AD-763 761

GROWTH AND CHARACTERIZATION OF GaAs AND MIXED III-V SEMICONDUCTOR COMPOUNDS

UNIVERSITY OF SOUTHERN CALIFORNIA

PREPARED FOR
ADVANCED RESEARCH PROJECTS AGENCY

JUNE 1973

Distributed By:

NTIS

National Technical Information Service
U. S. DEPARTMENT OF COMMERCE

USCEE Report 455

AD-763761

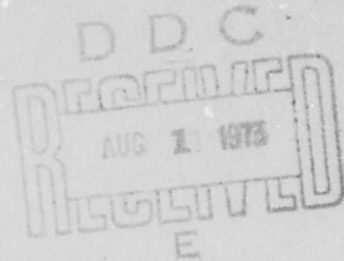

UNIVERSITY OF SOUTHERN CALIFORNIA

GROWTH AND CHARACTERIZATION OF GaAs AND MIXED III-V SEMICONDUCTOR COMPOUNDS

Vincent F. S. Yip

June 1973

A dissertation presented in partial fulfillment of the requirements for the degree of Doctor of Philosophy in Materials Science.

This research was supported by the Advanced Research Projects Agency of the Department of Defense under Grant DAHC-15-72-G7.

The views and conclusions contained in this document are those of the author and should not be interpreted as necessarily representing the official policies, either expressed or implied, of the Advanced Research Projects Agency or the U. S. Government.

ELECTRONIC SCIENCES LABORATORY

Approved for public release with unlimited distribution

233

Reproduced by
NATIONAL TECHNICAL
INFORMATION SERVICE
U S Department of Commerce
Springfield VA 22151

GROWTH AND CHARACTERIZATION OF GaAs AND MIXED III-V SEMICONDUCTOR COMPOUNDS

by

Vincent F. S. Yip

A Dissertation Presented to the

FACULTY OF THE GRADUATE SCHOOL

UNIVERSITY OF SOUTHERN CALIFORNIA

In Partial Fulfillment of the

Requirements for the Degree

DOCTOR OF PHILOSOPHY

(Materials Science)

June 1973

UNCLASSIFIED
Security Classification

DOCUMENT CONTROL DATA - R & D

(Security classification of title, body of abstract and indexing annotation must be entered when the overall report is classified)

1. ORIGINATING ACTIVITY (Corporate author) Electronic Sciences Laboratory University of Southern California Los Angeles, California 90007	2a. REPORT SECURITY CLASSIFICATION UNCLASSIFIED 2b. GROUP

3. REPORT TITLE

GROWTH AND CHARACTERIZATION OF GaAs AND MIXED III-V SEMICONDUCTOR COMPOUNDS

4. DESCRIPTIVE NOTES (Type of report and inclusive dates)

Dissertation (July 1969-June 1973)

5. AUTHOR(S) (First name, middle initial, last name)

Vincent F. S. Yip

6. REPORT DATE	7a. TOTAL NO. OF PAGES	7b. NO. OF REFS
June 1973	~~216~~ 233	49

8a. CONTRACT OR GRANT NO DAHC-15-72-G7 b. PROJECT NO. c. d.	9a. ORIGINATOR'S REPORT NUMBER(S) USCEE Report 455 9b. OTHER REPORT NO(S) (Any other numbers that may be assigned this report)

10. DISTRIBUTION STATEMENT

This document has been approved for public release and sale; its distribution is unlimited

11. SUPPLEMENTARY NOTES	12. SPONSORING MILITARY ACTIVITY
	Advanced Research Projects Agency

13. ABSTRACT

Gallium arsenide crystals were grown 1 cm in diameter by the gradient freeze technique and by the travelling heater method (THM) using a gallium zone. Optimal conditions for THM with a 1 cm long resistance heater were determined to be a heater temperature of 900°C, a lowering rate of 1.5 mm/day, a 6 to 10 mm long zone, a 1 cm long seed and a feed ingot over 2 mm long. Experimental results agreed well with a classical contitutional supercooling analysis. Preliminary experiments of THM growth of $Ga_xIn_{1-x}Sb$ and $Ga_xAl_{1-x}As$ were also performed. Classical constitutional supercooling theory was extended to multicomponent systems.

DD FORM 1 NOV 65 1473

UNCLASSIFIED
Security Classification

Preceding page blank

14. KEY WORDS	LINK A		LINK B		LINK C	
	ROLE	WT	ROLE	WT	ROLE	WT
Gallium arsenide, gradient freeze technique, travelling heater method, gallium indium antimonide, gallium aluminium arsenide, constitutional supercooling, crystal growth, dislocations						

TABLE OF CONTENTS

		Page
ACKNOWLEDGMENTS		iii
LIST OF FIGURES		ix
LIST OF TABLES		xiv
ABSTRACT		xvi
Chapter I	INTRODUCTION	1
Chapter II	LITERATURE STUDIES	6
	A. Temperature Gradient Zone Melting	6
	B. Travelling Heater Method Growth of Crystals	7
	C. Travelling Heater Method Growth of GaAs	14
	D. Travelling Heater Method Growth of Mixed III-V Compounds	19
Chapter III	VERTICAL GRADIENT FREEZE GROWTH OF GaAs	25
	A. Experimental	25
	1. Apparatus	25
	2. Sample Preparation	27
	3. Experimental Procedure	28
	B. Results and Discussions	33
	1. Crystallinity and Perfection	33

TABLE OF CONTENTS (Cont'd)

		Page
	2. Electrical Properties	38
	3. Mass Spectrometry	38
	4. Cathodoluminescence	44
Chapter IV	TRAVELLING HEATER METHOD GROWTH OF GaAs	49
	A. Experimental	49
	1. Original Apparatus	49
	2. Improved Apparatus	50
	3. Sample Preparation	52
	4. Experimental Procedure	58
	B. Results and Discussions	62
	1. Preliminary Growth Runs	62
	2. Influence of Feed and Crystal Lengths	71
	3. Influence of Zone Length and Interface Shape	78
	4. Influence of Heater Temperature and Lowering Rate	86
	5. Seeding and Impurity Doping	94
	6. Dislocation Etch Pits Studies	104
	7. Segregation in THM Growth	113
	8. Electrical Properties	116

TABLE OF CONTENTS (Cont'd)

		Page
	9. Temperature Profile Measurement During THM Growth	120
Chapter V	TRAVELLING HEATER METHOD GROWTH OF MIXED III-V COMPOUNDS	128
	A. Travelling Heater Method Growth of $Ga_xIn_{1-x}Sb$	128
	1. Sample Preparation	129
	2. Experimental Procedure	130
	3. Results and Discussions	132
	B. Travelling Heater Method Growth of $Ga_xAl_{1-x}As$	148
	1. Sample Preparation	148
	2. Experimental Procedure	149
	3. Results and Discussions	151
Chapter VI	CONSTITUTIONAL SUPERCOOLING IN TRAVELLING HEATER METHOD GROWTH	158
	A. Expression for Constitutional Supercooling	158
	B. Constitutional Supercooling in THM Growth of GaAs	164
	C. Constitutional Supercooling in Multicomponent Systems	175
Chapter VII	CONCLUSIONS	187
Chapter VIII	RECOMMENDATIONS	193
NOMENCLATURE		197

TABLE OF CONTENTS (Cont'd)

	Page
REFERENCES	201
APPENDICES	205

LIST OF FIGURES

Figure		Page
1.	Schematic of solution zone movement in crystal growth by travelling heater method.	3
2.	Schematic of temperature gradient zone melting in crystal growth.	7
3.	Temperature profile in casting process.	16
4.	Schematic of THM growth apparatus.	18
5.	Composition profile of $Ga_xAl_{1-x}As$ sample Al no. 20.	23
6.	Diagram of vertical gradient freeze apparatus for GaAs.	26
7.	GaAs ingot cast by vertical gradient freeze technique.	29
8.	Temperature profile in vertical gradient freeze growth of GaAs.	31
9.	Three GaAs ingots grown by vertical gradient freeze technique.	34
10.	Longitudinal section of GaAs ingot GF-32.	35
11.	Defects in GaAs ingots cast by vertical gradient freeze techniques.	37
12.	Cathodoluminescence intensity scans on GaAs crystal GF-25.	46
13.	Cathodoluminescence studies on GaAs crystal GF-25.	47
14.	Original apparatus for THM growth.	48

LIST OF FIGURES (Cont'd)

Figure		Page
15.	Diagram of THM apparatus for GaAs crystal growth.	53
16.	Assembled THM GaAs ampoule.	55
17.	THM apparatus partially filled with bubbled alumina.	60
18.	Quenched Ga zone.	60
19.	Longitudinal cross-section of THM-2.	65
20.	Longitudinal cross-section of THM-3.	65
21.	Cross-sections of THM-11.	67
22.	Schematic of THM growth of GaAs.	68
23.	(111)Ga etch pits of THM-9.	69
24.	Cathodoluminescence profile scan of THM-4.	70
25.	Cathodoluminescence linear scan brightness.	72
26.	Te x-ray linear scan spectrum.	72
27.	Position of the GaAs-Ga interfaces relative to the heater as a function of remaining length of crystal.	74
28.	Position of the GaAs-Ga interfaces relative to the heater as a function of the length of the feed.	75
29.	Steady state positions of the interfaces as a function of the length of grown solid for 0.55 cm initial zone length.	76
30.	Steadv-state positions of the interfaces as a function of the length of grown solid for 1.55 cm initial zone length.	77

LIST OF FIGURES (Cont'd)

Figure		Page
31.	Steady-state positions of the interfaces as a function of initial zone lengths.	80
32. a	Heat flow pattern and its relationship to interfaces shape.	82
32. b	Heat flow pattern and its relationship to interfaces shape.	82
32. c	Schematic of interface positions and shapes of experiments with different zone lengths.	84
33.	THM GaAs grown at 1.5 mm/day with different initial Ga zones.	85
34.	THM GaAs grown at 980°C with different lowering rates.	93
35.	GaAs crystal CZ-41.	95
36.	GaAs crystals THM-71.	97
37.	Longitudinal sections of THM-71 and THM-86.	97
38.	Longitudinal sections of THM-84.	99
39.a	(111) Slices of THM-72.	100
39. b	Geometry relationship between three (111) planes at 70.5° to the (111) seed plane in THM-72.	100
39. c	Side view of sandblasted crystal THM-72.	102
39. d	Polished side of THM-72.	102
40.	(111)Ga etch pits on THM-72 as a function of distance from the seed.	105
41.	Etch pit densities of THM-72 as a function of distance.	106

LIST OF FIGURES (Cont'd

Figure		Page
42.	Etch pit densities of THM-71 as a function of distance.	108
43.	Etch pit densities on longitudinal slices of THM-84 and THM-86.	110
44.	Assembled ampoule for temperature profile measurement during THM growth.	123
45.	Measured temperature profiles inside and outside THM growth ampoule.	124
46.	Excess crystal temperature versus cooling time.	127
47.	Five cast ingots of $Ga_xIn_{1-x}Sb$ material.	131
48.	THM grown $Ga_xIn_{1-x}Sb$ ingots and slow-cooled casting.	135
49.	Atom ratio Ga/(Ga+In) versus distance along growth direction of THM-77.	138
50.	Atom ratio Ga/(Ga+In) versus distance along growth direction of THM-87.	140
51.	Calculated solidus isotherms for the Ga-In-Sb system.	141
52.	$(X_{fi}-X_{ci})$ versus growth distance in THM-77 and THM-87.	147
53.	Assembled ampoule for THM growth of $Ga_xAl_{1-x}As$.	150
54.	A cross-sectional slice of THM-88.	154
55.	Atom ratio Ga/(Ga+Al) versus distance along growth direction of THM-88.	156
56.	Solute atom fraction and equilibrium temperature distribution in solution crystal growth.	159

LIST OF FIGURES (Cont'd)

Figure		Page
57.	Illustration of the factors which determine the maximum lowering rate for THM.	163
58.	Arsenic solubility in Ga over the temperature range 500-1000°C.	166
59.	Viscosity of pure Ga melt for temperature range 500-1000°C.	168
60.	THM GaAs experimental results shown with curves calculated from a criterion for constitutional super-cooling.	174

LIST OF TABLES

Table		Page
1.	Experimental data on material grown by THM or related methods.	11
2.	Growth parameters employed in GaAs crystal growth experiments.	20
3.	Growth details of GaAs ingots grown by vertical gradient freeze method.	39
4.	Hall measurement results for vertical gradient freeze GaAs crystals grown from different starting material.	40
5.	Spectrochemical analyses of vertical gradient freeze grown material.	41
6.	Mass spectrometric analyses of GaAs grown by different techniques.	43
7.	Summary of early travelling heater experiments on GaAs.	63
8.	THM runs with different initial zone lengths.	87
9.	Summary of THM growth runs at different heater temperatures and lowering rates.	88
10.	Details of THM runs at different heater temperatures and lowering rates.	90
11.	THM runs with controlled seeding and doping.	96
12.	Mass spectrometric analyses of feed rods and THM grown GaAs.	114
13.	Hall measurements of feed crystals and THM grown GaAs.	117

LIST OF TABLES (Cont'd)

Tables		Page
14.	Summary of travelling heater experiments on $Ga_xIn_{1-x}Sb$.	130
15.	Atom ratio x versus growth distance in THM-77.	137
16.	Atom ratio x versus growth distance in THM-87.	139
17.	Growth distance versus $(x_{fi}-x_{ci})$ for THM-77 and THM-87.	146
18.	Summary of THM $Ga_xAl_{1-x}As$ growth runs.	152
19.	Atom ratio x versus growth distance in THM-88.	155
20.	Calculated values of diffusion coefficient D of As in Ga for 500-1000°C.	168
21.	Calculations of critical growth rate V_c based on constitutional supercooling a criterion in THM growth of GaAs.	173

ABSTRACT

The travelling heater method (THM) is a crystal growth technique in which a liquid solvent zone is caused to move through a solid feed material by movement relative to the heater. In this research GaAs, $Ga_xIn_{1-x}Sb$ and $Ga_xAl_{1-x}As$ were grown by the THM and the material characterized by dislocation etching, Hall and conductivity measurements, mass spectrometry and cathodoluminescence.

The cylindrical feed GaAs for THM experiments was grown by the vertical gradient freeze method. The solvent used was high purity Ga and the single crystal GaAs seeds were shaped from Czochralski grown crystals. A systematic investigation was made on the influence of the various parameters such as temperature and lowering rate, feed and crystal lengths, zone length and growth interface shape on THM growth and the quality of GaAs grown. For the growth of 1 cm diameter GaAs using a 1 cm long resistance heater, the seed should be at least 1 cm long, the feed should be at least 2 cm long, and the ratio of the Ga zone length to the heater length should be about 0.6 to 1.0. The optimal growth temperature and growth rate were determined to be about 900°C and 1.5 mm/day respectively.

Single crystals of GaAs were grown up to 3.5 cm long by seeding in the ⟨110⟩, ⟨111⟩Ga and As directions. Some were not intentional-

ly doped while others were doped with Te, Zn or Cr. Characterization by Hall measurements, dislocation etching and mass spectrometric analyses was performed. The temperature profile inside GaAs during a THM growth run at a zone temperature of 931°C was measured. The temperature gradient in the Ga zone at the bottom growth interface was determined to be ~40°C/cm.

Based on a classical constitutional supercooling consideration, an expression for the "critical growth rate" V_c was derived and was found to depend on the temperature gradient G, the diffusion coefficient D, solubility X of the solute in the solvent, and the liquidus slope m at that temperature. Calculated values of V_c for THM growth of GaAs agree well with the experimental evidence obtained. A general expression for V_c was also derived for THM growth of a multicomponent system.

The THM growth of $Ga_xIn_{1-x}Sb$ with a Ga-In solvent zone at a growth temperature of ~550°C and the THM growth of $Ga_xAl_{1-x}As$ at a growth temperature of ~1000°C were also investigated.

Chapter I

INTRODUCTION

Conventional crystal growth techniques can be classified into three main categories:

1. Melt growth: Growth by directional solidification of the melt, or by movement of a molten zone through a solid ingot of the material.
2. Vapor growth: Growth by evaporation and condensation or by chemical reaction.
3. Solution growth: Crystallization by cooling or evaporation of the solvent or growth from chemical reaction in the liquid phase.

There are several typical advantages of growing a crystal from a liquid solution below its melting point:

1. Avoids incongruent melting and high vapor pressure at the melting point.
2. Avoids decomposition or undesired polymorphic phase changes during growth.
3. Solubilities and distribution coefficients of impurities are frequently smaller than at the melting point.
4. Increases experimental feasibility or convenience.
5. Lowers imperfections such as dislocations, vacancies and recombination centers in the grown crystals.

In recent years, crystal growth of electronic materials for use in fabrication of devices has gained great technological interest and importance. Liquid phase epitaxy techniques have been widely used in growth of thin films of semiconductor materials and their solid solutions. Growth by solvent zone techniques, such as the travelling solvent and the travelling heater methods, can satisfy the demand for bulk crystals and at the same time possesses the advantages of solution growth mentioned previously. Of the two, the travelling heater method (THM) is preferred for growth of large single crystals.

The travelling heater method of crystal growth is a technique in which a solvent zone is caused to move through a solid feed material by the movement of a heater. In practice, it is often more convenient to move the solvent zone and the feed charge relative to the heater, as illustrated in Figure 1(a) and (b). As the ampoule containing the solvent and the seed and feed sections are lowered through a stationary heater, feed material dissolves at the top hotter interface, is transported through the molten solvent zone and deposits onto the bottom cooler interface. In this manner, large crystals of different materials can be grown. In addition to increased perfection due to a lower growth temperature, the solvent zone has a zone-refining purification effect on the material regrown from the feed source.

Since the technique of travelling heater method was first

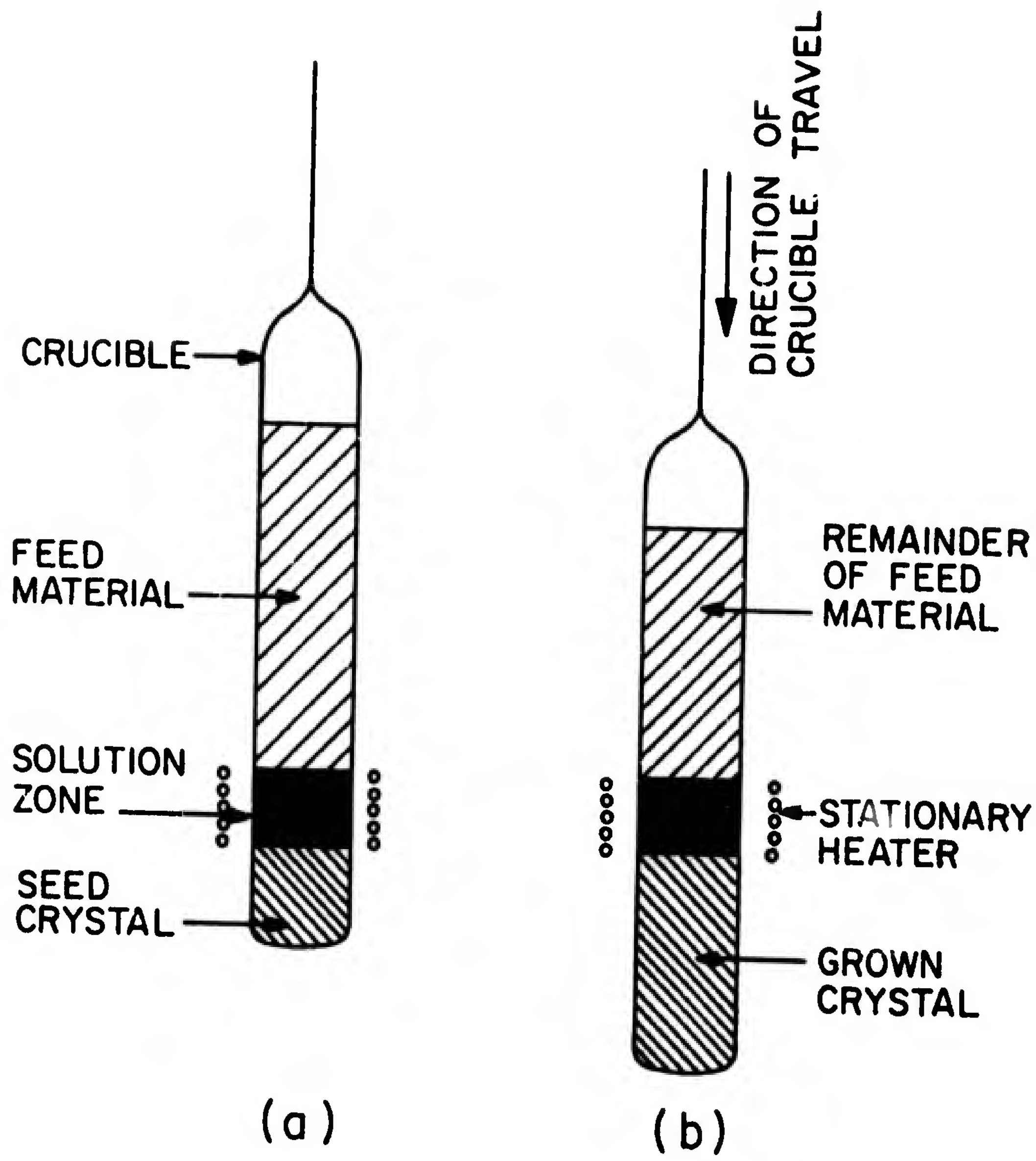

Figure 1: Schematic of solution zone movement in crystal growth by the travelling heater method.

conceived by Pfann[1] in 1955, most of the work to date on THM was done at Tyco Laboratories at Waltham, Massachusetts. Different researchers have demonstrated the feasibility of THM growth of a wide range of crystals of pure and mixed materials as summarized in Table 1 in the next chapter. However, very little has been published on the phenomena governing THM crystal growth or on the properties of the materials produced thereby. The purpose of this research was to fill some of the gaps in THM crystal growth knowledge and thereby enable growth of better crystals.

In our investigation, gallium arsenide was chosen for THM growth studies because it is an important semiconductor and also because of previous work on GaAs at U.S.C. Some work was also done on the vertical gradient freeze growth method, used to produce most of the cylindrical GaAs feed material for experiments on THM growth. A major part of the research was devoted to the systematic study of the influence of different growth parameters on the properties and perfection of the resultant crystals. High quality GaAs single crystals were produced and the latter part of the research centered on exploratory THM growth of mixed III-V compounds, the $Ga_xIn_{1-x}Sb$ and $Ga_xAl_{1-x}As$ systems.

The next chapter of this dissertation contains a review of the previous publications related to the THM. Chapter III describes the vertical gradient freeze technique for growth of GaAs and the

experimental results. The main body of this dissertation is contained in Chapter IV where the details of experiments and results on THM growth of GaAs are presented. The extension of THM growth to $Ga_xIn_{1-x}Sb$ and $Ga_xAl_{1-x}As$ is described in Chapter V, to be followed by a chapter which explores some theoretical considerations of constitutional supercooling in THM growth. The important interpretation and conclusions drawn from the research undertaking are summarized in Chapter VII. Recommendations on improvements and extensions of the present work are presented in the final chapter.

Chapter II

LITERATURE STUDIES

This chapter begins with a discussion of the original paper by Pfann[1] on Temperature Gradient Zone Melting (TGZM) and a later paper by Mlavsky et. al.[2] on the Travelling Solvent Method (TSM). Section B is a review of the Travelling Heater Method (THM) and contains an up to date tabulated summary of materials which were grown by the THM and related methods. The specific work on THM growth of GaAs by Hemmat and Wald[3] is reviewed in section C. That is followed by a review of studies on THM growth of mixed III-V compounds, in particular those on the $Ga_xIn_{1-x}Sb$ and the $Ga_xAl_{1-x}As$ systems, which were also investigated in our research.

A. Temperature Gradient Zone Melting or Travelling Solvent Method Growth of Crystals

In 1955, Pfann[1] gave a very comprehensive description of the fundamentals of Temperature Gradient Zone Melting (TGZM) and also outlined several applications of the technique. TGZM is applicable to any solute-solvent system in which one component lowers the melting of another component. For illustration, consider the system AB of Figure 2(a), where A is the solvent and B the solute, the distribution coefficient k for B is constant and less than one

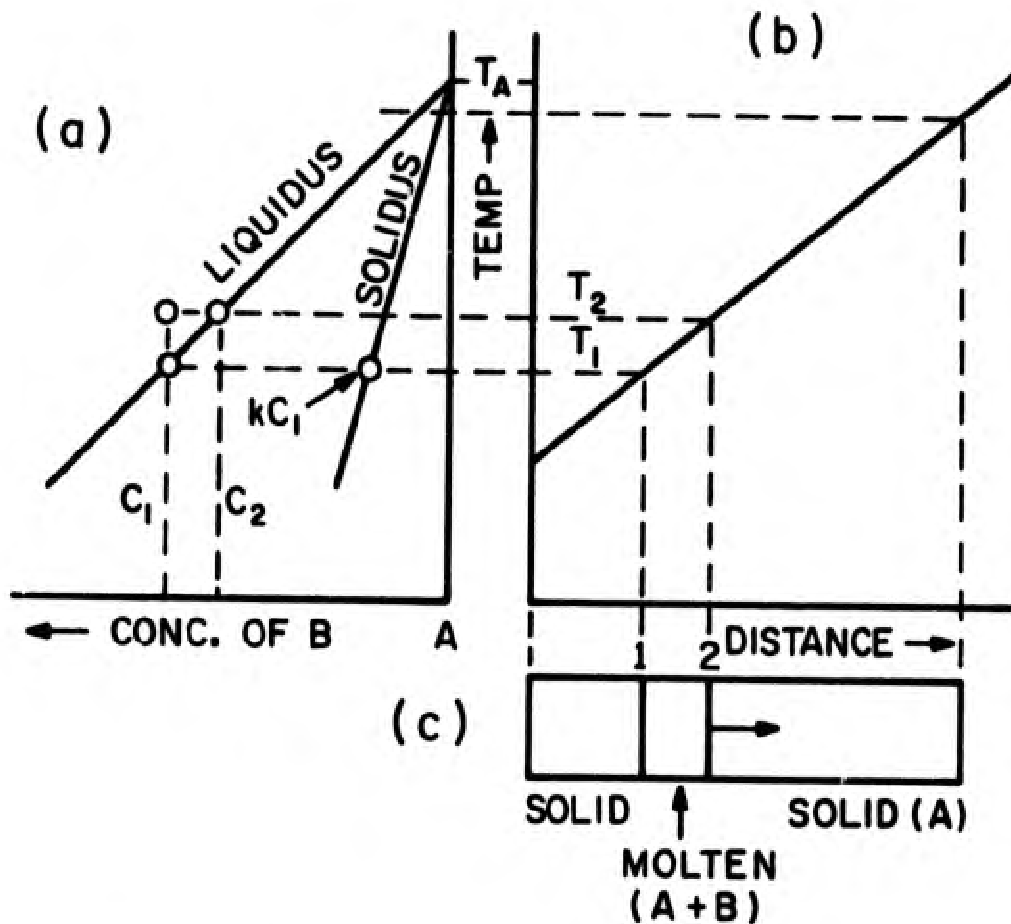

Figure 2: Temperature gradient zone melting showing (a)-portion of phase diagram, (b)-temperature gradient in system, (c)-physical system comprising molten zone containing A and B travelling through solid A. After Pfann.[1]

(as defined in the figure). If a thin layer of solid B is sandwiched between blocks of A and placed in a temperature gradient as shown in Figure 2(b), the layer becomes molten and dissolves A. The liquid at the interfaces 1 and 2 (Figure 2(c)) are at temperatures T_1 and T_2 respectively and become saturated with A at concentrations C_1 and C_2. The concentration gradient thus established causes A to diffuse toward the cooler interface 1 and B toward the hotter interface 2. As a result, the liquid at interface 2 becomes supersaturated and A containing concentration kC_1 of B deposits. Material A continues to dissolve at the hotter interface 2, diffuses through the zone and deposits at the cooler interface 1. As a result, the molten zone travels through the solid in the direction of increasing temperature.

Pfann considered the length, shape and compositional changes of the zone during travel. A high rate of travel of the zone is found to be favored by a large temperature gradient dT/dX, a large diffusivity D and a small liquidus slope dT/dC. The author noted that, "In principle, the zone could be held at one temperature for its entire travel distance." This would have the important feature that it would permit traversal of a charge at a high rate corresponding to a high temperature gradient, while at the same time permitting a low variation in impurity concentration. The travelling heater

Method later evolved from this idea described above. The application of TGZM to growing single crystals, fabrication of semiconductor devices, and measurement of diffusities in liquids are discussed in the concluding part of Pfann's original work.

In 1963, Mlavsky and Weinstein[2] of Tyco Laboratories(Waltham, Mass.) extended the TGZM technique to the growth of GaAs from a Ga solvent. They also suggested the name "Travelling Solvent Method" (TSM) of crystal growth and claimed that the name "has both denotative and connotative advantages over the term TGZM, particularly for crystal growth per se." The parameters influencing zone movement, including zone thickness, average temperature, temperature gradient, and seed orientation, were experimentally studied for the case of the GaAs-Ga system. The rate of zone movement was considered to be liquid diffusion limited. The diffusion coefficient D for arsenic in Ga liquid at the average temperature of 900°C (the temperature gradient ranged from 800-1050°C) was thereby estimated to be 1×10^{-4} cm^2/sec.

B. Travelling Heater Method Growth of Crystals

In his book "Zone Melting,"[4] Pfann discussed more extensively the idea of maintaining the solvent zone at constant thermal conditions by a ring heater. He concluded that while stationary thermal conditions may be good for moving a concentrated solution zone, this

technique of moving a heater might be more appropriate for dilute solution zones. Trumbore et. al.[5] first used this as yet unnamed technique to grow crystals of germanium and silicon in 1959. The name travelling heater method evolved subsequently and most of the work done to date can be credited to researchers at Tyco Labs. In 1965, Wolff and Mlavsky[6] reviewed crystal growth by TSM and THM techniques. Mass transport analysis were attempted for solvent zone techniques and were taken to be valid for both TSM and THM. The phenomena of purification and dislocation removal during growth by solvent zone techniques were briefly mentioned. The authors also described the application of solvent zone techniques to growth of peritectic compounds and solid solutions. They also noted that in THM growth of ternary system solid solutions, it is preferable to use a solution zone which is in equilibrium with the feed material. However, in any case, after some initial transient, the growing crystal will eventually reach final steady state composition equal to that of the feed.

In the decade following the first deployment of THM in crystal growth, a great variety of materials was grown by this technique, ranging from simple Si to the less common $CdIn_2Te_4$. The materials and the experimental data are summarized in the following Table 1.

TABLE 1. EXPERIMENTAL DATA ON MATERIAL GROWN BY THM OR RELATED METHODS (temperatures indicated by - are not available in reference)(RH-resistance heater, RF-radio frequency heating)

Material	Solvent	Heater	Growth Temp (^{o}C)	Growth Rate (mm/day)	Reference
$CaCO_3$	$CaCO_3$-Li_2CO_3	RH	700-800	5	[7][8]
$CdIn_2Te_4$	$InTe_3$-CdTe	RH	780-800	30 to 200	[9]
$CdCr_2Se_4$	$CdCl_2$	RH	-	≤ 1.5	[10]
CdS	Cd	RF	~980	2.5	[11]
CdTe	Te	RH	~700	≤ 5 to 7.5	[12]
CuCl	KCl	RH	~340	5 to 6	[13]
CuCl	KCl	RH	~200	3	[1[illegible]]
GaAs	Ga	RH	900-960	≤ 5.5	[3]
GaAs	Ga	RH	780-100	0.5 to 20	[15]
GaP	Ga	RF	~1160	4	[16]
GaSb	Sb	RF	-	40	[17]
Ga(As,P)	Ga	RF	900-1100	≤ 5 to 6	[18][19]

TABLE 1. (Continued)

Material	Solvent	Heater	Growth Temp (^{o}C)	Growth Rate (mm/day)	Reference
(Ga, In)P	Ga-In	RH	970-1040	$\leq$ 3 to 5	[20]
(Ga, Al)As	Ga-Al	RH	900-1050	$\leq$ 3	[21]
(Ga, In)Sb	Sb	RF	-	24	[22]
HgTe, ZnTe (Hg, Zn)Te	Te	RH	500-650	$\leq$ 3 to 5	[18]
HgCdTe	Te	RH	~730	5 to 7	[23]
Naphthalene	Benzoic acid	RF	~80	10 to 30	[24]
$(Pb, Sr)TiO_3$	Borate flux	RF	~1060	$\leq$ 1	[25]
$Pb(Ti, Zr)O_3$	Borate flux	RF	~1100	$\leq$ 1	[25]
Si	Au-Si	RF	-	0.4 to 20	[26]
SiC	Cr	RF	1650-1900	$\leq$ 3	[27]

TABLE 1. (Continued)

Material	Solvent	Heater	Growth Temp (^oC)	Growth Rate (mm/day)	References
YIG	$Fer0_3$-$YFe0_3$	RF	-	6	[28]
Zn0	PbF_2	RF	~900	≤ 3.5	[29]

C. Travelling Heater Method Growth of GaAs

It is interesting and also surprising when one examines Table 1 that it was not until 1969 that the THM growth of GaAs, a material of considerable technological interest and importance, was first reported by Hemmat et. al.[3] Beginning in 1970, research was conducted in our research laboratories on THM growth of GaAs from a Ga zone and the results were reported in two American Physical Society Conferences.[30, 31] The above mentioned references are in the form of abstracts and thus do not provide detailed discussions of the crystal growth experiments and results. Aside from our bi-annual USCEE technical reports to ARPA on "New Methods for Growth and Characterization of GaAs and Mixed III-V Semiconductor Crystals," the only other detailed information reported on THM growth of GaAs is by Hemmat and Wald[3] of Tyco Labs. Since this work is closely related to our effort on THM growth of GaAs in many aspects, it is reviewed and discussed here in detail:

1. Mass Transfer: The understanding of the mass transfer and crystal growth processes described is the same as that in other Tyco work. The THM growth of GaAs was presented as a crystal growth process which takes place under steady-state, near equilibrium conditions with the diffusion through the liquid zone being the rate limiting factor. A diffusion coefficient of D of 10^{-4} cm^2 sec^{-1} was quoted for

arsenic in a gallium melt and since THM growth was assumed diffusion controlled, the maximum growth rate was predicted to be about 0.4 in/day (~1 cm/day). Any attempt to enforce an increased growth rate past this critical growth rate would interrupt single crystal growth, the authors contended. Of course, as will be discussed in this dissertation, our work has demonstrated that THM growth is also convection dependent. The "critical growth rate" for simple crystal growth depends not only on D but also on growth temperature, geometry and stirring. For GaAs it was raised here to much greater than the 1 cm/day given by these authors.

2. Sample preparation and experimental procedure.

The feed inputs of GaAs was prepared by a method similar to the vertical gradient freeze method employed in our research (see Chapter III). Figure 3 shows the initial position of the furnace. Prereacted polycrystalline GaAs was melted in the carbonized fused silica crucible at about 1260°C and gradually lowered through the cooler section of the furnace. The crystal cast was 0.8 cm in diameter, 2.4 cm long. No growth from elemental Ga+As was attempted. Apparently, for later growth runs where longer feed ingots were needed, they were not obtained by casting but by "mechanically shaping" polycrystalline material. Seed crystals of approximately 1 cm long by 1 cm diameter were shaped from GaAs

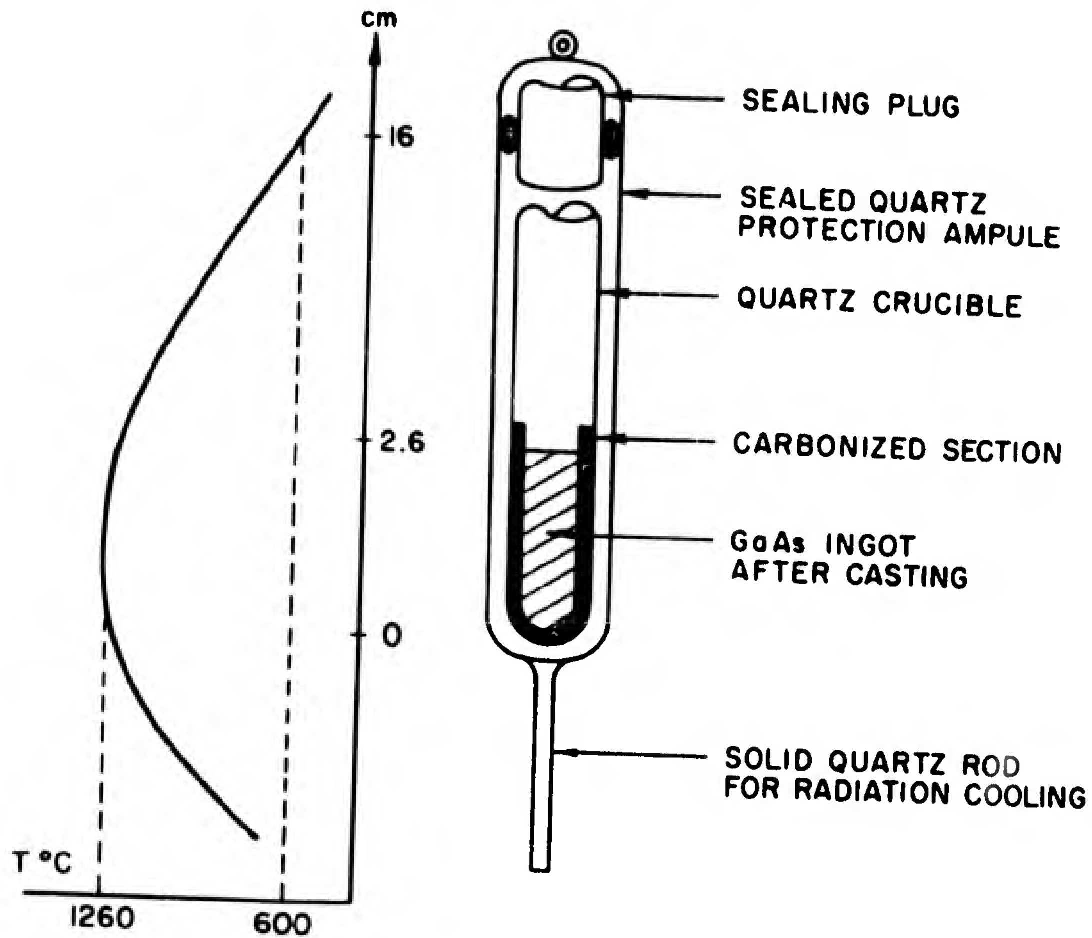

Figure 3: Initial position of the GaAs charge relative to the temperature profile of the furnace in the casting process. After Hemmat and Wald.[3]

which contained two to three grains. The Ga solvent zone length used was 1 cm throughout. Crystal growth was accomplished in carbonized fused silica crucibles which were supposed to prevent the gallium solvent from adhering to the crucible wall during crystal growth and to allow easy removal of the ingot after growth.

The apparatus used for THM growth is shown in Figure 4. The furnace consisted of two separately-controlled resistance heaters made of Kanthal wire wound on a clear fused silica muffle. The short top heater (about 1.5 cm long) provided the growth temperature while the bottom longer after-heater could subject the grown ingots to annealing, although this was not done in the GaAs runs. Another clear fused silica tube was placed concentrically around the heater muffle to protect it from atmospheric convection and to allow direct viewing of the ampoule. The authors noted that during the entire THM crystal growth process the Ga zone maintained its position within the heater.

3. Experimental results and characterization.

A total of five runs were performed as summarized in Table 2. The solution zone temperature used was in the range 900-960°C and the growth rate was 0.3 to 0.55 cm/day. Discussion of the results of growth and characterization of the crystals was minimal. From previous experiments on growth of GaAs by cooling a Ga melt,

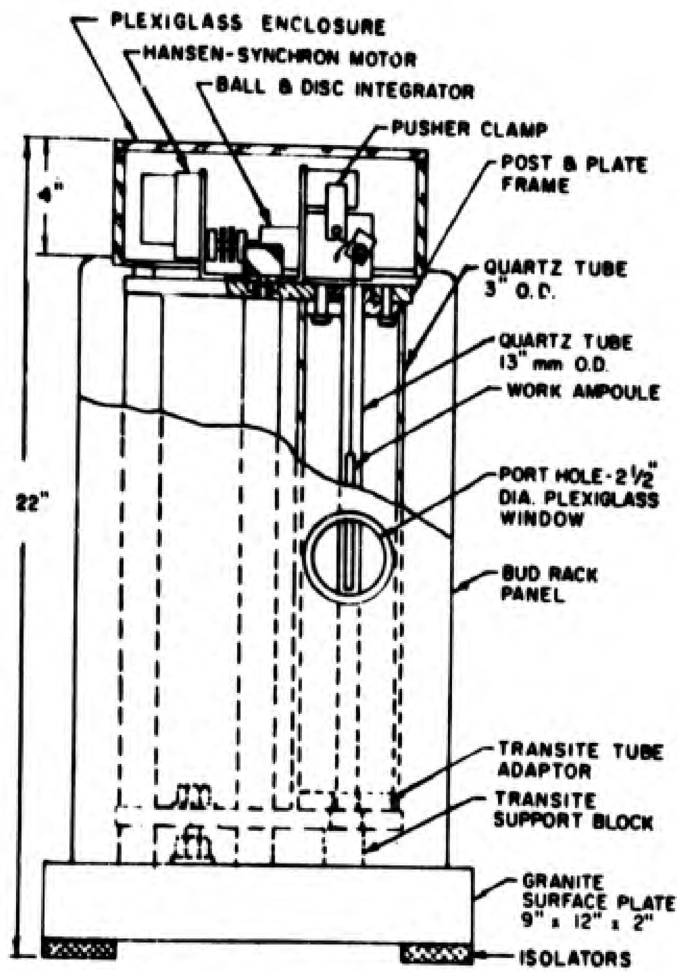

Figure 4: Schematic of apparatus specially designed for crystal growth by THM. After Hemmat and Wald.[3]

the authors noted that the $\langle 111 \rangle$ Ga and As directions were least favorable growth directions, while the $\langle 110 \rangle$ and $\langle 112 \rangle$ are the most favorable. However, this contention was not supported experimentally as selective seeding was not done in their THM growth of GaAs. In general, the crystals grown were found to be p-type and had an etch-pit density on the order of $10^3/cm^2$. The authors determined that THM produced GaAs had lower impurity concentrations than material prepared by other techniques. Results from emission spectrography analysis was presented as:

Impurity Elements	ppm
Si	0.5
Cu	0.05
Mg	0.01
Al	1.0
Ca	0.1
Fe	0.5
Ni	0.5
Ag	0.1

In conclusion, Hemmat and Wald contended that they demonstrated the feasibility of growing bulk GaAs by the THM. The main advantages of this technique were considered to be the purification factor and the lack of contamination by the container. Finally, the authors suggested using low dislocation content seeds and annealing by the afterheater to produce still lower dislocation crystals.

D. Travelling Heater Method Growth of Mixed III-V Compounds

TABLE 2. GROWTH PARAMETERS EMPLOYED IN THE GaAs CRYSTAL GROWTH EXPERIMENTS (After Hemmat and Wald[3])

Exp. No.	GaAs Charge Material	GaAs Charge Length and Diameter, cm	Solvent Ga-Zone Length cm	Solution-Zone Temperature °C	Growth Rate, cm/day	Seeding	Length of Ingot Produced cm
1	Precast	2.4 x 0.8	1	900	0.55	-	2.4
3	Mechanically shaped ingot	7.0 x 1	1	930	0.3	1-cm-long seed; contained 2 grains	4
4	Mechanically shaped ingot	7.0 x 1	1	960	0.3	1-cm-long seed; contained 3 grains	5
5	Precast	5.0 x 1	1	900	0.5	0.7-cm-long seed; contained 3 grains	3

Despite the fact that THM method is a very promising technique for the growth of mixed III-V compounds, there have been few reports on such work. Wolff et.al.[18] grew small crystals (0.5 cm diameter, 1.5 cm long) of GaP_xAs_{1-x} in BN crucibles at solution zone temperature between 900 and 1100°C with a heater movement less than 5 mm/day. The feed material used was a pasty mixture of GaP and GaAs obtained by grinding in liquid gallium. Single crystals of GaP were used as seeds in some runs. This work demonstrated the ease and feasibility of growing crystals having a high vapor pressure at their melting point. $Ga_xIn_{1-x}P$ was also grown by Tyco personnel[20] by THM for electroluminescent light sources. As for the $Ga_xIn_{1-x}Sb$ system which we are concerned with in our research, there appears to be no previous reports of its growth by THM using a Ga-In zone. Plaskett and Woods[22] did mention the growth of GaSb-rich alloys by horizontal zone leveling using an Sb-rich zone. The THM growth of $Ga_xAl_{1-x}As$, the second mixed III-V system selected in our investigation, was extensively covered by the work of Bell et.al.[21] of Tyco Labs. This reference will be discussed here in greater detail. Some aspects of the report will also be discussed later in this dissertation in relation to our effort on THM growth of $Ga_xAl_{1-x}As$.

The purpose of their research was to produce $Ga_xAl_{1-x}As$

which could conceivably be used to fabricate more efficient laser diodes. The first major task was the preparation of the feed material. After different approaches were tried, an Al wire was axially inserted along with a GaAs ingot as feed. Fused silica, AlN, Al_2O_3 and BN were used as crucible material, with BN producing the most satisfactory results. A total of over thirty different runs were performed, some self-seeded and some with single crystal GaAs as seeds. The rate of zone movement was between 1.5 and 3.2 mm/day and the solvent zone temperature ranged from 930°C to 1100°C. X-ray lattice parameter measurements were made on many of the samples. The axial composition profile of two samples was determined by optical absorption edge measurements. Figure 5 shows the composition variation of $Ga_xAl_{1-x}As$ sample no. 20 grown at a 1050°C zone temperature from a feed of $Ga_{0.95}Al_{0.05}As$. A GaAs seed was used and the total grown length was 2.3 cm.

A paper on THM growth of solid solutions of electronic compounds by Hemmat et.al. [32] maintained that the maximum growth rate in THM growth is limited by "the highest possible diffusion rate of the most slowly diffusing constituent species through the solution zone." In the case of growth of solid solutions, the solution zone used should be in equilibrium with the feed material in order to grow material of uniform composition. At the same time, the

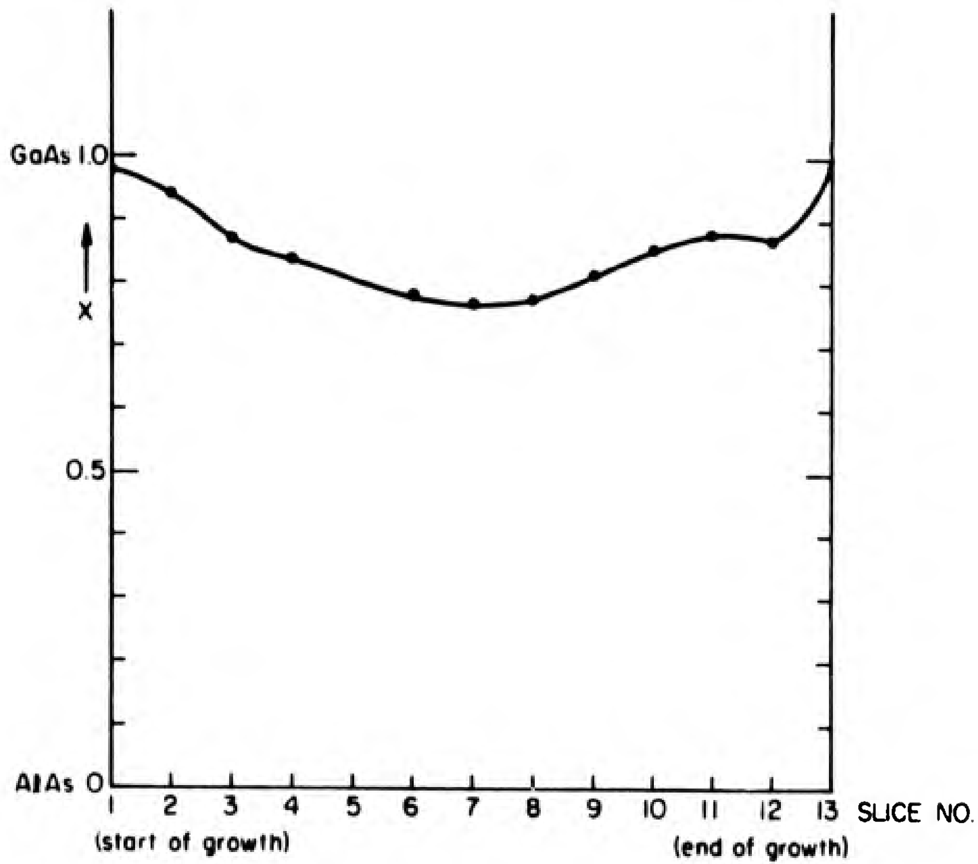

Figure 5: Composition profile of $Ga_xAl_{1-x}As$ (sample Al no. 20) in axial direction as determined by optical absorption edge measurements (sample was seeded with GaAs). After Bell et. al.[21]

temperature used should be high enough so that the solubility of the slowest diffusing component is still sufficient for THM growth. The THM growth of $Ga_{0.9}Al_{0.1}As$ from a Ga-Al solvent was taken as a practical example and the conclusion was that a solution zone temperature in excess of $1000^{o}C$ is necessary.

Chapter III

VERTICAL GRADIENT FREEZE GROWTH OF GaAs

Cylindrical rods of GaAs are needed for use as feed material in THM growth of GaAs. Initially, they were mechanically shaped from rectangular slices of polycrystalline material cut from horizontal Bridgman grown GaAs. This process was tedious and wasteful. The vertical gradient freeze method described below was subsequently developed to prepare cylindrical ingots of GaAs for use in THM growth.

A. Experimental

1. Apparatus

The basic experimental setup of the two-zone furnace is shown in Figure 6. The bottom melt zone firebrick furnace measured 15'' x 17'' and had a central circular cavity of diameter 7 inches and length 7 inches. Six, 18 inches long (heater length 14 inches) one-half inch diameter carborundum globars were used. They were equally spaced around the furnace at two inches from the center. A 46 x 50 mm silica tube was placed in the center to even out the heat from the heating rods and to protect them from direct shock and damage in case of an arsenic explosion during growth. The top furnace was used for controlling the arsenic pressure and was

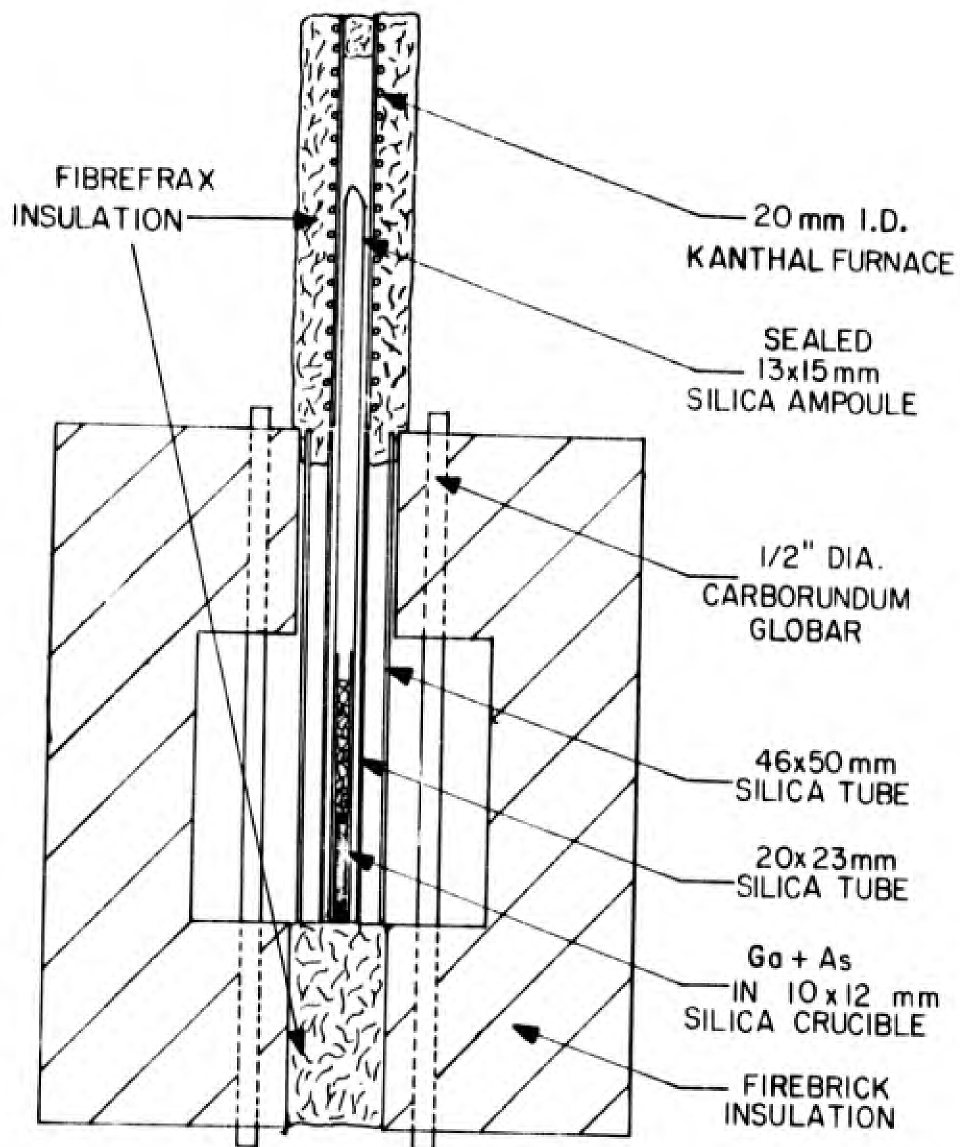

Figure 6: Diagram of vertical gradient freeze apparatus for GaAs.

constructed by winding gage 20 Kanthal wire on a grooved (1/16 in. pitch), 20 mm I.D., 12-inch long alumdum furnace core (from Norton Refractories Company, Worcester, Massachusetts). Fibrefrax (from Carborundum Corp., Niagara Falls, New York) was used as insulation.

The power for the globar furnace was provided by a 240-volt line and controlled by a Superior Electric Company type 246 Powerstat which had a capacity of 4.2 KVA. An Allis Chalmers transformer (10.6 KVA capacity) was placed between the Powerstat and the globar elements to lower the maximum voltage from 240 volts to 30 volts while the current capacity was increased. The Kanthal furnace was connected to a 10 amp, 20-volt Variac with the voltage input regulated by a 60 VA Sola transformer (from Sola Electric Company, Elk Grove Village, Illinois).

2. Sample Preparation

The starting material used was either pre-reacted GaAs or elemental Ga and As. If the requirement on purity was not stringent, it was easier to use scrap material from Czochralski, horizontal Bridgman or other vertical gradient-freeze runs. The pre-reacted GaAs was broken into small pieces, etched in 1 HF:3 HNO_3 and washed in deionized water. It was then loaded into a 10 x 12 mm 20-cm long silica tube closed at one end. This was then placed inside a 13x 15

mm, 45-cm long silica tube which was in turn evacuated to 1-3 microns Hg pressure and sealed with a torch. An assembled ampoule and several grown ingots are shown in Figure 7.

The earlier exploratory vertical gradient freeze growth runs were all performed using GaAs as starting material. Realization that this crystal growth method should be more than a mere regrowth of pre-reacted material brought about the investigation which resulted in successful growth of GaAs from elemental Ga and As. The appropriate measured amount of high purity (typically six 9's) gallium was placed in the inner 10 x 12 mm crucible with the corresponding necessary amount of arsenic. Surface oxide was removed from the arsenic pieces before use by carefully heating them in a closed tube with a torch. The arsenic oxide sublimed and condensed at the cold end of the tube. The cleared arsenic pieces were then weighed and placed into the crucible. A small amount of arsenic in excess of stoichiometry was added to provide approximately 1 atm. arsenic pressure during growth. The preparation of the evacuated growth ampoule was similar to that described earlier but with the additional precaution of avoiding any spilling of gallium outside of the inner growth crucible. It was not necessary, however, to have the arsenic chunks within the inner crucible.

3. Experimental Procedure

The sealed ampoule was loaded and positioned inside the furnace

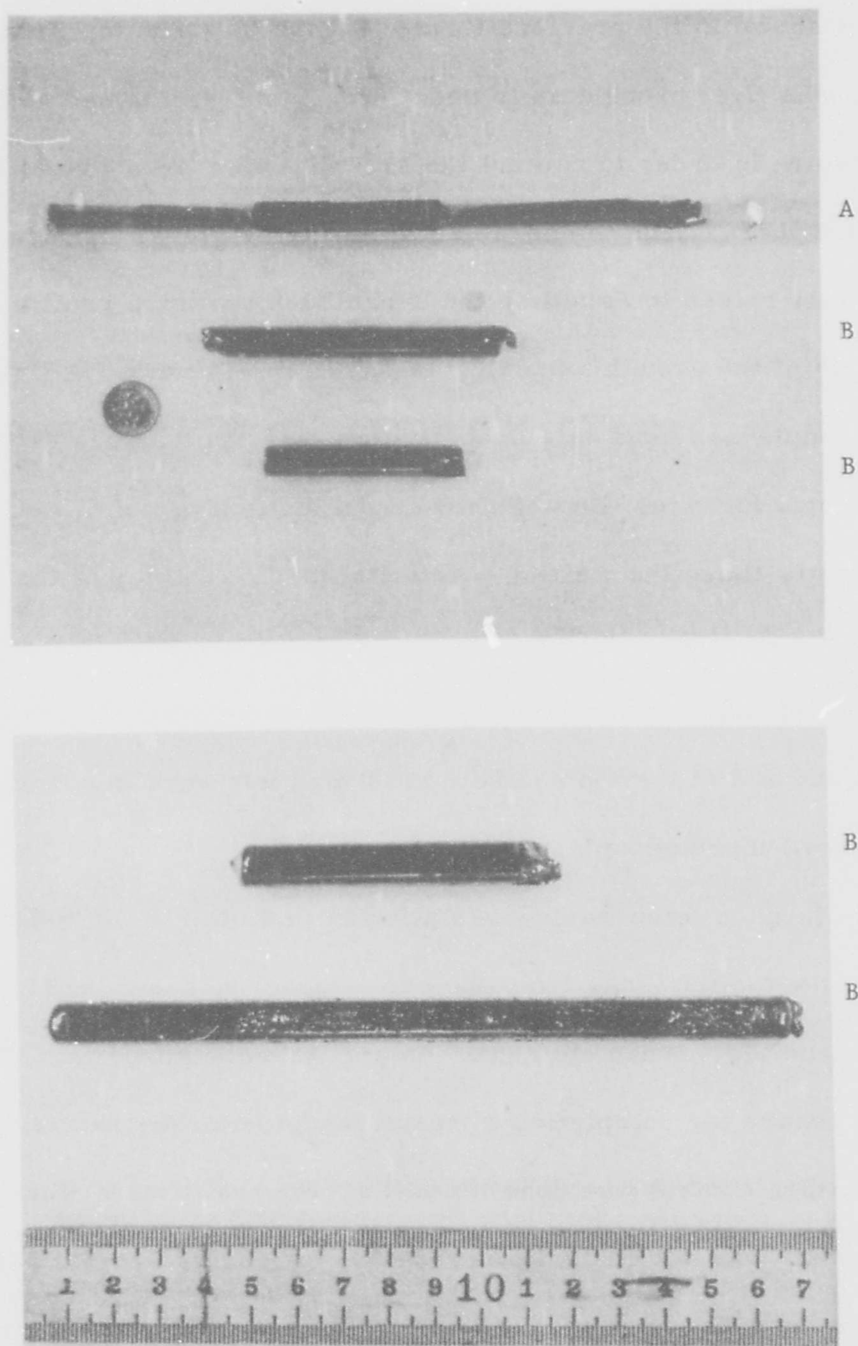

Figure 7: GaAs ingot cast by vertical gradient freeze technique.
A. Assembled ampoule before casting;
B. Cast ingots.

setup as shown in the previous figure (Figure 6). The top Kanthal furnace was first brought up to about 610°C and maintained at that temperature in order to control the arsenic vapor pressure at about one atmosphere. The temperature of the lower globar furnace was then slowly raised to establish the overall temperature profile over the length of the growth ampoule, as shown in Figure 8. A Cr-Al thermocouple was used as a probe to measure the temperature profile in the empty furnace. During growth, the bottom of the GaAs melt was slightly above the melting point of 1238°C. The top of the 10-cm long melt was about 1300°C. The temperature gradient in the furnace was approximately linear at 6°C/cm. The temperature at the arsenic control end and at the top and bottom of the melt were monitored by three Cr-Al thermocouples throughout growth.

The furnace temperature was allowed to stabilize for 6-7 hours to allow the molten GaAs from the pre-reacted pieces to settle in the growth crucible. When elemental Ga and As were used, this time was necessary for completion of reaction and homogenization. Temperature control was done manually. Several times, when the temperature was not controlled properly, excessive arsenic vapor pressure built up and caused violent explosions which terminated the growths and sometimes damaged the globar elements. When the conditions were satisfactorily established and controlled, the temperature of the melt zone was steadily lowered by reducing the furnace

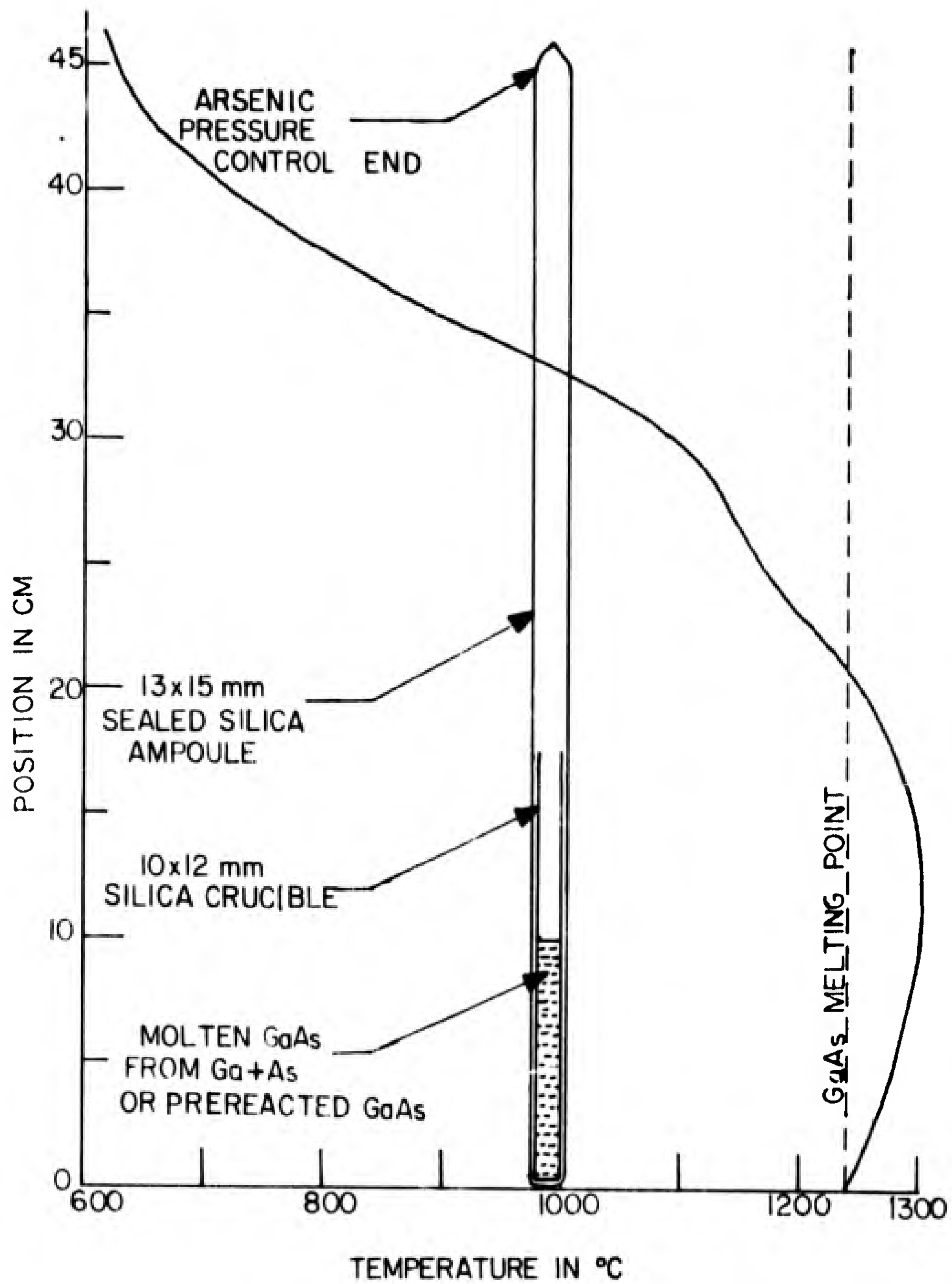

Figure 8: Ampoule and empty furnace temperature used for vertical gradient freeze growth of GaAs.

voltage at a constant rate with a low-speed motor connected to the Powerstat. The cooling rate was typically 0.3°C to 3°C/minute. Solidification occurred first at the bottom of the melt and the subsequent vertical growth rate for a 10 cm ingot is estimated to be about 0.05 to 0.5 cm/minute. The total time period from loading to extracting the grown crystal was about 24 hours. Throughout the growth, the top of the sealed ampoule was kept at 610°C to avoid loss of arsenic or excessive arsenic pressure which could cause an explosion. At the end of a run, the inner silica growth crucible was often found to be broken, but the GaAs ingot was usually intact. A typical ingot measured 1 cm in diameter, 10 cm in length and weighed approximately 40 grams. Shorter ingots and ingots as long as 17 cm, as shown in Figure 7, have been successfully produced by the vertical gradient freeze method. This success was beyond the original expectations.

Breakage of the silica crucible and frequent fracture of the ingots were due to GaAs adhering to the silica wall. Several crucibles were precoated on the inside with carbon by pyrolysis of acetone vapor passed into the silica tubes situated in the furnace at about 900°C. Ingots grown in carbonized crucibles were always intact and could be extracted from the silica container with ease. However, coated crucibles were not generally employed because of the probability of

carbon and silicon contamination. Carbon could come from the coating itself and silicon could come from the silica ampoule when the silicon dioxide is reduced by the carbon coating at high temperature.

B. Results and Discussion

1. Crystallinity and Perfection

The vertical gradient freeze method produced ingots of GaAs with few or no fractures. Figure 9 shows three typical ingots. In addition, much to our initial surprise, roughly the top half of each ingot was a single crystal or occasionally a bi-crystal. Apparently, nucleation occurred at the bottom of the crucible and growth proceeded upward with rapid grain selection, as shown by the longitudinal section of a typical ingot pictured in Figure 10. Of the forty or more ingots grown, in no case was the ingot more polycrystalline in the second half than in the first half. Theoretical investigation of heat transfer in the vertical gradient freeze growth system predicted that the freezing solid melt interface should be concave for approximately the first half of the 1 cm diameter, 10 cm long GaAs ingot and convex for the remaining half.[33] If one agrees with the basic hypothesis that a concave freezing interface yields polycrystalline growth while a slightly convex interface results in single crystal growth, then the theoretical prediction corresponds nicely with the observation on the transition from polycrystalline to single crystal

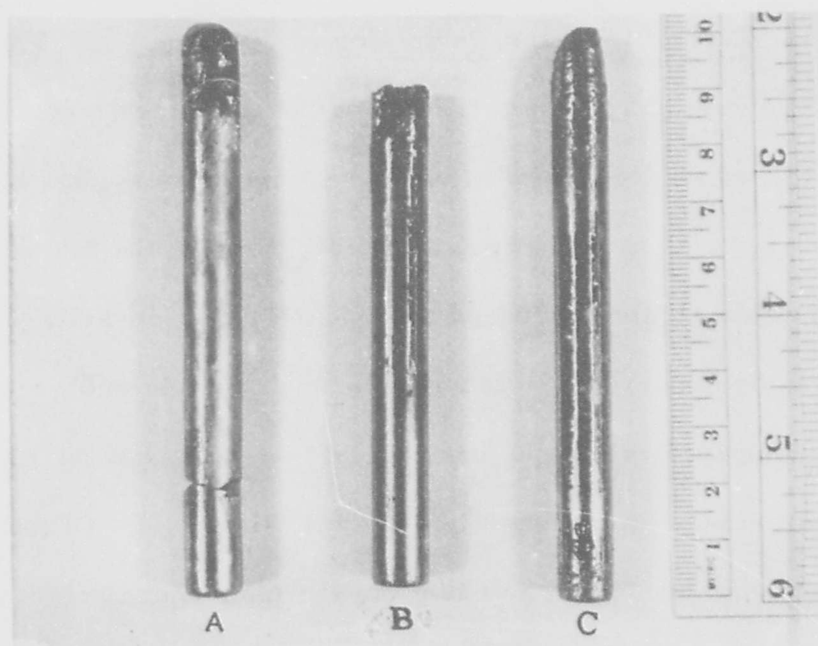

Figure 9: Three GaAs ingots grown by the vertical gradient freeze technique.
A. Ingot GF-30
B. Ingot GF-31
C. Ingot GF-32

Figure 10: A longitudinal section of a vertical gradient freeze grown ingot GF-3F (T-Top, B-Bottom) showing the grain selection during growth.

growth.

When pre-reacted GaAs was used as starting material, occasionally voids were found along the periphery of the ingot as shown in Figure 11. These were thought to be caused by incomplete settling of the molten GaAs and trapping of gas bubbles during melt-down. Frequently, the As-grown surfaces of the ingots were smooth and mirror-like. Occasionally, there was a central void or crack, as shown in Figure 11. Just as with the peripheral voids, this defect occurred at random parts of the ingots and its origin is not completely established. One hypothesis is that residual gas dissolved was released and trapped by the solidifying GaAs. Another hypothesis is that cracking resulted from the thermal strain associated with an extremely convex freezing surface. Dislocation densities in the cast crystals were in the range of 10^5 to $10^7/cm^2$.

The above mentioned defects make GaAs crystals grown by vertical gradient freezing unattractive for use as quality material. Perhaps improvements such as better temperature control and slower growth rates could overcome these problems. The greatest contribution of this growth method so far seems to be in providing cylindrical ingots of GaAs to be used as feed material for the travelling heater method and for floating zone melting, processes in which the crystallinity and perfection of the starting material are not of great importance.

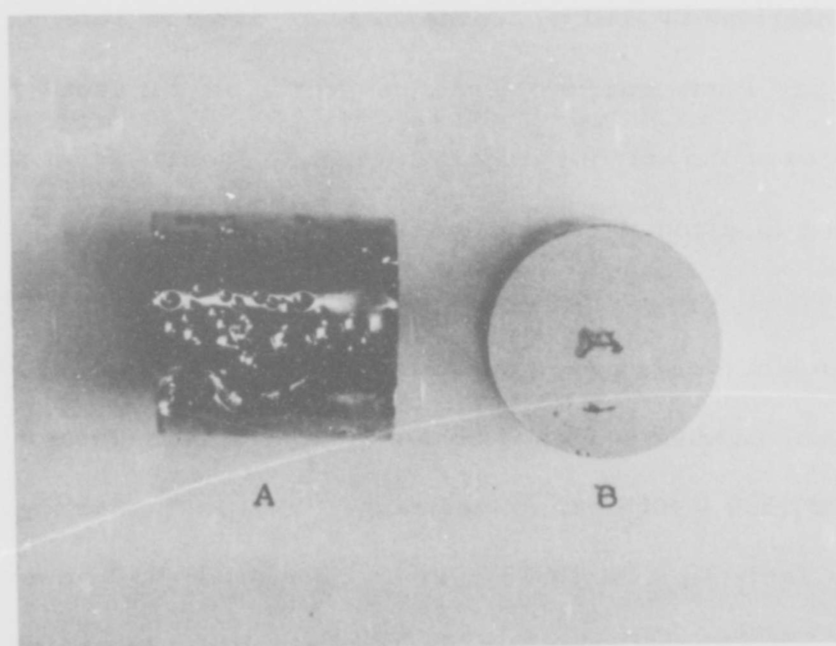

Figure 11: Defects in GaAs ingots cast by vertical gradient freeze technique.
A. Voids at periphery
B. Central void or crack

2. Electrical Properties

Impurity doping was not attempted in vertical gradient freeze growth of GaAs. In general, undoped crystals produced were n-type and of high conductivity, as shown in Table 3. Several crystals, grown from pre-reacted GaAs as well as from elemental Ga and As, were characterized by Hall measurements, as listed in Table 4. Two points are worth noticing: first, re-growth did not vastly alter the properties of the starting material; second, growths from pre-reacted GaAs (horizontal Bridgman or Czochralski) or elemental Ga and As produced crystals of similar properties. It appeared that vertical gradient freeze grown crystals typically had resistivities of 10^{-2} ohm-cm, carrier concentrations of $10^{17}/cm^3$ and electron mobilities of 1500 - 4000 cm^2/v-sec range. One particular ingot, GF-30 (see Table 3), exhibited a very high resistivity of almost 10^8 ohm-cm and an unmeasurably low electron mobility. A possible explanation of this special case is discussed in the following section.

3. Mass Spectrometry

For undoped crystals, a property of interest is the quantity of unintentional impurities present. Preliminary indications were given by spectrochemical analyses (results shown in Table 5) performed on four crystals, the electrical properties and growth conditions of which were listed previously in Table 3. Starting material for GF-1 was from a horizontal Bridgman ingot while feed for GF-25 was prepared

TABLE 3. TYPICAL GaAs INGOTS GROWN BY VERTICAL GRADIENT FREEZE METHOD

Ingot	Starting Material	Cooling Rate	Results
GF-1	Horizontal boat grown GaAs (undoped).	3°C/min.	N-type, low resistivity.
GF-25	Czochralski grown GaAs (undoped).	3°C/min.	N-type, low ρ.
GF-30	Six nines purity Ga + As.	0.3°C/min.	N-type, high ρ.
GF-31	Six nines purity Ga + As.	0.3°C/min.	N-type, low ρ.
GF-32	Czochralski grown undoped GaAs.	0.3°C/min.	N-type, low ρ.

TABLE 4. HALL MEASUREMENT RESULTS FOR GRADIENT FREEZE GaAs CRYSTALS GROWN FROM DIFFERENT STARTING MATERIALS

Crystal	Resistivity, ρ Ω-cm	Carrier Concentration cm^{-3}	Electron Mobility cm^2/volt-sec.
HBT-1 (Horizontal Bridgman)	0.0130	2.75×10^{17} n	1750
GF-1 (Grown from HBT-1)	0.0130	3.00×10^{17} n	1600
GF-1A (Grown from GF-1)	0.0100	1.67×10^{17} n	3747
GF-25 (Grown from Czochralski feed)	0.0336	1.00×10^{17} n	1890
GF-31 (Grown from Ga + As)	0.0164	1.53×10^{17} n	2500

TABLE 5. SPECTROCHEMICAL ANALYSES

Element	GF-1 wt.%	GF-25 wt.%	GF-30 wt.%	GF-31 wt.%
Ga	Rem.	Rem.	Rem.	Rem.
As	49	49	48	48
Si	nil	TR < 0.002	nil	nil
Mg	nil	TR < 0.0001	nil	nil
Cu	ND < 0.00002	0.000058	0.000041	0.000049
Ca	0.00022	0.00045	0.00021	0.00042
Li	ND < 0.005	ND < 0.005	ND < 0.005	ND < 0.005
Te	ND < 0.10	ND < 0.10	ND < 0.10	ND < 0.10
Other Elements	nil	nil	nil	nil

ND = not detected

TR = trace

using a liquid-seal Czochralski technique developed by Allred.[34] The higher impurity content of GF-25 is felt to reflect the greater handling of the pre-reacted material. GF-30 and GF-31 were grown from high purity Ga and As and show lower impurity contents. Comparison was made with results of analyses on horizontal Bridgman and Czochralski GaAs performed by the same facility (Pacific Spectrochemical Laboratory, Inc., Los Angeles). It appears that the Bridgman and Czochralski crystals contained more Cu and Ca and also detectable amounts of other impurities such as Si, Mg, Fe, Li and Al which were not detected in the gradient freeze crystals.

It is understood that spectrochemical analyses are not accurate. In GaAs, the detection limit in parts per million weight for the following impurities are given by Pacific Spectrochemical Lab. as: Si (20 ppmW), Ca (1 ppmW), Pb (100 ppmW) and Te (900 ppmW). Therefore, ingots GF-30 and GF-31 were sent for mass spectrometric analysis to Battelle Columbus Laboratories. The results are summarized in Table 6 together with those for a horizontal Bridgman crystal, HB-105, and a Czochralski crystal, CZ-169. It is clear that GF-30 was considerably "dirtier," a fact which was not suggested by the spectrochemical analysis results in the previous table (Table 5). Since all four crystals were grown starting from elemental Ga and As of identical purity, it appears that it is possible

TABLE 6. MASS SPECTROMETRIC ANALYSES OF GaAs GROWN BY GRADIENT FREEZE, HORIZONTAL BRIDGMAN AND LIQUID-SEAL CZOCHRALSKI TECHNIQUES

Element (ppm W)	GF-30	GF-31	HB-105	CZ-169
Li	< 0.003	< 0.003	< 0.003	< 0.003
Be	0.04	0.07	0.01	0.04
B	< 0.05	0.003	0.002	0.006
Mg	< 0.3	< 0.1	< 0.3	< 0.3
Al	< 0.1	< 0.04	< 0.07	< 0.07
Si	0.1	0.1	0.04	0.1
Cl	0.7	0.2	4	2
K	0.02	0.05	0.05	0.05
Ca	0.06	0.06	0.06	0.06
Cr	< 0.03	0.02	0.02	0.03
Mn	< 0.02	0.02	< 0.01	< 0.01
Fe	0.2	0.3	0.2	0.2
Co	0.03	0.02	< 0.01	< 0.01
Ni	0.1	0.06	0.03	0.02
Cu	0.6	0.04	0.02	0.04
Zn	0.2	0.1	0.1	0.2
Sn	0.1	< 0.06	< 0.06	< 0.06
Te	< 0.06	< 0.06	< 0.06	2
Pb	0.6	< 0.06	< 0.06	< 0.06

to grow vertical gradient freeze crystals, such as GF-31, which are of comparable purity to the other common GaAs growth methods. Notice that the gradient freeze grown crystals contained less Si, probably due to a shorter contact period with the silica crucibles. It is suspected that poor quality deionized water was used for preparing the GF-30 run as the resultant crystal contained considerably greater amounts of Mg, Cu and Pb, elements which are present in untreated or poorly treated water. This significantly less pure ingot GF-30 was later used as feed material for travelling heater method growth. The considerable change in impurity concentrations are discussed in Section B. 7 of Chapter IV.

4. Cathodoluminescence

The uniformity of the GaAs crystals was studied by the electron microprobe. The cathodoluminescence intensity is an indication of the minority carrier lifetime of the material at the site where the electron beam is focused. This is so because the radiation emitted from recombination is proportional to the excess minority carrier density, which in turn is proportional to the minority carrier lifetime. Thus the relative intensities at different points of a crystalline slice indicate the uniformity of the material.

A semi-elliptical (110) section of about 10 mm wide, 20 mm long was cut at 20° to the growth direction of the single crystal section of

GF-25. The surface was mechanically lapped down to 3200 grit silicon carbide and then chemically polished using "Mirrolite" (Materials Development Corporation, Los Angeles). Using an electron beam voltage of 40 KV and a sample current of 0.5μ A, the total cathodoluminescence intensity was measured at 2 mm intervals in the radial and longitudinal directions across the polished GaAs slice. The results, as plotted in Figure 12, show that the crystal was non-uniform.

Profile scans on a square area of about 10^{-3} cm^2 at the four corner points and the center of the slice were made. The resultant photomicrographs (Figure 13) strongly suggest cellular solidification, which would be expected from the very rapid freezing rates (~ 0.5 cm/minute for GF-25) employed. Cellular formation and its relation to interface breakdown due to constitutional supercooling are discussed in Reference [35]. The linear scan of 300 μ at the central point also revealed the quantitative inhomogeneity at this particular locality.

From the results discussed in the previous sections, it is quite clear that the vertical gradient freeze grown GaAs crystals as grown herein leave much to be desired. With the exception of purity, improvements on other properties of the GaAs would have to be made to render it desirable for use as an electronic material. This could

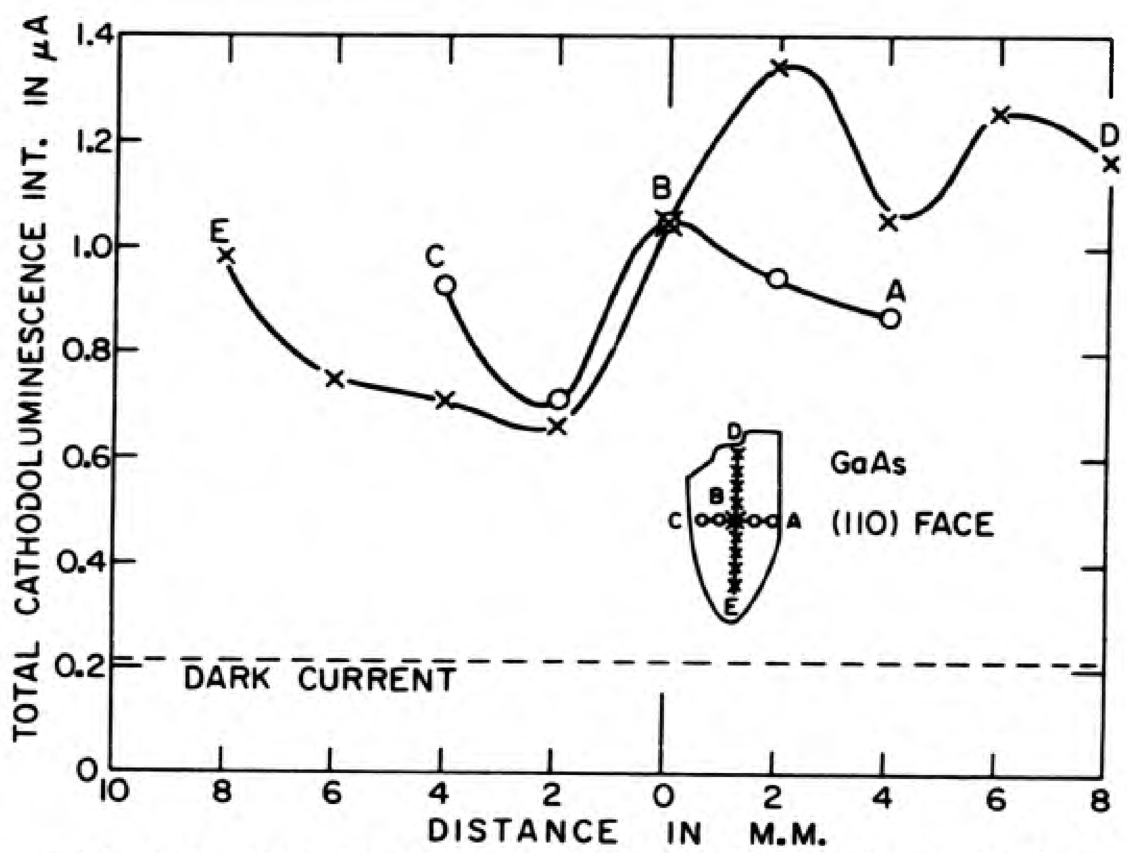

Figure 12: Cathodoluminescence intensities at 2mm intervals in scans across (110) face of vertical gradient freeze grown GaAs crystal GF-25.

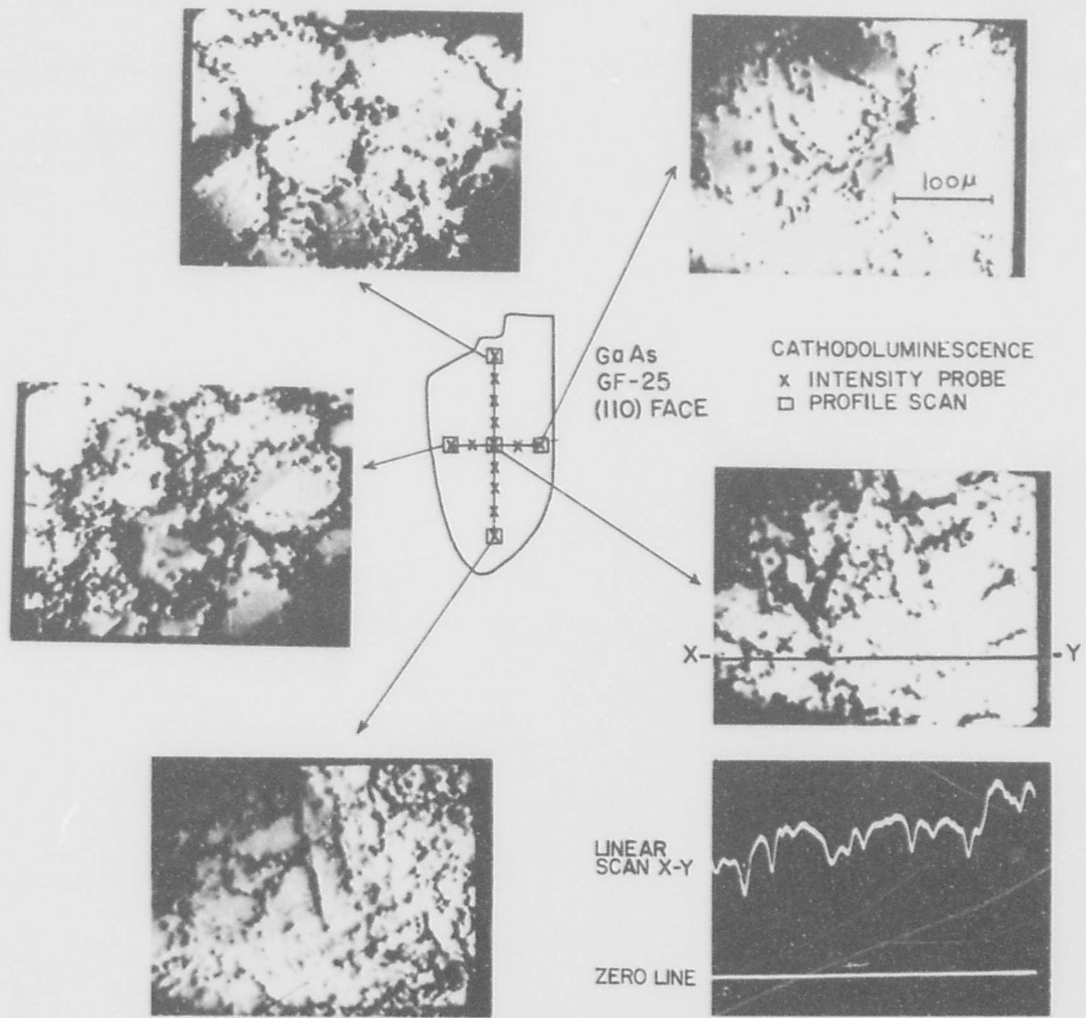

FIGURE 13. CATHODOLUMINESCENCE OF VERTICAL GRADIENT FREEZE GROWN GaAs

be partially achieved by having better temperature control and slower cooling rates. However, as emphasized previously, the main interest here was in producing cylindrical GaAs feed material to be used for THM growth. This objective was successfully accomplished.

Chapter IV

TRAVELLING HEATER METHOD GROWTH OF GaAs

The major portion of our research investigation was on the travelling heater method solution growth of GaAs. The THM configuration is similar to that of zone melting except that a solution zone replaces the molten zone which traverses through the solid feed. This chapter describes in detail the development of the apparatus and experimental procedure for growth of GaAs. The results of the crystal growth and the characterization performed are also presented here.

A. Experimental

1. Original Apparatus

The first apparatus build was based on the bare minimum technical requirements for travelling heater method growth of GaAs. The approximately 1 cm diameter by 1 cm long heater was made of gage 22 Kanthal wire wound on a grooved, 1 foot long alundum furnace core. The 110 volt line input was regulated by a 120 VA constant voltage transformer (from Sola Electric Company) and the power input to the heater was controlled by a 110 volt variable autotransformer (from Superior Electric Company). The heater was situated at the center of a larger (10 cm I.D.) Pyrex tube which was secured between two

asbestos boards with four steel rods at the corners. Fibrefrax served as thermal insulation. Four 4.5 to 10 pound capacity "Met-L-Flex" shock absorbers (from Robinson Aviation, Inc., Teterboro, New Jersey) were situated at the four corners to isolate the apparatus from disturbance and vibration. Lowering rates in the range of several mm per day were provided by a low-speed synchronous motor (Bristol Motors, Old Saybrook, Conn.) in conjunction with a miniature speed reducer (Metron Instruments, Inc., Denver, Colorado). The THM growth ampoule containing the GaAs feed and seed and the Ga zone was lowered by a gage 30 nichrome wire from a pulley connected to the reducer.

A photograph of the simple setup is shown in Figure 14. The actual growth unit (i.e., excluding the power supply components) cost less than $50. This economical factor could override disadvantages of THM growth, such as the long growth time and small product crystals, and help make the growth method attractive.

2. Improved Apparatus

Although the first version of the apparatus contained all of the essential features, it suffered from several serious defects. The main problem was that the Kanthal wire heater could operate at 1000°C for only three to four weeks, which was only long enough for two to three THM runs, before it burned out and had to be replaced. The

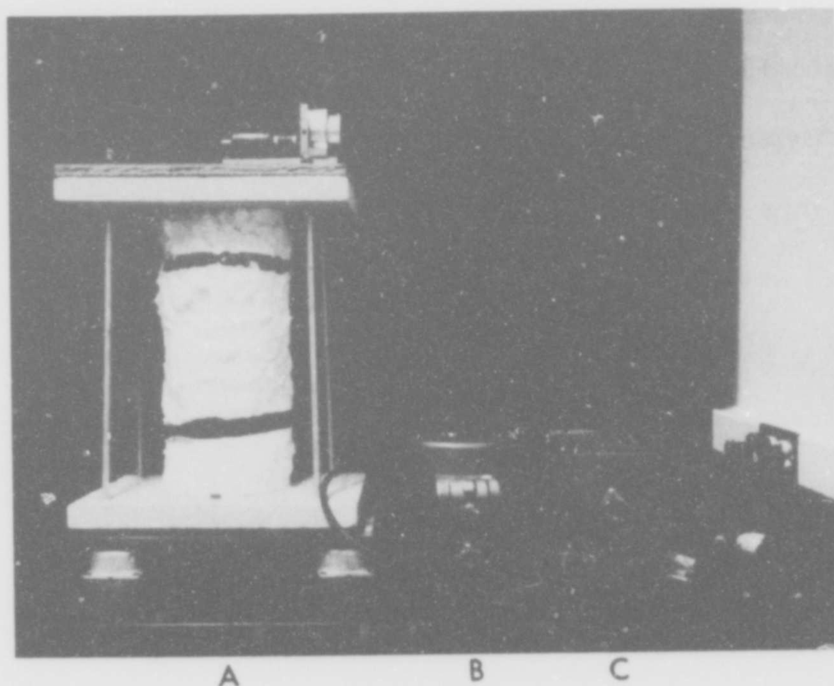

Figure 14: Original apparatus for THM growth.
A. Furnace
B. 110 volt variable autotransformer
C. Sola constant voltage transformer

opaque alundum furnace core was not convenient for loading and positioning of the growth ampoule because of lack of visibility. Another concern was that the transformer combination was not adequate for supplying a constant voltage to the heater.

The first problem was solved by replacing the Kanthal heater element with Pt - 10% Rh wire, which prolonged the heater life considerably (typically to two to three months), so that the interruption of growth runs due to heater failure was a rare occurrence. The noble metal was also capable of producing a furnace temperature of up to 1200°C without much difficulty, which was not possible with Kanthal wire. Visibility of the zone was provided by winding the heater wire on a transparent 13 mm I.D., 1 foot long silica tubing. Bubbled alumina replaced Fibrefrax as the insulating material and provided a more symmetrical and repeatable thermal surrounding for the heater. It could also be easily added to or drained from the outer Pyrex tube which contained the insulation. This final improved version of the apparatus, as shown in Figure 15, was used for most of the THM crystal growth runs described in this dissertation report. Even with the use of Pt - 10% Rh wire, the cost of constructing such a model was still relatively low because the amount of wire needed was small and the labor required was also not excessive.

3. Sample Preparation

A typical GaAs growth ampoule prepared for a THM run is

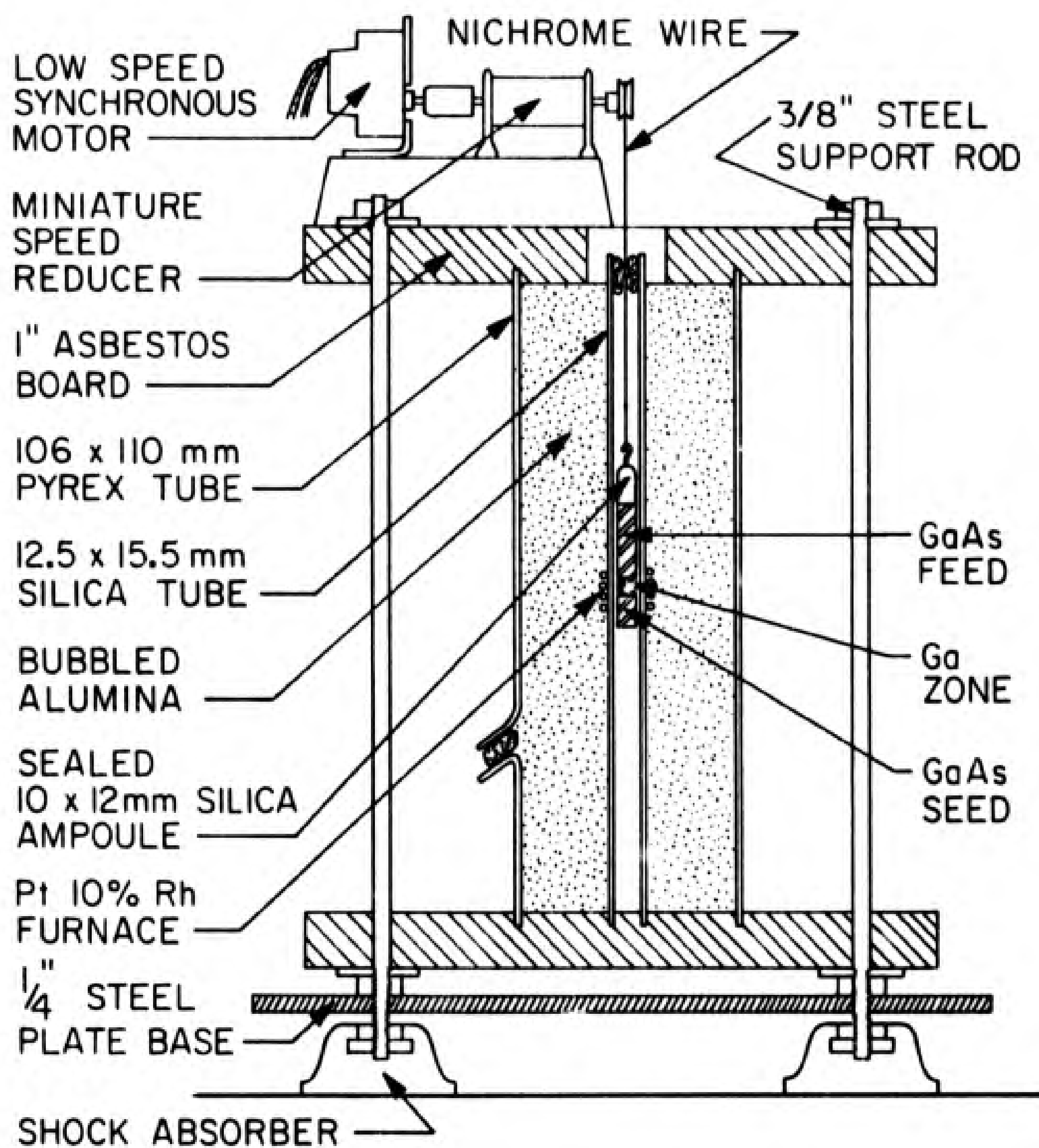

Figure 15: Diagram of the travelling heater apparatus for GaAs crystal growth by THM.

shown in Figure 16. It consisted of a short single crystal GaAs seed and a longer ingot of polycrystalline GaAs with a zone of pure Ga sandwiched in between. The three parts were contained in a 10 mm I.D. flat-bottom evacuated silica ampoule about 10 cm long.

Cylindrical ingots of GaAs which fit snugly into the 10 mm I.D. crucible were needed as feed material. A close fit was necessary for THM growth, otherwise the amount of feed dissolved was considerably less than that necessary for deposition onto the seed and the volume difference gradually built up and eventually caused the Ga zone to detach from the feed, stopping the growth. This occurred in some early runs. For the initial set of experiments, rectangular slices of GaAs were cut from horizontal Bridgman grown ingots. The individual slice was mounted on a specially designed grinding tool and was ground down to the 1 cm diameter with a 1/2 inch thick silicon carbide grinding wheel. This tedious and wasteful process of preparing feed material was later abandoned in favor of casting GaAs ingots of the same diameter by the vertical gradient freeze method described in the previous chapter. However, the short section of single crystal seed with specific orientation still had to be ground from a Czochralski grown single crystal because it could not be readily grown by the gradient freeze technique. Both seed and feed crystals had to fit loosely enough to slide into place, but

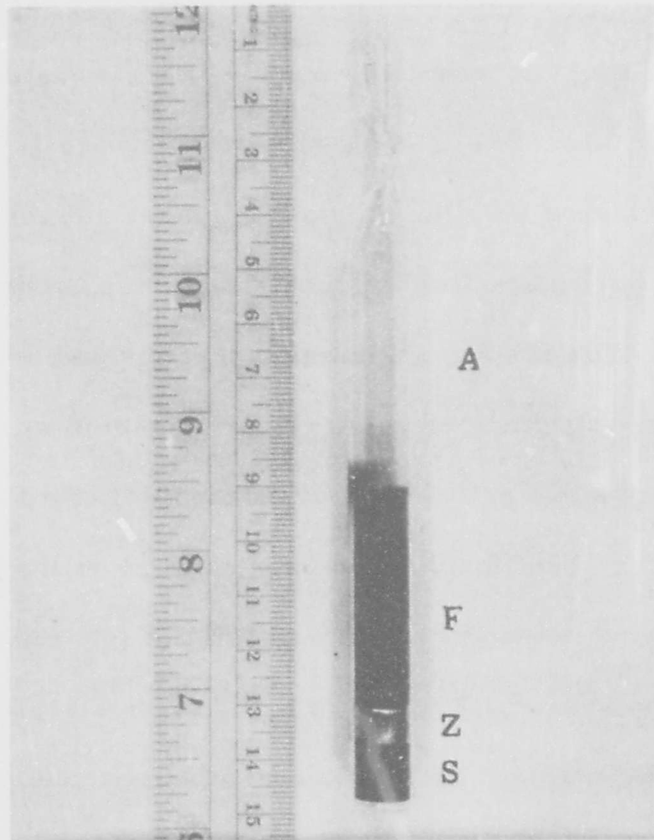

Figure 16: A typical assembled THM fused silica ampoule (A) showing the GaAs feed (F) the Ga Zone (Z) and the single crystal seed (S).

not so loosely that liquid Ga would readily flow around them.

The presence of a liquid zone of Ga between two fitted sections of GaAs presented a host of problems during evacuation and loading of the ampoule. All too frequently the liquid metal was sucked around the close-fitting feed rod when the ampoule was evacuated, rendering the ampoule unusable. Even when evacuation down to 1-5 micron Hg pressure was achieved with the Ga zone in place, any disturbance to the ampoule in loading and handling could force the Ga down around the seed GaAs. This happened a number of times and new ampoules had to be prepared for replacement. Many problems were encountered even in placing a desired amount of the liquid Ga into the ampoule before evacuation. The liquid Ga frequently stuck to the quartz wall or splashed around the seed when it was dripped into the ampoule from the container bottle. The use of a rod or small tube to guide the flow of the Ga was not considered desirable because of the contamination likely to be introduced.

Several possible solutions to these difficulties were tried and the one finally adopted was simple and convenient. Liquid Ga droplets were extracted from the original container and placed on chemically clean glassine power paper (from Eli Lilly and Company, Indianapolis, Indiana). They were cooled slightly and solidified into droplets of different sizes and weight. Any amount of the metal could then be

weighed and readily dropped into the crucible without any of the host of problems connected with the placing of liquid Ga. The solid droplets of Ga were easily melted and the proper Ga zone configuration assumed after the ampoule was evacuated, sealed and loaded into the furnace. This perfected technique of THM and ampoule preparation was found to be most efficient and convenient. The only drawback was the possibility of additional contamination during preparation of the solid Ga droplets. Fewer difficulties were encountered in preparing ampoules for self-seeded growth, in which the Ga zone was situated at the bottom of the crucible. As a whole, the proper preparation of THM ampoules was found to be a non-trivial matter necessitating the skill and techniques described in this section. A step-by-step summary is presented below:

1. A cylindrical feed rod of GaAs was ground from a horizontal Bridgman crystal or grown by the vertical gradient freeze technique.

2. A single crystal seed of a specific orientation was ground from a GaAs crystal grown by the liquid-seal Czochralski technique.

3. Liquid Ga was dripped from the container and solidified into droplets on chemically clean paper.

4. The single crystal seed, the Ga droplets and then the close-fitting feed rod were placed into a 10 mm I.D., flat bottom silica tube.

5. The ampoule was evacuated down to 1-5 μ Hg pressure and sealed to a total length of 10 cm.

6. The Ga droplets were melted to form a Ga zone. After the proper seed-zone-feed THM configuration was assumed the ampoule was ready for loading and growth.

4. Experimental Procedure

After the THM ampoule was properly prepared, several other precautions were necessary in loading and growth to ensure that the run would be successful. The ampoule should be able to be lowered through the heater with a small clearance. Frequently, lack of uniformity of the diameter and length of the heater tube, or the accidental introduction of small bubbled alumina particles, would arrest the motion of the lowering ampoule and terminate an otherwise successful run. The proper positioning of the Ga zone relative to the heater was critically important and this was made possible by viewing through the initially empty silica furnace tube. Locating the zone too high relative to the heater was responsible for the complete dissolution of the seed and the resultant failure in most of the earliest runs.

When all the proper steps were taken and the ampoule correctly loaded, the bubbled alumina insulation was added and the outside of the Pyrex tube was protected and insulated from the room air drafts with a sheet of Fibrefrax wrapped around it. The voltage required to

produce the desired heater temperature was then turned on instantaneously. The furnace was left for 10-12 hours for the steady state temperature to be attained and then the lowering motor-reducer mechanism was activated to begin the growth run. No attention or further work was necessary for the entire growth period of one or two weeks. At the end of that period, the heater was turned off and the ampoule retrieved after the system had cooled. The grown crystal was then extracted by using a small hammer to carefully break off the silica wall surrounding it, usually without fracturing the GaAs in the process. The crystal was put into warm dilute hydrochloric acid to dissolve any adhering elemental Ga.

While growing THM crystals, considerable investigation was done on the relationships between the steady state positions and lengths of the GaAs seed, the Ga zone and the GaAs feed relation to the heater. For such studies, the loaded ampoule was allowed to come to thermal equilibrium and then the power was abruptly shut off in order to quench the ampoule. The bubbled alumina was later drained below the heater, exposing the ampoule. The positions of the upper and lower solid-liquid interfaces of the Ga zone relative to the heater were observed and recorded through a stereo-microscope (Bausch and Lomb) located outside the Pyrex furnace tube. The setup is shown in Figure 17. The photograph of a quenched Ga zone

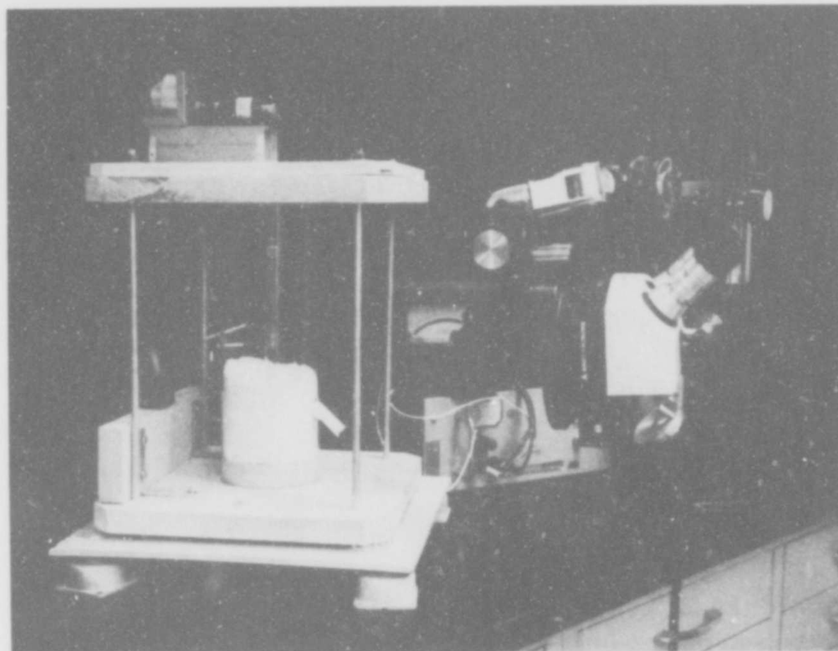

Figure 17. Photograph of travelling heater III-V growth apparatus partially filled with bubbled alumina.

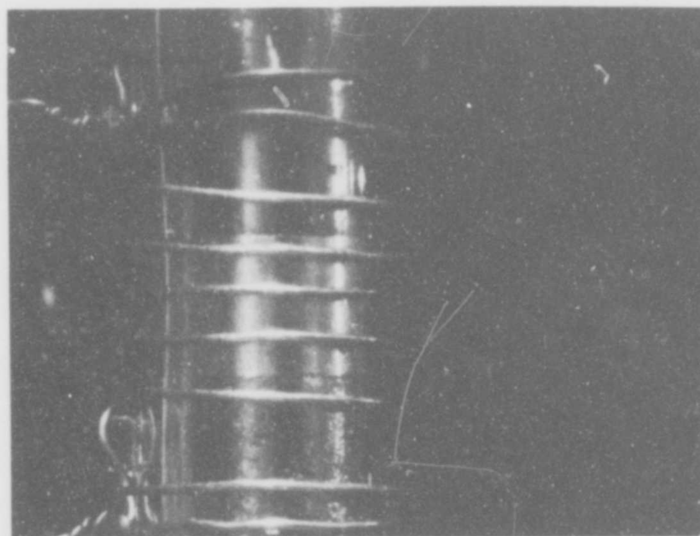

Figure 18: Photograph of quenched Ga zone.

shown in Figure 18 was taken with a Polaroid camera attached to the microscope.

The assumption that the tube position did not change appreciably during the cool-down to room temperature is reasonable. The linear expansion coefficient of quartz glass is of the order of 5.8×10^{-7} cm/^{o}C[36] for the temperature range of 16-1000°C. The nichrome wire (expansion coefficient approximately 1.4×10^{-5} cm/^{o}C) used for hanging the ampoule was usually located 5-8 cm away from the heater zone at a temperature of below 300°C. Therefore the maximum position change due to contraction of the silica ampoule and the nichrome wire was on the order of 10^{-3} cm, an error which can be neglected.

Since opaque insulation as above does not permit in-situ observation of the interface position, an investigation was made of the use of a silica tube coated on the inside with a semi-transparent gold film to act as insulation by reflecting most of the infrared radiation while at the same time allowing visual monitoring of the growth. The idea was abandoned when it was found that this provided poor thermal insulation, the visibility was poor and the convection currents created in the air space between the tubes caused considerable fluctuation in the heater temperature. Consequently, the interface positions and the lengths of the crystal and feed were measured by the procedure described earlier.

B. Results and Discussions

1. Preliminary Growth Runs

At the beginning, there was insufficient information in the literature on THM GaAs growth which could provide guidelines for this research investigation. About a dozen exploratory runs were made using the original THM growth apparatus described earlier in Section A. 1. There was no systematic control of the lengths of seed and feed GaAs, Ga zone or the heater temperature and lowering rate used. The growth details and the results of these preliminary growth runs are listed in Table 7. For the first six growth runs, the Ga zone was placed at approximately the center of the 1 cm long heater, the exact location was not visible because of the opaque aluminum furnace tube used. Consequently, it was discovered that the short sections of 0.3-0.6 cm of single crystal seeds were completely dissolved and that subsequent growths were actually by self-seeding. Two such ingots (Figures 19 and 20), from THM No. 2 and No. 3, were found to contain large grains and twins, but no Ga inclusions. Tries were made with self-seeded growth from different shaped crucibles. The intended grain selection which should lead to single crystal growth did not materialize and the method was abandoned in favor of seeded growth.

Some insight into the requirements for good growth was gained from the early failures. Longer seed sections were used and the Ga

TABLE 7. SUMMARY OF EARLY TRAVELLING HEATER EXPERIMENTS ON GaAs (JULY 1970-JUNE 1971)

Run THM No.	Heater Temp.	Original Seed length (cm)	Original Ga Zone length (cm)	Original Feed length (cm)	Lowering Rate (mm/day)	Results
1	1000°C	0.6 <111> direction	0.3	4.2	4.7	Seed was dissolved. Growth started by self-seeding and grains grew inwards towards center where Ga inclusions were found. Total growth about 3.5 cm.
2	1010°C	0.6 <111>	1.0	2.5	4.7	Seed dissolved. Self-seeded poly-crystal measured 2.5 cm with large twinned crystals several mm in center. Evidence of nucleation near wall. No Ga inclusions.
3	1025°C	0.6 <111>	1.0	2.5	5.0	Seed dissolved. Large grain of 4 mm x 10 mm in center with polycrystalline nucleation near ampoule wall. No Ga inclusions. Total length 2.3 cm.
4	1055°C	0.3 <111>	1.0	2.0	5.0	Seed dissolved. Grains nucleated at bottom of ampoule and propagated along the length for 2.0 cm polycrystalline growth. No Ga inclusions.

TABLE 7. (Continued)

Run THM No.	Heater Temp.	Original Seed length (cm)	Original Ga Zone length (cm)	Original Feed length (cm)	Lowering Rate (mm/day)	Results
6	1000°C	0.3 <111>	0.8	2.5	1.0	Growth was quenched after 1 cm growth from self-seeding (seed dissolved). The quenched solid-liquid interface was convex and the ingot showed grain selection.
7	950°C	1.3 <110>	0.8	2.5	2.0	Successfully seeded. 90% of the 1.5 cm grown was single crystal of <110> direction.
9	935°C	2.0 <110>	0.8	1.5	5.0	Successfully seeded and grown 1.0 cm. Ingot began single but rapidly became polycrystalline due to the fast growth rate.
11	950°C	0.8 <110>	0.8	1.0	3.0	Successfully seeded and grown 0.8 cm. Ingot was in <110> direction and nearly completely single crystal.

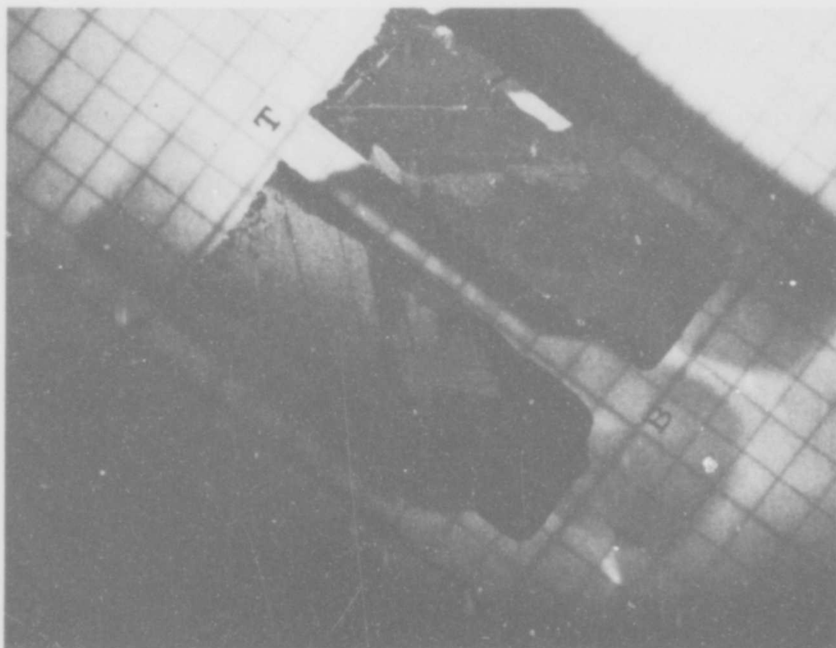

Figure 19: Longitudinal cross-section of THM-2 grown by self-seeding (T-Top, B-Bottom).

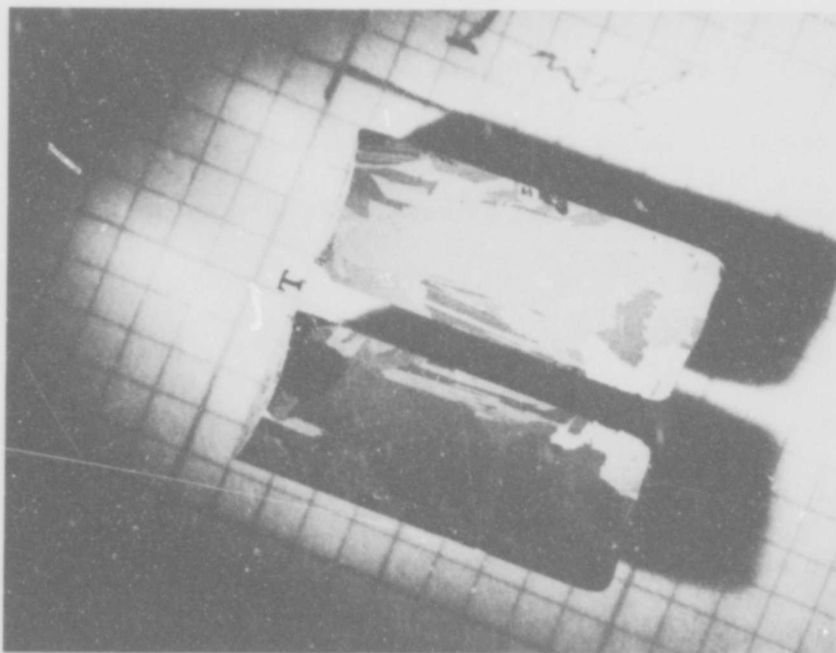

Figure 20: Longitudinal cross-section of THM-3 grown by self seeding (T-Top, B-Bottom).

zones were located slightly lower than the heater to prevent excessive dissolution of the seed. The lowering rate was reduced to 2-3 mm/day instead of the 5 mm/day used earlier. Crystals in the resultant runs were successfully seeded. Figure 21 shows cross-sectional slices of crystal THM-11, seeded in the ⟨110⟩ direction. The heater temperature was 950°C and the lowering rate was 3 mm/day. A schematic of a THM GaAs ampoule and its location relative to the heater temperature profile is shown in Figure 22.

Some preliminary characterization of the crystals were performed. The seed crystal of THM No. 9 contained about 10^6 etch pits/cm^2 while a ⟨111⟩ grain grown from this seed had areas with an etch pit density in the 10^2-10^3/cm^2 range (Figure 23(a) and (b)). Etching was done at 60°C for 10 minutes in Schell's etch (1 HNO_3 : $3H_2O$).

Electron microprobe studies were made on a polycrystalline slice cut from THM No. 4. A cathodoluminescence profile scan over an area (about 10^{-3} cm^2) which contained different grains and grain boundaries is shown in Figure 24. Notice that the grains were of different but uniform brightness, which could be due to different contents of impurities and imperfections in the grains. There was no evidence of cellular formation as shown in the cathodoluminescence scan on a vertical gradient freeze grown crystal described in

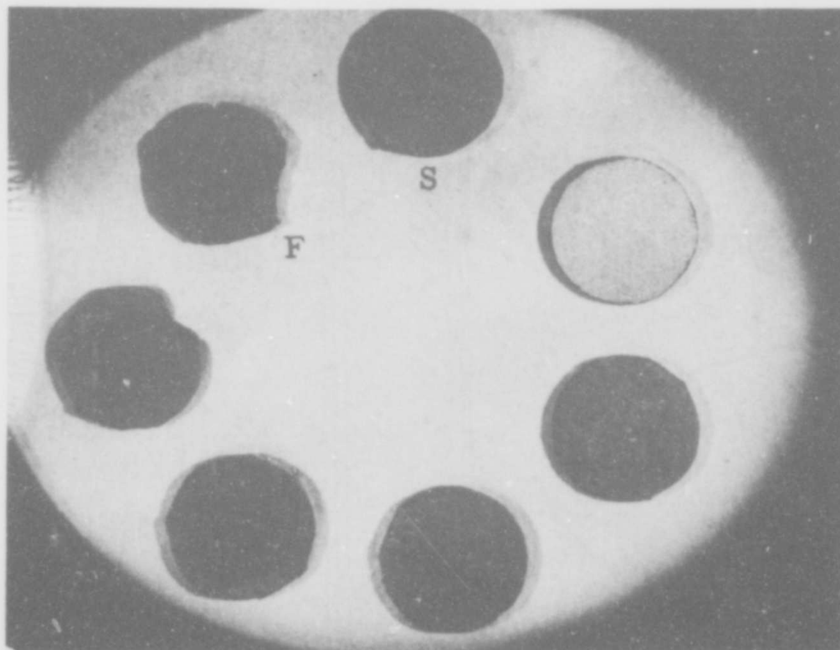

Figure 21: Cross sections of THM-11 taken perpendicular to the 110 seeding direction (S-seed slice, F-final slice).

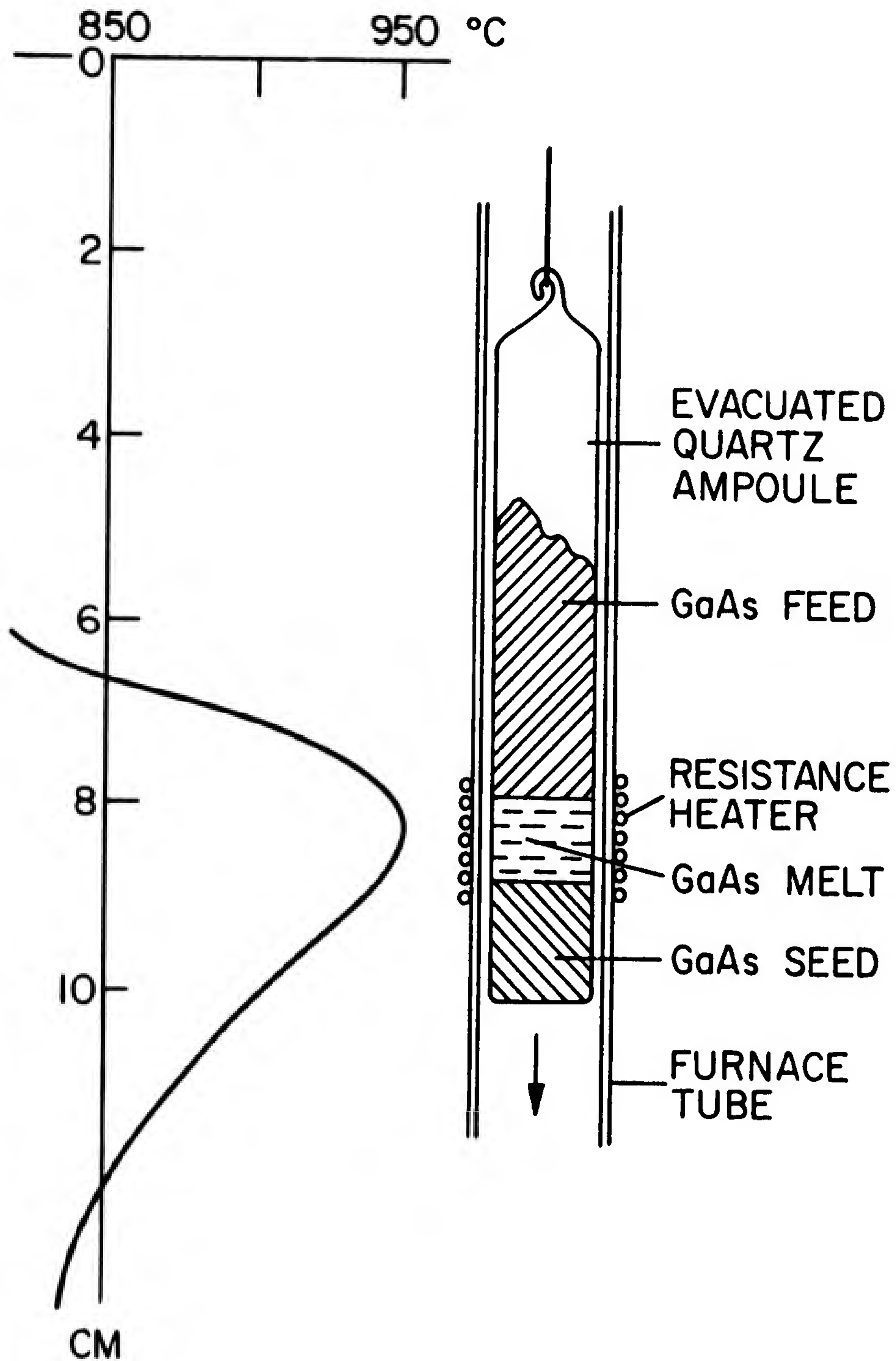

Figure 22: Diagram of THM GaAs ampoule relative to temperature profile in empty furnace.

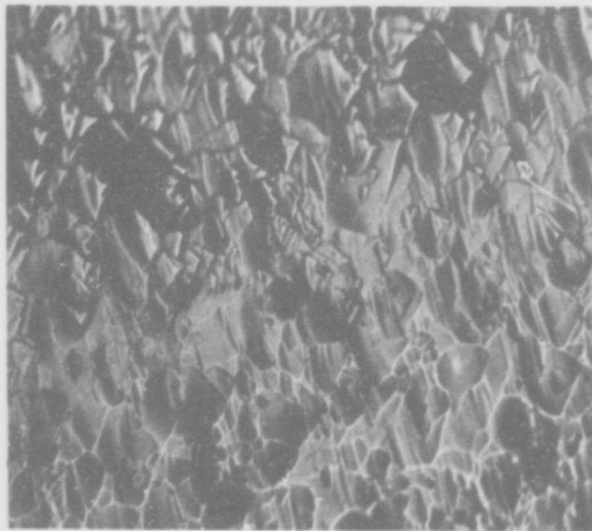

a. Melt grown seed

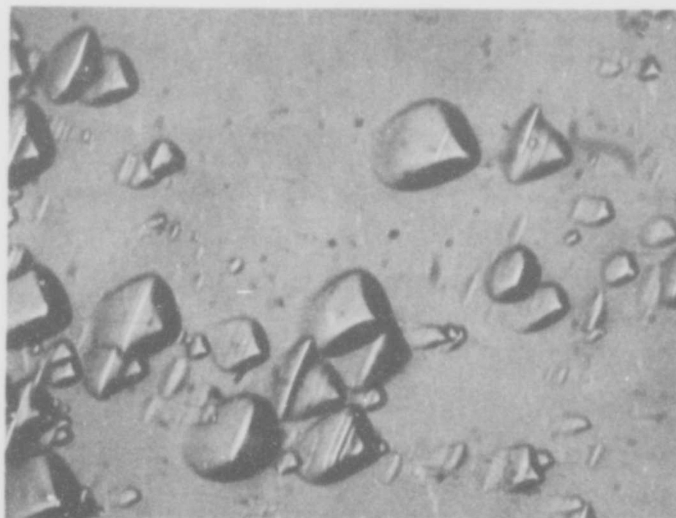

b. THM grown crystal

Figure 23: (111)Ga etch pits of THM-9

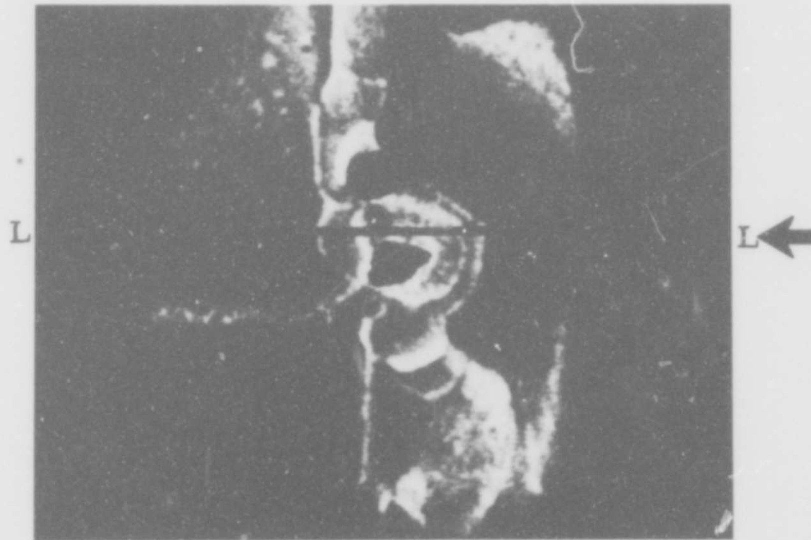

Figure 24: The cathodoluminescence profile scan of a polycrystalline slice from THM-4 showing the grains and grain boundaries. Area covered was $\sim 10^{-3} cm^2$.

Chapter 2, Section C4. This indicates that the slower growth rates in THM growth produced crystals free of some of the problems in vertical gradient freeze melt growth of GaAs. Ingot THM No. 4 was grown with a Te doping of about 5×10^{19} atoms/cc in the initial Ga zone. The Te X-ray spectrum scan across line L-L of Figure 24 is shown in Figure 25. The concentration of Te was approximately 1×10^{17} atoms/cc. Figure 26 shows the cathodoluminescence intensity from the linear scan L-L.

After the preliminary set of THM experiments, it was apparent that there should be a systematic study of the role and influence of different parameters such as seed, feed and zone lengths, heater temperature and lowering rate on the quality of the THM grown crystals. As a result of such investigation, a set of "optimal conditions" for good single crystal could then be determined for use in subsequent growths. The crystals grown under the controlled conditions could then be analyzed and characterized by the different methods and the results would then be meaningful. Such a planned sequence of investigation was successfully carried out, with the details and results discussed in the following sections of this chapter.

2. <u>Influence of Feed and Crystal Lengths</u>

In preparing an ampoule for THM growth, the lengths of the seed and feed sections were often chosen arbitrarily or based on

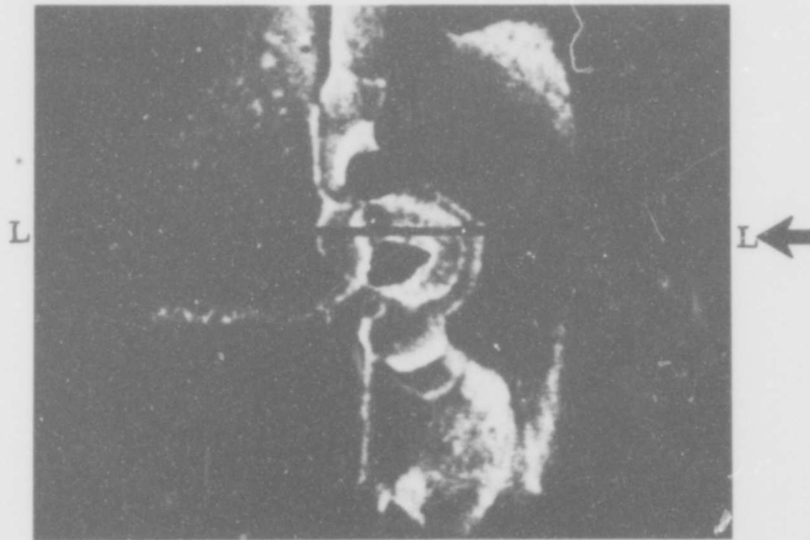

Figure 24: The cathodoluminescence profile scan of a polycrystalline slice from THM-4 showing the grains and grain boundaries. Area covered was $\sim 10^{-3} cm^2$.

availability of the material. Ampoules with 0.55 cm initial Ga zone length, 3.8 cm initial GaAs feed length and different initial GaAs seed lengths were brought to steady state at a heater temperature of 850°C and then quenched. The resultant GaAs-Ga interfaces positions and shapes were recorded and plotted in Figure 27. Changes in seed length had no influence for lengths beyond about 1 cm.

Similar experiments were performed at 980°C heater temperature, with the initial seed lengths all 1.0 cm, the initial zone lengths all 0.55 cm, and a variation in feed lengths. The results, plotted in Figure 28, show that it is undesirable to use a feed which is less than twice the diameter, because this results in deposition of GaAs onto the seed even before lowering is commenced. Such growth is undesirable because it is uncontrolled.

From the above, it became obvious that the position of the zone was strongly dependent on the lengths of the crystalline sections above and below it. Starting with Ga zone lengths of 0.55 cm and 1.55 cm (the choice of the dimensions will be discussed in the next section), different lengths of crystals were grown and quenched. The interface positions and shapes were then determined. An important phenomenon in THM growth became apparent when the results, as shown in Figures 29 and 30, were examined. It was found that, for both Ga zone lengths, the positions of the interfaces shifted relative

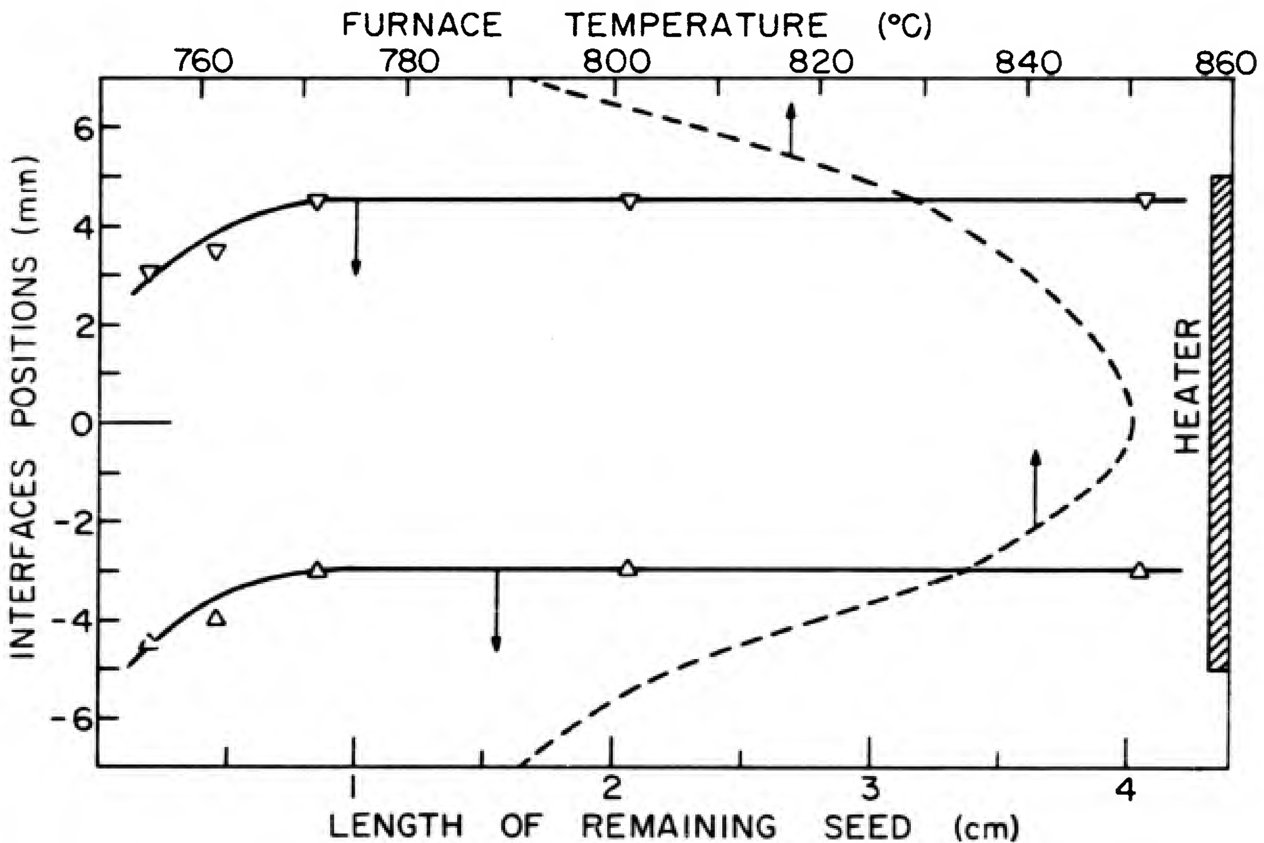

Figure 27: Steady state positions of the GaAs-Ga interfaces relative to the heater as a function of the remaining length of the crystal below the solvent zone in the travelling heater method apparatus with zero travel rate and a 3.8 am initial feed length above zone. Initial Ga zone length was 0.55 cm, maximum heater temperature was 850°C.

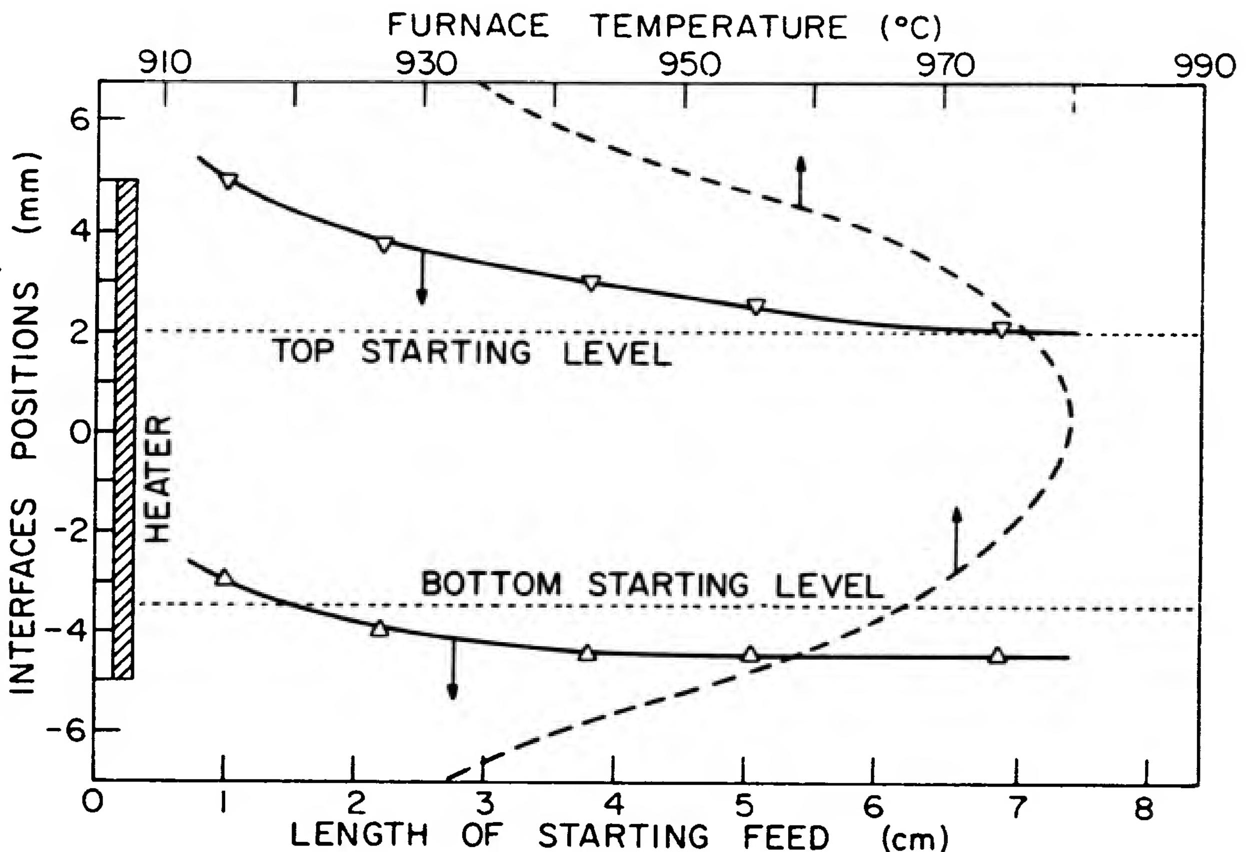

Figure 28: Steady state positions of the GaAs-Ga interfaces relative to the heater as a function of the initial feed length above the solvent zone in the travelling heater method apparatus with zero travel rate and 1.0 cm intial seed length below zone. Initial Ga zone length was 0.55 cm, maximum heater temperature was 980°C.

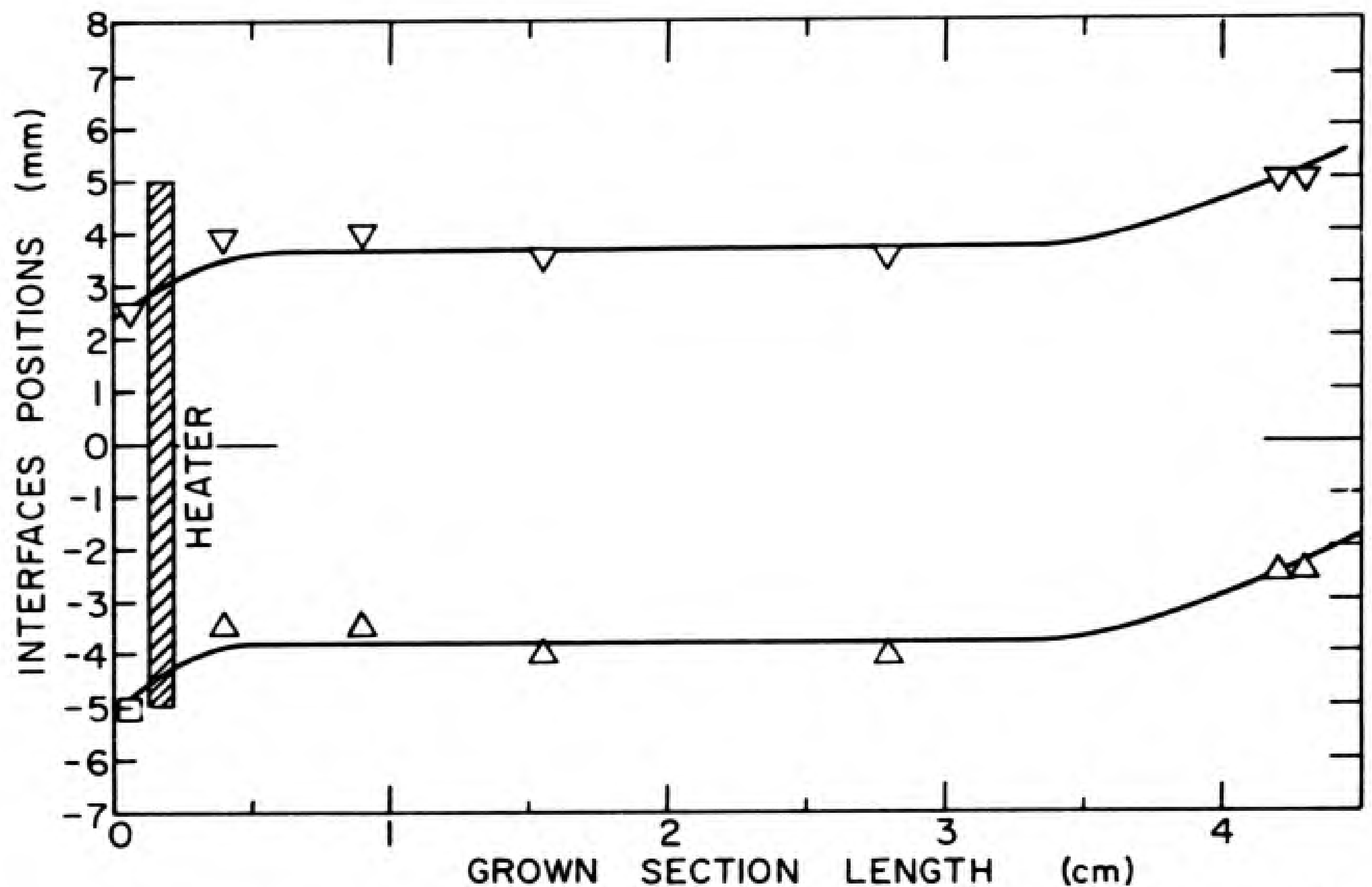

Figure 29: Steady state positions of the GaAs-Ga interfaces as a function of the length of solid below the zone. Initial Ga zone length was 0.55 cm.

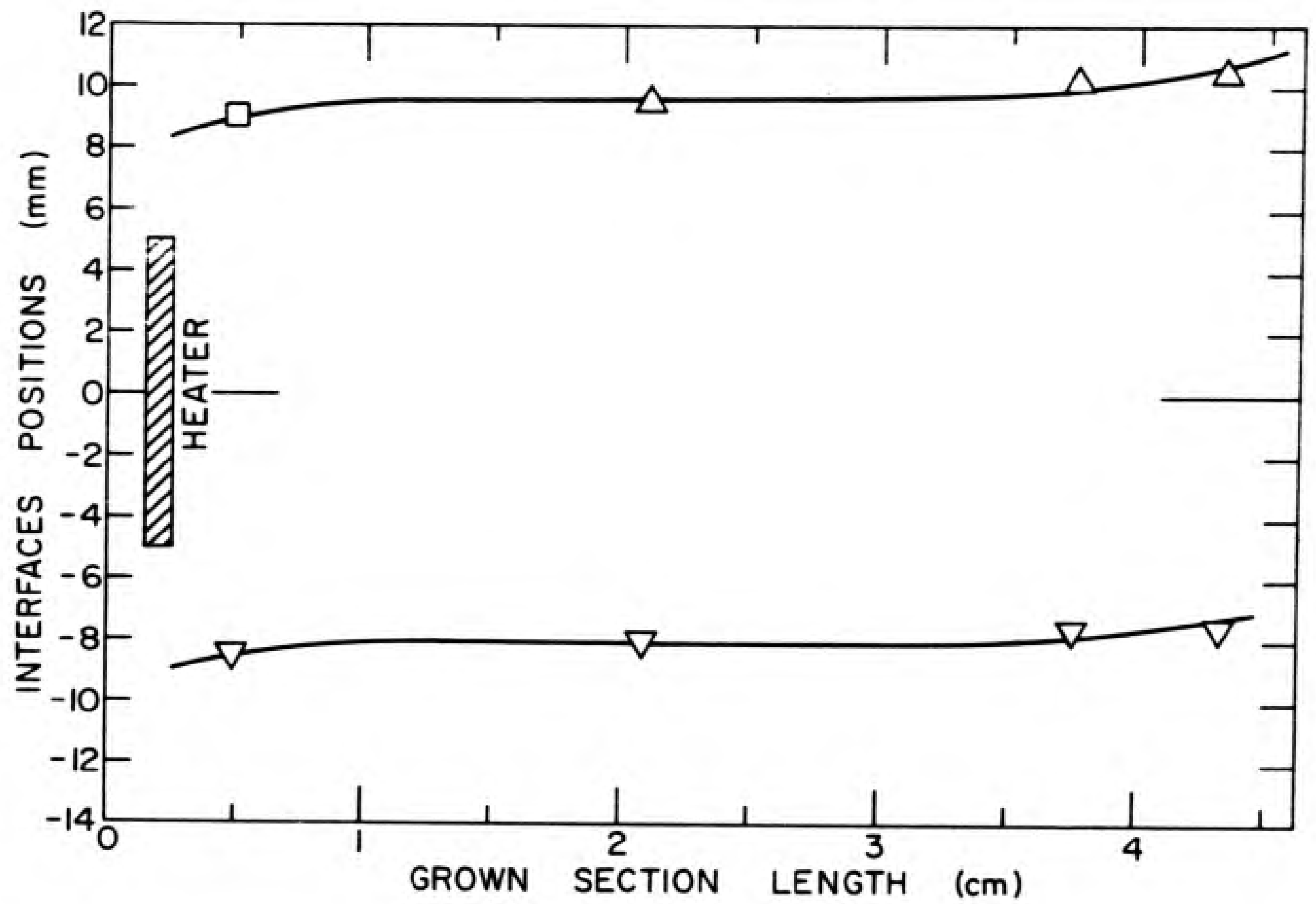

Figure 30: Steady state positions of the GaAs-Ga interfaces as a function of the length of solid below the zone. Initial Ga zone length was 1.55 cm.

to the heater as growth took place because of the gradual change in heat transfer conditions. This upward shift of the zone was especially significant at the beginning and the end of the growth runs, producing an accelerated growth which should be taken into consideration in THM growth. Therefore, only during the middle portion of the growth run was the growth rate equal to the lowering rate of the ampoule. One could interpret this to mean that the initial growth (unless a sizeable seed was used) and the final growth of a THM crystal occur at accelerated rates which could result in problems in uniformity and other properties of the crystal. If a growth run were performed at close to the critical lowering rate for inclusion-free single crystal growth, such accelerated growth would cause problems. In the case of growth of mixed compounds where the quality and composition of the growing crystals are especially sensitive to the lowering rate and other growth conditions, such deviations in growth rates are definitely undesirable. One could compensate for this effect by programming the lowering rate, rather than leaving it constant.

3. Influence of Zone Length and Interface Shape

In this study, it was discovered that a very important parameter influencing the crystallinity and perfection of the THM grown crystal is the length of the Ga zone relative to the heater length, a parameter

which has often been neglected. The heater length used throughout was 1 cm with a 1 cm diameter ampoule--both dimensions were standard for all experiments. A 1 cm seed and a 3.8 cm feed section was used for the present experiments. The steady state length and position of the Ga zone at a heater temperature of 980°C were determined for 0.3, 0.55, 0.7, 1.0 and 1.55 cm initial Ga zone lengths, as shown in Figure 31. (These values actually represent averages, inasmuch as the interfaces were frequently curved, as described below.) The resultant zones were about 1.5 to 2.5 mm larger than the initial Ga lengths due to dissolution of GaAs and the consequent expansion of the metallic zone at high temperatures. It might be expected that the increase in solution zone size should be directly proportional to the amount of solvent. This was not the case because as the zone size was increased the interfaces moved farther and farther away from the center of the heater thus lowering the interfaces temperature and the GaAs solubility.

The qualitative shapes (convex, planar, or concave with respect to the solid) of the interfaces are also indicated in Figure 31. It should be realized that the 1.0 cm physical length of the heater was actually smaller than its "effective length," which could be defined as the length over which heat flowed into the ampoule. The effective heater length should be larger than the physical length by about twice

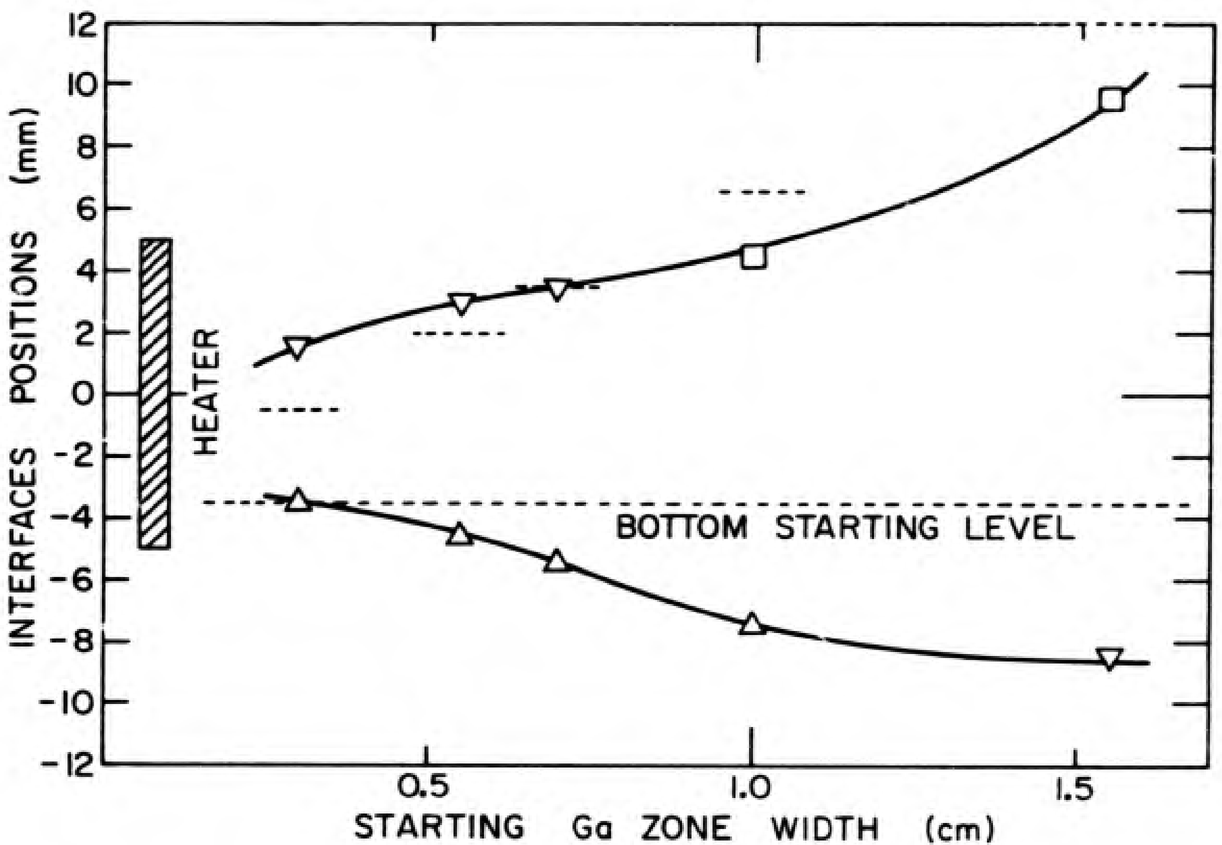

Figure 31: Steady state positions of the GaAs-Ga interfaces as a function of initial Ga zone length in the travelling heater method.

Δ - convex interface shape

▽ - concave interface shape

□ - approximately planar

----- - initial position of interface

the thickness of the furnace core and it should be larger the higher the heater temperature. It was then observed that the bottom solid-liquid interface was convex or approximately planar when the zone was smaller than the effective heater length, such as in the cases of 0.55, 0.70, 1.0 cm initial Ga zones. When the starting zone was much smaller than the heater, as in the case of the 0.3 cm zone, a GaAs bridge formed between the seed and feed in the colder center portion of the zone, thus rendering it unusable for THM growth. The bottom interface for the 1.55 cm Ga zone was located outside the heater and was found to be concave towards the liquid zone.

The above mentioned experimental knowledge of the GaAs-Ga interface position and shape in relation to the size and location of the Ga zone confirmed predictions based on considerations of the heat flow in the respective cases. If the Ga zone was located within the effective heater, as in Figure 32(a), the solid adjacent to the top and bottom interfaces received heat from the surroundings, causing the interfaces to assume convex shapes which are very nearly isotherms. Figure 32(b) shows the thermal conditions in the case of a large Ga zone where the interfaces were located at positions such that the heat flow was outwards away from the ampoule, causing the concavity of the interfaces. The interfaces should be approximately planar when the zone and the heater are approximately of the same size. The

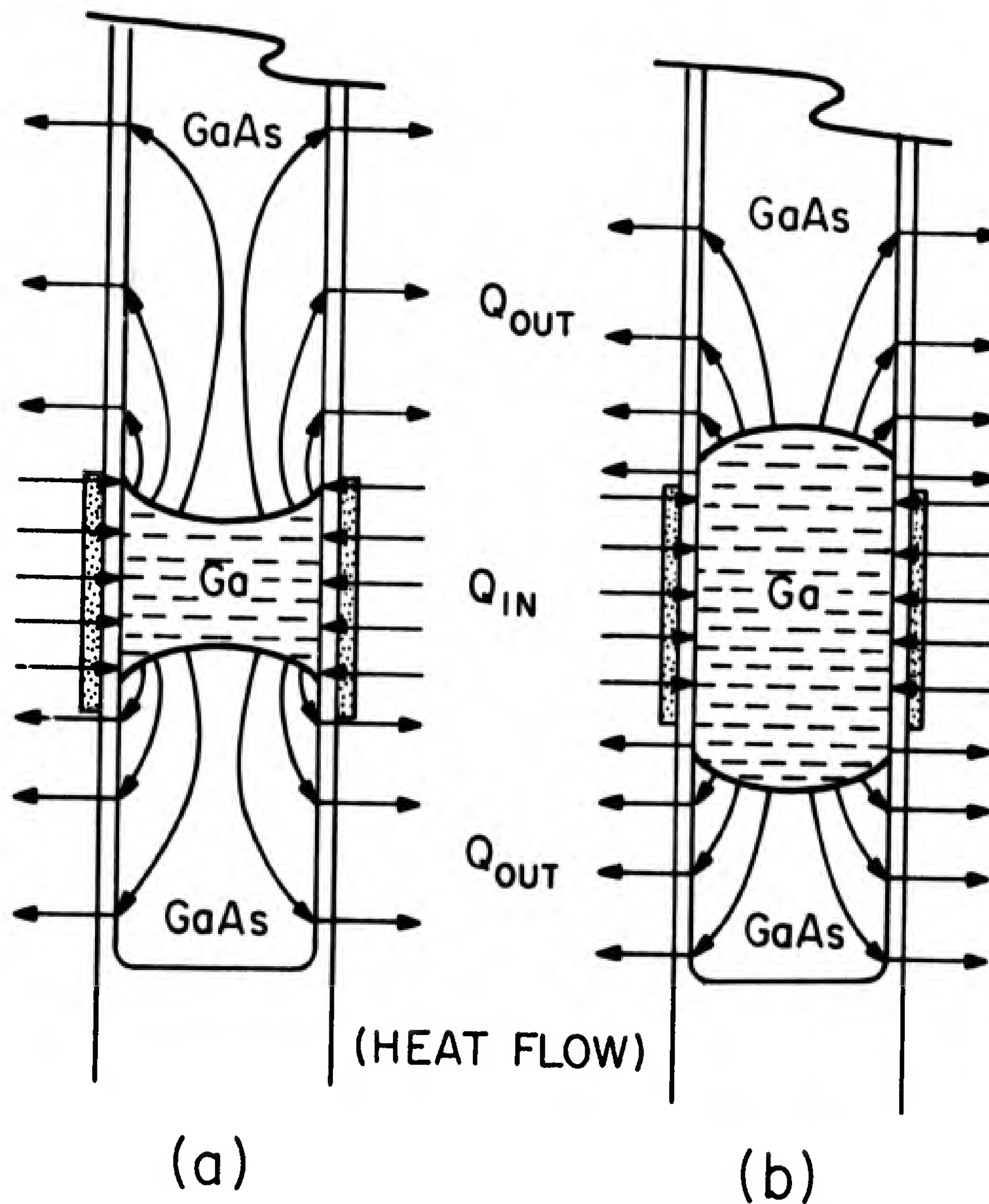

Figure 32· Schematic showing the heat flow pattern and its relationship to the interfaces shapes for the cases where the Ga zone is (a) smaller (b) larger than the effective heater length AA'. The radial component of the heat flow at the surface of the ampoule are indicated by the arrows.

approximate interfaces positions and shapes for different zone sizes are shown in Figure 32(c).

Since the thermal conditions in THM growth are stable and completely determined by the physical arrangements of the growth system, the knowledge described above could be applied to investigate the influence of the Ga zone size (and thereby the GaAs-Ga growth interface shape) on the crystallinity and quality of THM-grown crystals. Identical ampoules were prepared with 0.55, 0.7, 1.0 and 1.55 cm starting Ga zone lengths. Growths were performed at a 950°C heater temperature with a 1.5 mm/day lowering rate. The longitudinal sections of the resultant crystals, which were seeded with bi-crystal sections obtained by vertical gradient freeze growth, are shown in Figure 33. Strong differences are evident. With 0.55 and 0.7 cm initial Ga zones, the solid-liquid growth interfaces were expected to be convex (as explained earlier) and were confirmed to be so in the quenched samples. The crystals grown with the convex interface had fewer grains and the grain boundaries tended to grow out. The near-flat interface of the 1.0 cm zone was responsible for the lengthwise propagation of grains in THM-62. In THM-41, in which the zone was larger than the heater and the growth interface concave, many grains nucleated at the wall and grew inwards. Traces of trapped Ga were also found in the center, throughout the

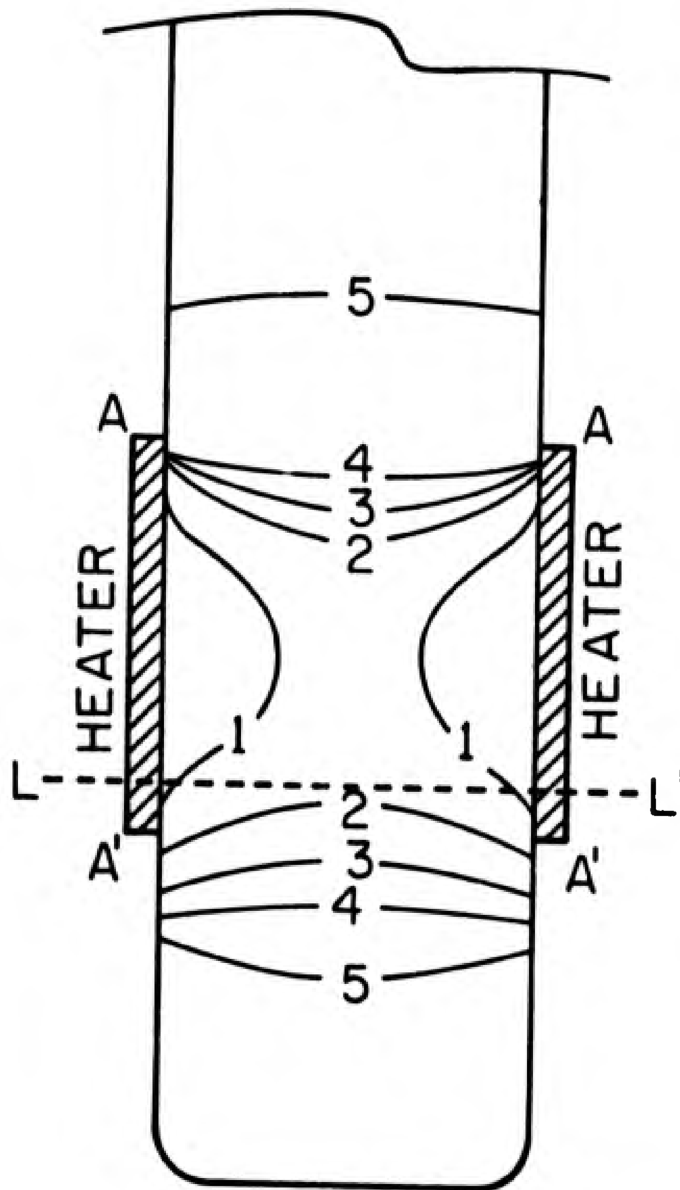

Figure 32(c): Schematic of interface positions and shapes in the same experiments as in Figure 31 at 980°C maximum heater temperature. Curves 1 to 5 are steady state interfaces for Ga zones of initial lengths: curve 1:0.3 cm, curve 2:0.55 cm, curve 3:0.7 cm, curve 4:1.0 cm, curve 5:1.55 cm.

AA' - Physical length of 1 cm long heater.

LL' - Starting level of bottom interface of Ga zone.

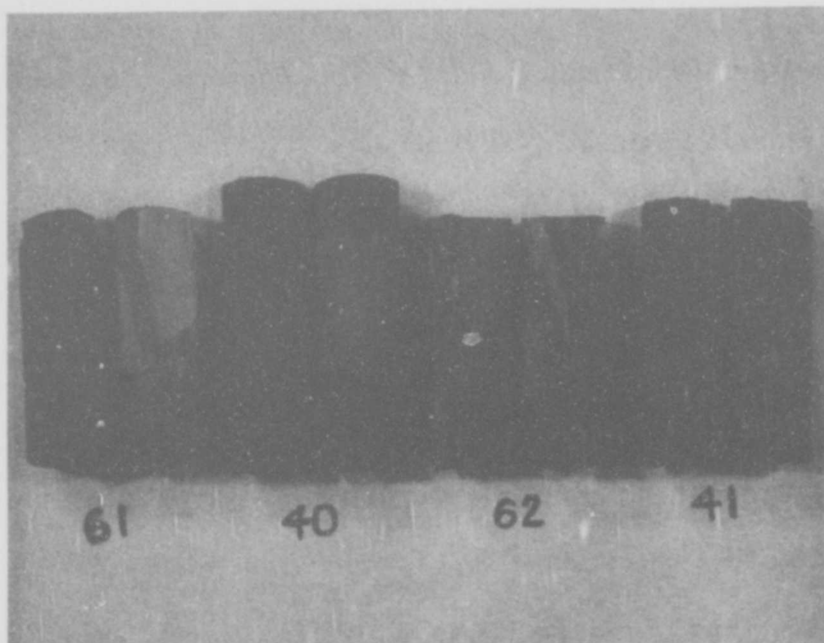

Figure 33: Travelling heater GaAs grown at 1.5 mm/day with different initial Ga zones.
THM-61 - 0.55 cm
THM-40 - 0.70 cm
THM-62 - 1.0 cm
THM-41 - 1.55 cm

length of the ingot. This was probably due to trapping by the inward growth of grains. Another contributing factor could be the fact that the temperature gradient at the center would be expected to be smaller because of the greater distances to heat sources and sinks. A lower gradient would more readily permit interface breakdown and solvent inclusion formation, as discussed in Chapter VI.

The experimental details and results of the four THM growth runs using different Ga zone sizes are summarized in Table 8. It seemed that to obtain a good single crystal by THM growth, the ratio of the length of the Ga zone to the heater length should be greater than 0.6 but less than 1.0. This important observation was found to be true in all the controlled THM growth runs performed. This also explained the erratic results in the early runs in which the size of the Ga zone and its position were randomly chosen.

4. Influence of Heater Temperature and Lowering Rate

As will be discussed in Chapter VI, the heater temperature and lowering rate were expected to influence gallium inclusion formation. In addition, it is reasonable to assume that there is a maximum travel rate corresponding to a given thermal configuration and level. In order to investigate these effects, eleven different THM runs were performed at temperatures of 800°C, 950°C, 980°C and 1100°C and lowering rates ranging from 0.5 mm to 20 mm/day. The growth runs are summarized in Table 9 and the growth details

TABLE 8. DETAILS OF THM RUNS WITH DIFFERENT INITIAL Ga ZONE LENGTHS.

Run THM No.	Heater Temp.	Original Seed length(cm)	Original Ga Zone length(cm)	Original Feed length(cm)	Lowering Rate (mm/day)	Results
61	980°C	1.0	0.55	3.8	1.5	2.8 cm successful growth. Grain selection by convex interface was apparent as grain boundaries grew outwards toward crucible wall.
40	980°C	1.0	0.75	3.8	1.5	3.0 cm growth. Seeded crystals appeared to have grown outwards due to presence of convex solid-liquid growth interface. Quality of crystal good with no Ga inclusion.
62	980°C	1.0	1.0	3.8	1.5	Growth interface was near-flat. As a result, the grain propagation was generally parallel to the growth direction.
41	980°C	1.0	1.55	3.8	1.5	2.8 cm polycrystalline growth completed. Grains appeared to have nucleated on wall and grown towards center due to the concave solid-liquid growth interface. Trains of Ga inclusions present in center of crystal.

TABLE 9. SUMMARY OF THM GROWTH RUNS AT DIFFERENT HEATER TEMPERATURES AND LOWERING RATES

Heater Temp. (°C)	Estimated Interface Temp. (°C)	Estimated As Solubility (wt. %)	Lowering Rate in mm/day							
			0.5	1.0	1.5	2.22	4.44	6.66	13.2	20.0
800	740	1.2%		#33**						
850	775	2 %	#83*	#45*		#32**	#31**			
980	900	6 %			#61	#89	#39**	#44**		
1100	1010	12 %							#58	#79*

*Growth completed with some polycrystalline nucleation, but no Ga inclusions.

**Growth run failed, Ga zone detached or Ga inclusions trapped.

concerning each run listed are separately described in Table 10. The interface temperatures listed in Table 9 are estimates which are 60° to 90° lower than the heater temperatures (see discussion in Section C9). It appeared that it was nearly impossible to have any growth at a heater temperature of $800^{o}C$. The Ga zone remained at its original position at the end of the run. At $850^{o}C$ the crystal quality was poor even at the inconveniently slow rate of 0.5 mm/day. Speeds greater than 2 mm/day produced crystals with Ga inclusions. At a heater temperature of $980^{o}C$ (corresponding to a interface temperature of about $900^{o}C$), results of growth runs at four different lowering rates show a definite difference in the quality of the crystals grown. The 6 at. % As solubility at $900^{o}C$ seemed to be sufficient for good single crystal growth up to a critical rate of about 2.2 mm/day, after which growth became polycrystalline and Ga inclusions were trapped (Figure 34). The highest heater temperature employed was $1100^{o}C$. Any further increase in temperature would have softened the silica ampoule, caused the ampoule and heater tube to stick, and shortened the life of the heating element. It would also have resulted in higher contamination of the grown crystal by the crucible material and defeat the advantages of solution growth. It was found that using a very large lowering rate not previously used for THM growth, 20 mm/day, it was possible to grow good

TABLE 10. DETAILS OF THM RUNS AT DIFFERENT TEMPERATURES AND LOWERING RATES

Run THM No.	Heater Temp.	Original Seed length (cm)	Original Ga Zone length (cm)	Original Feed length (cm)	Lowering Rate (mm/day)	Results
61	980°C	1.0	0.55	3.8	1.5	Successfully completed 2 to 8 cm of growth. Grain selection by convex interface quite evident. Growth rate could be considered ideal for growth.
89	980°C	1.0	0.55	3.8	2.22	Growth of 2 cm completed before run was terminated because of power shut down. Crystal contained a <111> twin. No inclusions were observed. It appeared that 2.22 mm/day was close to the maximum rate for single crystal growth at 980°C.
39	980°C	1.0	0.55	3.8	4.44	Successfully completed 3.5 cm growth. Polycrystalline with some Ga inclusions; travel rate apparently too fast for good quality crystal.

TABLE 10. (Continued)

Run THM No.	Heater Temp.	Original Seed length (cm)	Original Ga Zone length (cm)	Original Feed length (cm)	Lowering Rate (mm/day)	Results
44	980°C	1.0	0.55	3.8	6.66	2.8 cm growth completed. Crystal very polycrystalline with trails of Ga inclusions.
58	1100°C	1.0	0.55	3.8	13.2	Completed 2.0 cm growth. No Ga inclusions present.
79	1100°C	self-seed	0.55	3.8	20	Good quality, inclusion free crystal.
33	800°C	1.0	0.75	3.8	1.0	Ga zone detached after 0.8 cm growth indicating 800°C is too low for THM growth, even at 1 mm/day.
83	850°C	1.0 <111> Ga	0.55	2.0	0.5	Ga inclusions were present, as well as small crystals scattered in the grown crystal.
45	850°C	1.0	0.75	3.8	1.0	Successfully completed 2.5 cm growth. Crystal quality poor, indicating 850°C and 1 mm/day as lower limit for THM growth.

TABLE 10. (Continued)

Run Thm No.	Heater Temp.	Original Seed length (cm)	Original Ga Zone length (cm)	Original Feed length (cm)	Lowering Rate (mm/day)	Results
32	850°C	1.0	0.75	3.8	2.22	Ga zone detached after 1.0 cm growth. Travel rate too fast for growth.
31	850°C	1.0	0.75	3.8	4.44	Ga zone detached after 0.7 cm growth.

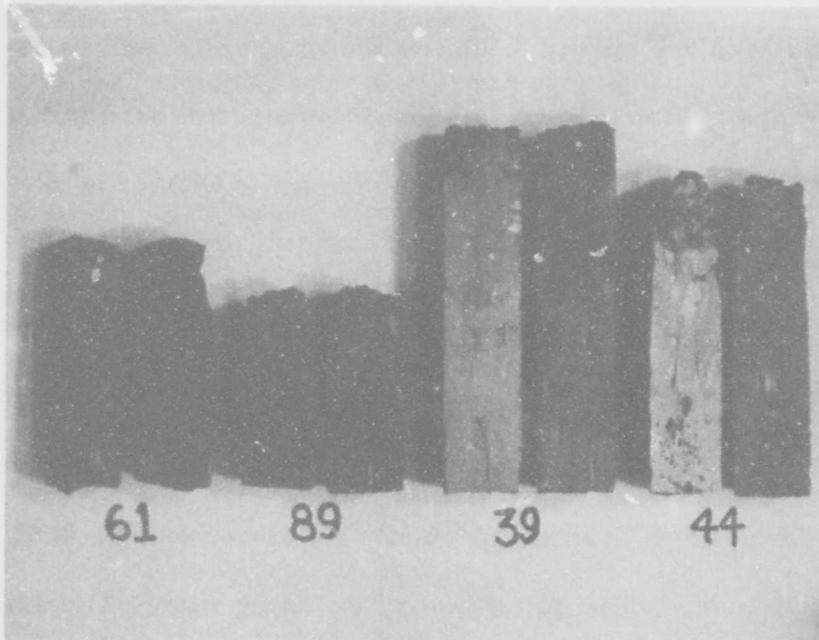

Figure 34: Sectioned THM GaAs grown with a heater temperature of $980^{o}C$ at four different lowering rates.
THM-61 - 1.5 mm/day
THM-89 - 2.22 mm/day
THM-39 - 4.44 mm/day
THM-44 - 6.66 mm/day
Voids at bottom 1 cm of ingots are gas bubbles in the vertical gradient freeze grown seeds used.

quality, inclusion-free crystals. A detailed theoretical analysis on the transport processes and problems of constitutional supercooling in THM growth of GaAs is included in Chapter VI.

Although there was considerable variation in the degree of crystallinity, it is the author's feeling that higher growth rates tended to produce more grains. However, grain generation is influenced by a variety of factors, so that a strong correlation with growth rate is not possible.

5. Seeding and Impurity Doping

After the different aspects of THM growth of GaAs were investigated and understood, five single crystals were successfully grown under the proven conditions of 980°C heater temperature, 0.55 cm Ga zone length and ~1.0 to 1.5 mm/day lowering rate. The seeding directions used were ⟨111⟩Ga, ⟨111⟩As and ⟨110⟩. The seeds were prepared from liquid-seal Czochralski[34] single crystal CZ-41 (Figure 35) grown in the ⟨111⟩Ga direction. The THM crystals were either not intentionally doped (No. 72) or were doped with Te (No. 71), Zn (No. 81) or Cr (No. 84 and No. 86). The details concerning the runs and the product crystals are listed in Table 11. Figure 36 shows the ⟨111⟩ As seeded crystal, THM-71. The completely single crystalline (110) section of THM-71 is shown in Figure 37 along with the (111) section of single crystal THM-86, which was grown in the

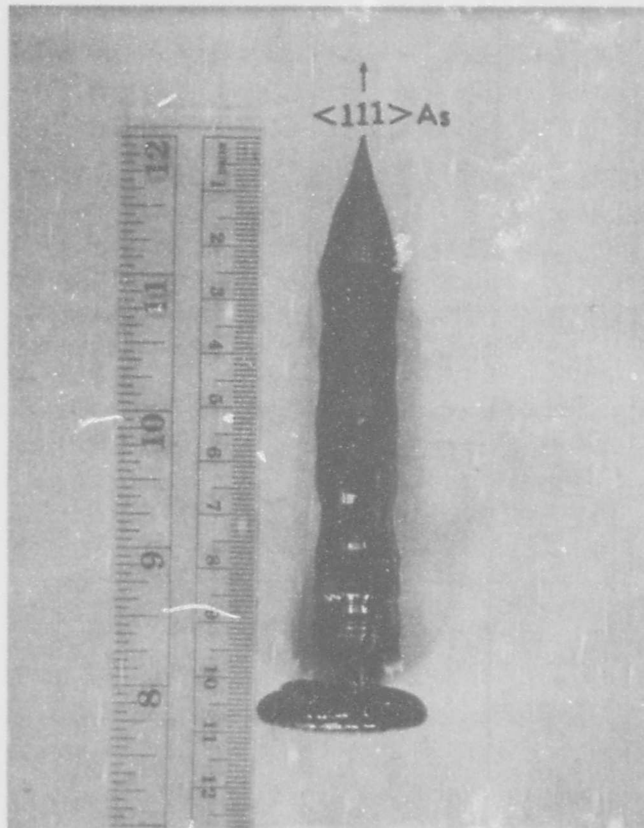

Figure 35: Single GaAs crystal CZ-41, grown by liquid-seal Czochralski technique, from which ± 111 and 110 seed crystals were obtained for seeding THM growths.

TABLE 11. THM RUNS WITH CONTROLLED SEEDING AND DOPING

Run THM No.	Heater Temp.	Original Seed length (cm)	Original Ga Zone length (cm)	Original Feed length (cm)	Lowering Rate (mm/day)	Results
71	980°C	0.6 <111> As	2.578 g Ga 0.001 g Te	3.8	1.5	2.0 cm single crystal with a separate small grain in the second cm.
72	980°C	1.0 <111> As	2.80 g Ga no dopant	3.5	1.5	95% single crystal. Three tiny strip-like (111) twins nucleated near the circumference and grew into the center of the crystal at 70.5° to <110>.
81	930°C	0.6 <111> Ga	2.95 g Ga 0.001 g Zn	2.0	1.5	Seeding poor. Polycrystalline from 0.5 cm to 1.5 cm.
84	980°C	1.0 <110>	3.39 g Ga 0.012 g Cr	2.0	1.5	After 0.3 cm growth in the <110> direction a (111) twin developed from the side and grew preferentially for the remaining 1.5 cm.
86	980°C	1.0 <110>	2.4 g Ga	2.0	1.0	Completely single.

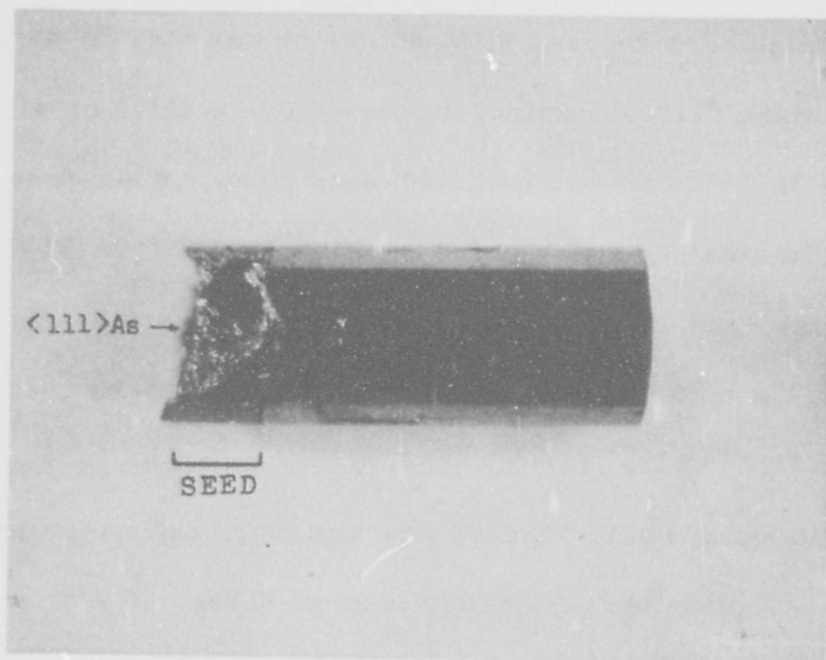

Figure 36: THM-71. Te doped and grown in 111 As direction.

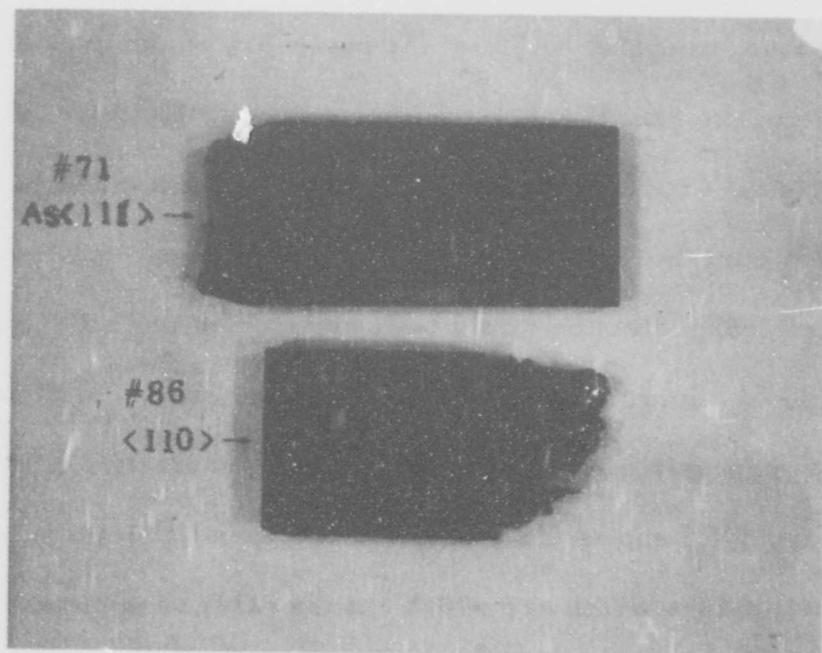

Figure 37: THM-71. Te doped and grown in the 111 As direction.
THM-86. Cr doped and grown in the 110 direction.

⟨110⟩direction. However, THM-84, which was also Cr-doped and seeded in the ⟨110⟩ direction, developed into a ⟨111⟩ crystal at an angle of $35^{o}16'$ to the original (110) seed plane, as shown in Figure 38. An interesting case was the undoped crystal THM-72 (Fig. 39a). Three tiny strip-like ⟨111⟩twins, spaced 120° apart, nucleated at or near the circumference and grew into the center of the crystal at an angle of 70.5^{o} to the (111) As seeding face.

Twin formation in THM-72 was a puzzling and interesting phenomenon. A plausible explanation is given below. The crystal was grown with relatively short Ga zone of about 0.5 cm and thus the bottom growth interface was expected to be quite convex. It is conjectured that at certain points of the periphery of the crystal, the curvature of the growth interface approximated the three (111) planes at an angle of $\sim 70.5^{o}$ to the (111) seed plane. Because of lack of convection currents at these three wedge-like sites, the corresponding arsenic concentration would be lower than in the bulk liquid. The constitutional supercooling resulting from the arsenic deficiency was probably responsible for twinning and grain generation.

Figure 39(b) shows the geometric relationship between the three (111) planes which are $\sim 70.5^{o}$ to the (111) seed plane. The diameter of the crystal was ~ 1.0 cm, so that the three twins should meet at point D at a distance about 1.46 cm above the seed plane,

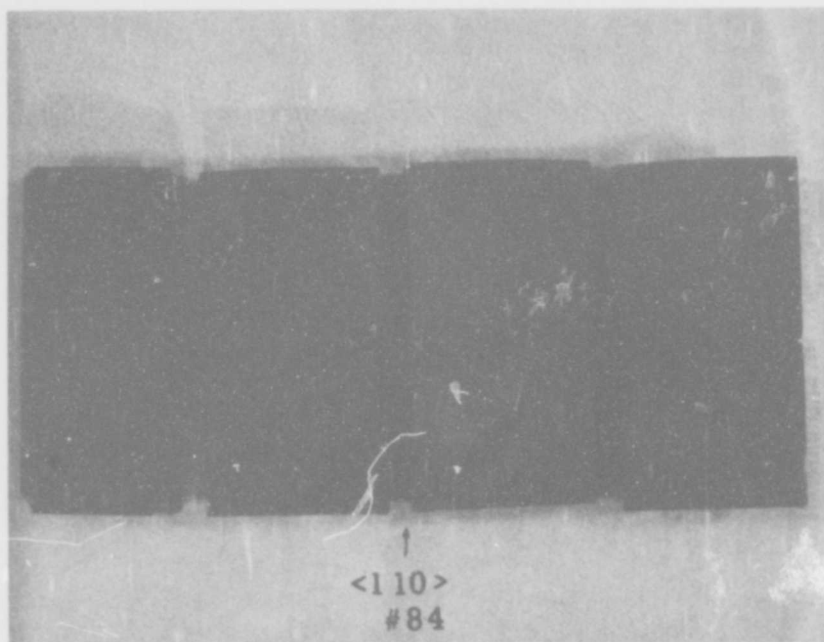

Figure 38: THM-84. Cr doped, crystal developed into a 111 grain at an angle of 35°16' to the original (110) seed plane.

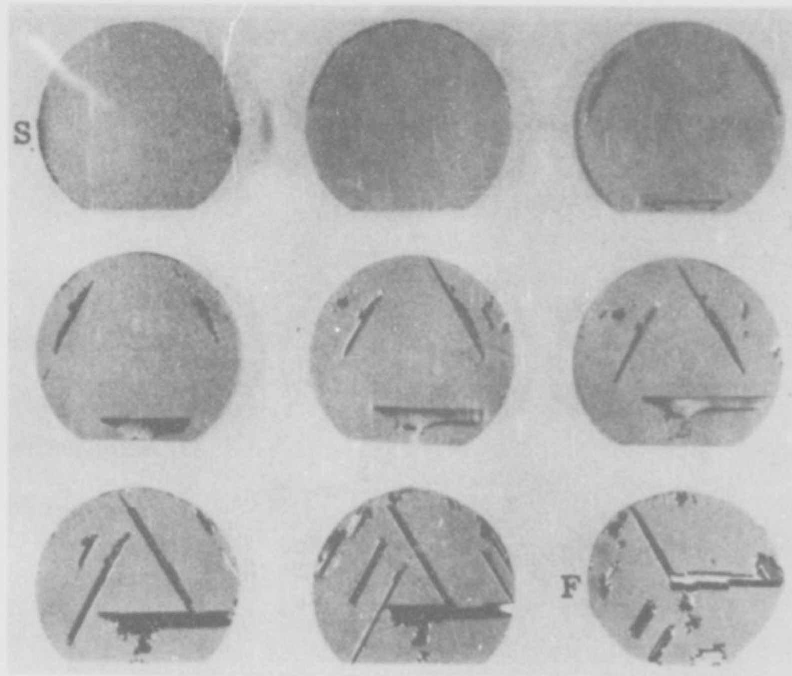

(b)

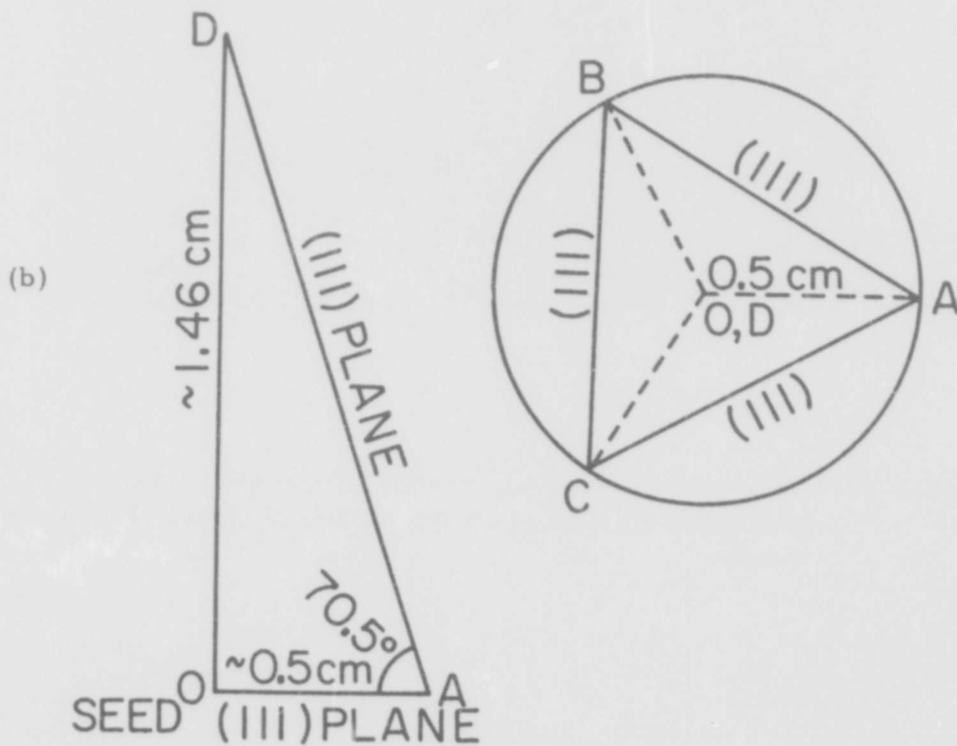

Figure 39(a): (111) slices of THM-72 showing the sequence of formation and propagation of the three (111) twins (Slice S-O mm, Slice F-19 mm from seed).

Figure 39(b): Schematic showing geometric relationship between the three (111) planes and the (111) seed plane.

which was what happened in THM-72 (see Figure 39a).

As will be discussed extensively later in Chapter VI, constitutional supercooling in GaAs could lead to interface breakdown with Ga inclusions, and twin and grain formation. Traces of trapped Ga and polycrystallinity were indeed observed near the three (111) sites as shown in Figure 39 (c). The polished side showing the grain sturcture (Figure 39(d)) further confirms our explanation. The flat-bottomed grain near the seed was one of the ⟨111⟩ twins initiated at the beginning of the growth. There was intermittent generation of new grains along the side. This is because the initial growth of a grain would eliminate the slow growth (110) wedge geometry and thus the supercooling temporarily. However, as the grain grew out due to the convex interface, the (111) wedge of the original seeded growth interface formed again and the supercooling, inclusion and polycrystalline as twin formation recurred.

We noted earlier that THM-84, which was seeded in the ⟨110⟩ direction, developed into ⟨111⟩ grain instead (see Figure 38). This probably is because ⟨111⟩ is a more stable growth direction compared to the ⟨110⟩ in GaAs, rather than because of supercooling at the (111) "wedges." The two (111) planes are at an angle of $35^{\circ}16'$ to the (110) seed plane, the convection currents could certainly reach growth planes of such shallow angles. Indeed, in both ⟨110⟩ seeded

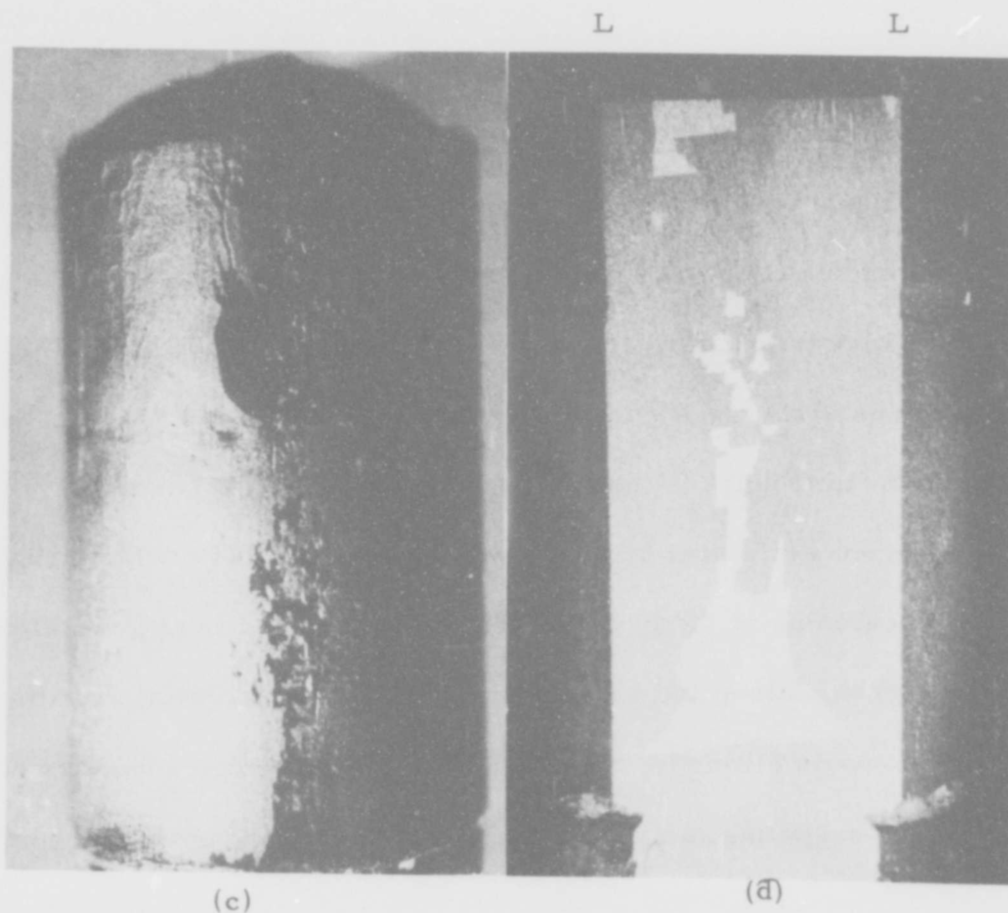

Figure 39(c): A side view of sandblasted crystal THM-72 showing traces of Ga inclusions, twinning and grain generation approximately parallel to one of the three (111) planes at 70.5° to the (111) seed plane.

Figure 39(d): The Figure 39(c) side polished, showing initiation of (111) twin near bottom (111) seed interface and later sequence of grain and twin formation. L-L' is the polished side as shown in Figure 39(a).

THM-84 and 86 no Ga inclusions or intermittent twin and grain formation were observed.

The five growth runs cited above were not sufficient to establish which seeding orientation is best for THM GaAs growth. Hemmat and Wald[3] concluded from growth of GaAs platelets from Ga solutions that the $\pm\langle 111\rangle$ directions are the least favorable because they grow slowest while the $\langle 110\rangle$ and $\langle 112\rangle$ are the most favorable for THM growth because they grow more rapidly. Such inference is debatable as the evidence from our research on THM and experience on GaAs melt growth by many other researchers have shown that the $\pm\langle 111\rangle$ orientations are more stable and generally preferable for use in seeding. However, as discussed above, there are problems with (111) twin formation if the growth interface is too convex. Therefore, the best technique probably is to seed in the $\langle 111\rangle$ direction with a slightly convex growth interface.

Impurity doping was accomplished by including the calculated amount of dopant in the Ga zone when the ampoule was prepared. From the mass spectrometric data of THM-71 (grown with 1 mg of Te in 2.578 g of Ga) the Te concentration was 0.784×10^{16} atoms/cc. This yields a Te segregation constant k of about 1.0×10^{-3} for growth from a Ga solution at an estimated growth temperature of about 900°C. This k value is lower than the true value, because before the sample

grew, Te was depleted from the zone by incorporation into previously crystallized material and by evaporation from the zone and condensation into the cooler part of the seeded ampoule.

6. Dislocation Etch Pits Studies

In earlier studies (Section III) of the effect of zone length on the growing interface shape, it was shown conclusively that a zone smaller than the heater (such as the 0.55 cm Ga zone used in all the later controlled seeded growths) would produce a slightly convex solid-liquid growth interface. One would expect dislocations to grow out to the periphery and gradually be eliminated with a convex interface shape. In order to prove this hypothesis, studies were made of the (111) Ga dislocation etch pits (Schell's etch; 1 HNO_3: $3H_2O$) developed on cross sections of two crystals (No. 71 and No. 72) grown in the ⟨111⟩ As direction and two others (No. 84 and No. 86) grown in the ⟨110⟩ direction.

For THM-72, the etch pit density increased from 0.5×10^4 per cm^2 to 1.0×10^5 per cm^2 at the seeding interface and then decreased approximately exponentially by two orders of magnitude to 0.3×10^3 per cm^2 after only 2 cm of growth (see Figures 40 and 41). The linear negative slope approximates a "dislocation elimination rate" of about 17% per mm of growth. Run THM-71 was terminated by rapidly withdrawing the ampoule from the furnace, thus quenching it

Seed Slice

Magnification 100X

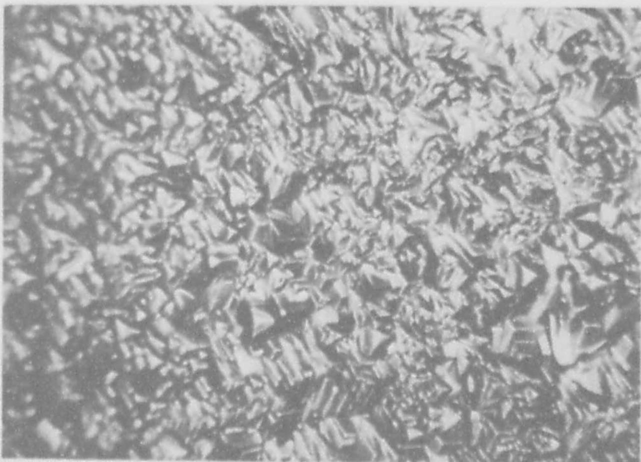

Slice 1: 0 mm from seed

Slice 6: 8 mm from seed

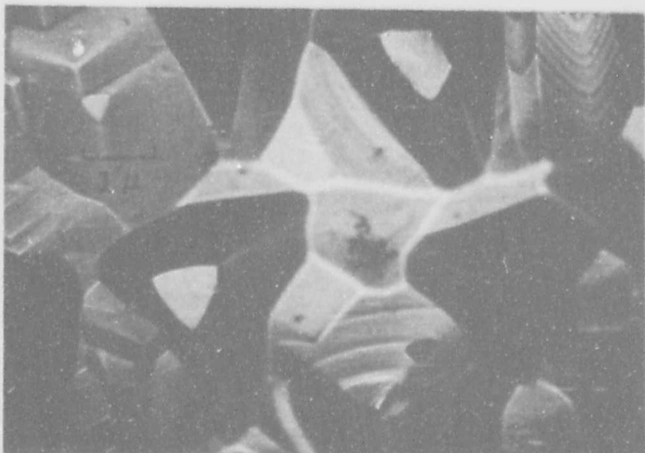

Slice 10: 19 mm from seed

Figure 40: (111)Ga etch pits on THM-72 as a function of distance from the seed. Slices were taken perpendicular to growth direction.

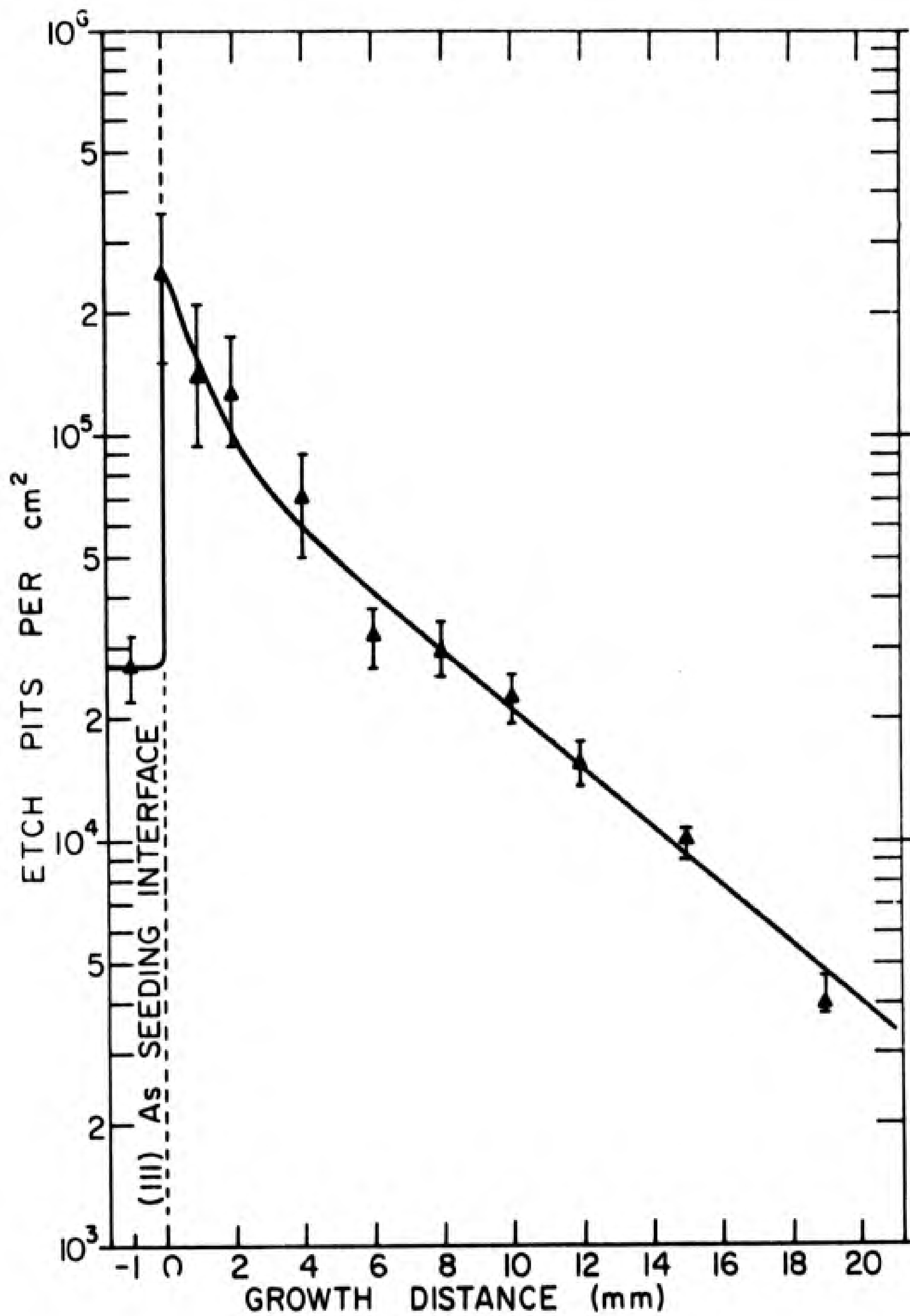

Figure 41: Etch pit densities on cross-sections perpendicular to growth direction as a function of growth distance in THM-72.

to room temperature rather than leaving the ampoule in the furnace and turning the heater off to allow relatively slow cooling, as in run THM-72. The study on the resultant dislocations (Figure 42) in the crystals showed that there was the same sudden increase in the dislocations at the seeding interface and the exponential decrease afterwards. However, the etch pit density increased by one order of magnitude from 7.5 mm to 16.5 mm, which was probably caused by thermal strain during the rapid cooling of this part of the crystal which was closer to the heater. The discontinuity occurred at a distance in the crystal approximately 9 mm below the bottom interface. The temperature at this point was estimated to be approximately 650°C by extrapolating the data from the temperature measurement in a THM crystal which will be discussed later in Section C9. This value is approximately half of the melting temperature of GaAs (1238°C), which is a rough estimate of the brittle-ductile transition temperature above which dislocations are mobile.

The sudden increases in etch pit density at the seeding interface were of the same order of magnitude in both crystals and were possibly due to lattice mismatch at the initiation of growth. The exponential rate of decrease in etch pit density in the first part of THM-71 was 27% per mm of growth, which is about the same magnitude as that of THM-72, indicating that it is indeed the effect of a

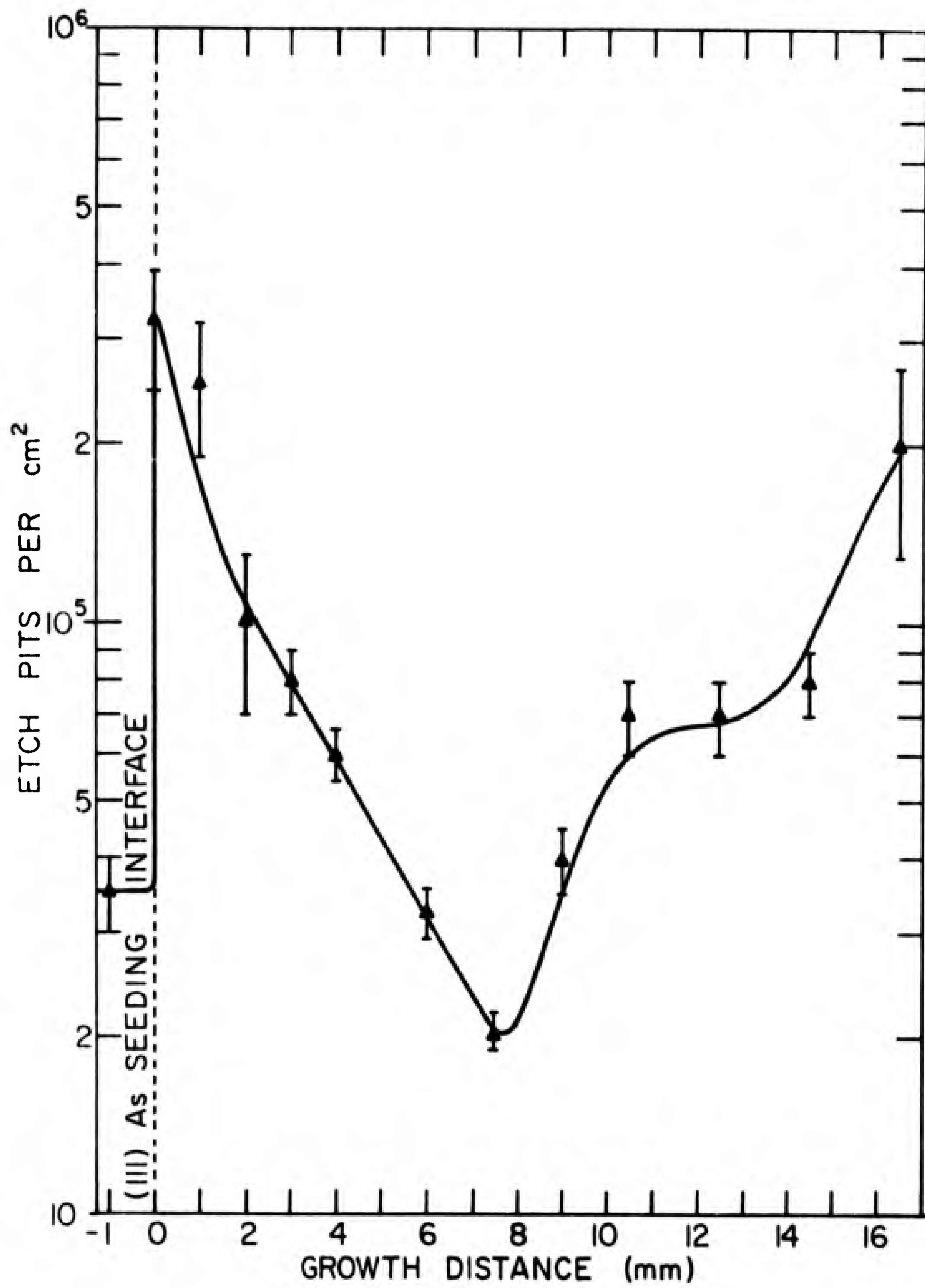

Figure 42: Etch pit densities on cross-sections perpendicular to growth direction as a function of growth distance in THM-71.

definite dislocation elimination mechanism.

Further evidence was found to be convincing in favor of the hypothesis mentioned. Crystals THM-84 and THM-86, seeded in the ⟨110⟩ direction and doped with Cr, were sliced longitudinally on the (111) plane and dislocation etch pit counts made along the length of the crystals. As shown in Figure 43, the etch pit density did not change appreciably at seeding and remained approximately at a constant value of around 2-3.5 x $10^4/cm^2$. These results suggest that the dislocations perpendicular to the growth direction were not affected by the elimination process of the convex growth interface and thus remained at the same level as the seed throughout the crystal.

No previous reports were uncovered on such dislocation elimination in THM crystal growth. However, Wolff and Mlavsky in their review of crystal growth by solvent zone techniques[6] described reports of dislocation removal in TSM-grown GaAs, GaSb, $SrTiO_3$ and SiC. In all cases the dislocation density of the grown crystals, revealed by etching and x-ray techniques, was one or more orders of magnitude lower than the seed material. The specific work on dislocation annihilation in TSM-grown GaAs was Weinstein et.al.[37] The GaAs seed slice was in the ⟨111⟩ Ga direction and the Ga layer was about 0.5 mm thick. The TSM "sandwich" of diameter 6.35 mm was subjected to a temperature gradient of about 60°C/mm with an average temperature of about 850°C. In the grown crystal, the

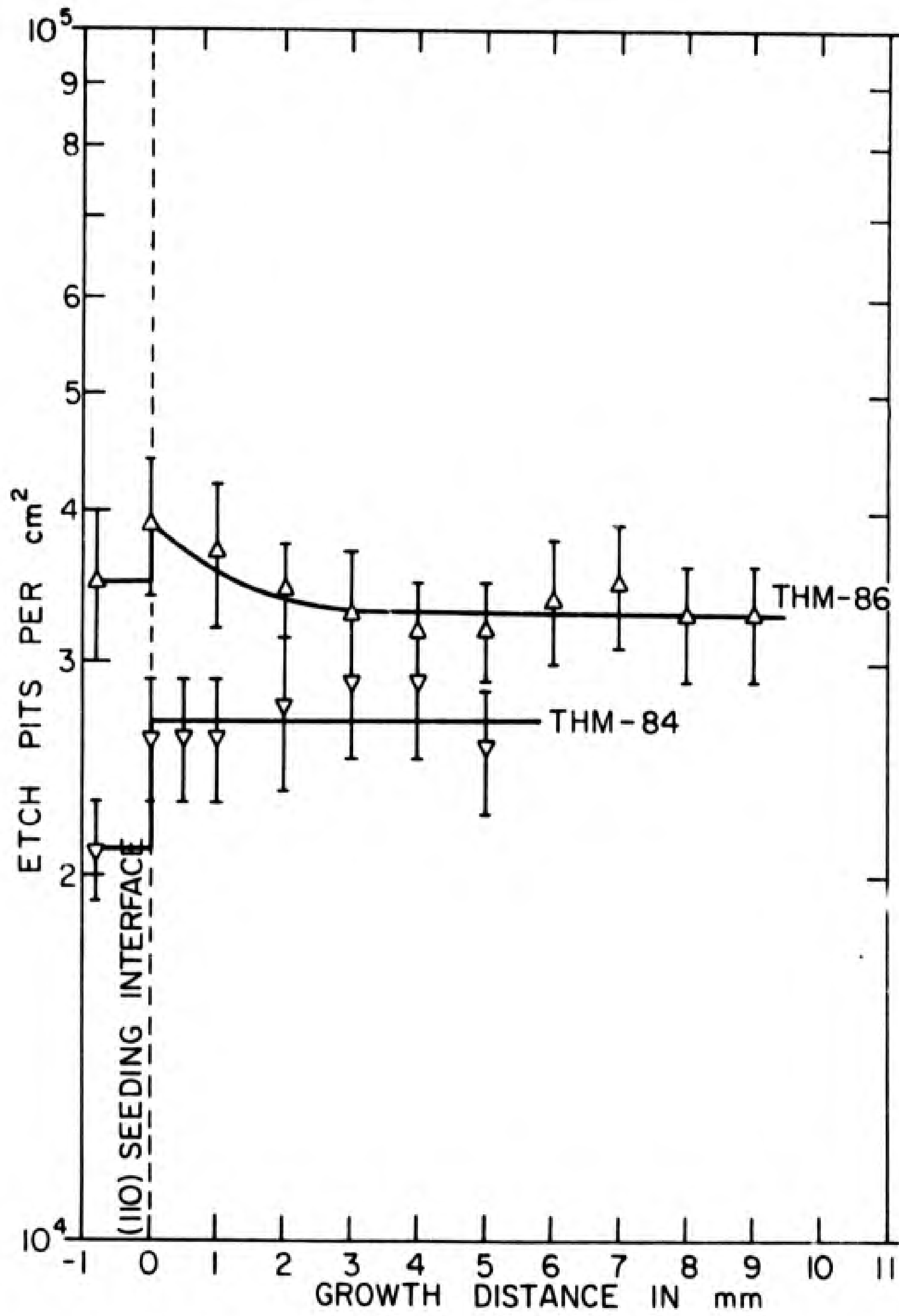

Figure 43: Etch pit densities on longitudinal slices of THM-84 and THM-86.

dislocation density at the seeding interface was the same as that of the seed, $8 \times 10^4/cm^2$. It decreased abruptly to 1×10^4 cm^2 in the first 0.15 mm of growth and then remained constant thereafter. GaAs grown directly from a Ga solution by cooling without radial temperature gradients also showed a similar decrease in dislocation density. The authors concluded that the phenomenon was characteristic of growth from a metal solution rather than any inherent property of the TSM sandwich approach. No satisfactory theoretical model was proposed. It was conjectured that the dislocations normal to the growth interface disappear because of closed loop formation or degeneration through transformation to other types of dislocations. In the TSM geometry, the diameter to thickness ratio is large and the solid-liquid growth interface is relatively flat. Thus there was little possibility that the edge type dislocations grew out of the sides. Were this the case, these would have been a radial variation in dislocation density, which was not observed in the TSM-grown GaAs.

The work discussed above shed some light on our observations on THM GaAs dislocation elimination. As evident from the previous two Figures 41 and 42, the etch pit density increased at the seeding interface, then decreased markedly for the first 2 mm of growth after which it followed an exponential path of decrease. The initial increase was explained as the effect of lattice mismatch. Since the

growth interface in the THM growth here was convex, the growing out of the edge dislocations probably accounted for most of the exponential decrease. The presence of this mechanism was confirmed by the observed radial variation in etch-pit density in our THM crystals. The density decreased towards the edge but there was a large increase at the periphery which was probably due to dislocation generation from thermal stress during cooling.

The combination of this "growing out" effect and the "loop formation" effect observed in TSM growth was probably the cause of the larger than exponential decrease at the beginning of THM growth. The dislocation density normal to the growth direction in THM grown crystals remained relatively constant as shown previously in Fig. 43. This is because the growth interface was only slightly convex in the growth direction so that few such dislocations were affected by the two effects which helped to eliminate dislocations parallel to the growth direction. Apparently, more experimental work and theoretical considerations are necessary to fully understand this phenomenon of continuous dislocation elimination with growth in the THM. It seems that seeding with very low dislocation seeds and slow cooling at the end of growth (instead of quenching) could produce THM crystals with very low dislocation density, perhaps at the 10^2 per cm^2 level. This could make the THM very attractive as a controllable growth method for low dislocation crystals.

7. Segregation in THM Growth

One of the most important features of the zone melting process is the purification effect on the material with the molten zone passes. The purification by solution zone passages[38] should be greater than for melt growth since the growth temperature is considerably lower and the segregation constant of most impurities is much smaller in growth from Ga solution than growth from GaAs melt. Mass spectrometric analyses of feed GaAs and THM crystals grown from them bore out this fact, as shown in Table 12. The impurity concentrations before and after THM growth are shown.

Crystal THM-72 was grown using a zone of 2.8 g of six 9's purity Ga and seed and feed rods ground from the same Czochralski single crystal CA-41. There appeared to be a reduction in the amount of B, K, Cr and Fe by factors of 2 to 5. Most of the other elements remained at approximately the same level after one zone pass.

The purification in crystal THM-76, which was the result of three separate Ga zone passed performed on vertical gradient freeze grown crystal GF-30, was marked. Almost all of the impurities decreased in concentration, some by a factor as large as 20 (as in Be) or 30 (as in Cu). The three exceptions were the slight increase in Cl, Ca and Fe concentrations, which were probably contaminants accumulated from the acid etches and tweezer handling during preparation for the three separate growth runs. Most significantly, however, is

TABLE 12. MASS SPECTROMETRIC ANALYSES OF FEED RODS AND THM GaAs GROWN FROM THEM

(Concentrations in 10^{16} atoms/cm^3)

Element (D - donor) (A - acceptor)	Feed CZ-41	Crystal THM-72	Feed GF-30	Crystal THM-76
Li (A)	< 0.14	< 0.14	< 0.14	< 0.09
Be	≤ 0.14	≤ 0.14	< 1.4	< 0.07
B	0.15	< 0.09	< 1.5	< 0.09
F	< 1.7	< 1.7	< 5.0	< 1.7
Mg (A)	0.4	0.4	< 1.3	≤ 0.04
Si (D/A)	<11.4	<11.4	8.0	6.8
Cl	0.9	0.9	0.02	0.04
K	< 1.6	0.8	0.49	0.26
Ca	< 2.4	< 2.4	0.24	< 0.48
Cr (A)	0.6	< 0.12	< 0.18	< 0.06
Mn (A)	< 0.02	< 0.12	< 0.12	< 0.06
Fe (A)	2.28	0.40	1.14	5.7
Co (A)	< 0.05	< 0.05	0.16	< 0.05
Ni (A)	< 0.22	< 0.22	0.54	< 0.11
Cu (A)	< 0.15	< 0.15	3.0	< 0.1
Zn (A)	0.47	0.47	0.9	< 0.09
Sn (D)	< 0.27	< 0.27	0.27	< 0.13
Te (D)	< 0.13	< 0.13	< 0.15	< 0.15
Pb (D)	< 0.09	< 0.09	0.9	< 0.09

the fact that the most common and important impurities in GaAs, such as B, Mg, Si, Cr, Mn, Cu, Zn and Te, all decreased in concentration. Most of the impurities have been reduced down to, or even below the 1×10^{15} atoms/cm^3 concentration level. This means that THM-73 had one of the lowest impurity concentrations in GaAs grown in this laboratory.[29] This significant purification effect and the dislocation elimination effect are indeed favorable attributes of THM.

It is appropriate here to consider the question of accuracy and reliability of the mass spectrometry results. More than a dozen GaAs samples grown by various techniques were submitted at different times to the same facility (Batelle Columbus Labs.) for analysis. It is difficult to determine the absolute reliability of the results, but more of them were surprising or inconsistent with results on control samples sent to other facilities. Results on crystals grown routinely by the established techniques of horizontal Bridgman and liquid-seal Czochralski were consistent with each other. Variation in impurity concentrations of the same order of magnitude cannot be taken to be accurate. However, this concentration in GF-30 are generally more than one order of magnitude higher, and in THM-76 they are generally more than one order of magnitude lower than that appearing in CZ-41 and THM-72. It is felt that such large differences can be regarded as significant indication of the actual difference in impurity

concentrations. To support and supplement such inferences, results of other analytic techniques such as infra-red local mode absorption studies and electron microprobe analysis can be compared with the mass spectrometry results.

8. Electrical Properties

As described earlier in Section 5, five THM crystals were grown with controlled seeding and doping. Hall measurements were made on samples from several of these, as summarized in Table 13. It is interesting to examine the electrical properties in relation to the impurities present. The properties of THM-72 correspond to those of the GaAs grown from a Ga-rich solution at 925°C by Vieland, et. al,[40] which are $\rho = 0.64\text{-}0.96\Omega\text{-cm}$, $p \simeq 10^{16}/cc$, $\mu_p \simeq 340$ $cm^2/v\text{-sec}$. The five-fold reduction in chromium concentration from feed CZ-41 to THM-72 may account for the lowering of ρ by one order of magnitude.

The crystal GF-30 had relatively high concentrations of impurities. The poor electrical properties (very high ρ, very low mobility) reflect that fact. After three separate THM Ga-zone passes, the feed material was significantly purified, as discussed previously, and was reflected in the much improved electrical properties

TABLE 13. HALL MEASUREMENTS OF FEED CRYSTALS AND THM GROWN CRYSTALS

Crystal	Resistivity Type	Resistivity ρ ohm-cm	Carrier Concentration cm^{-3}	Electron or Hole Mobility, μ cm^2/volt-sec.	Discussion
CZ-41 (undoped, liquid-seal Czochralski method grown.)	N	45.2	3.3×10^{15} n	very low	The presence of Cr in the mass spectrometric data could account for the moderately high ρ. The low μ could be due to Fe, C and other deep level acceptors.
THM-72 (grown from CZ-41 by THM growth.)	p	3.69	6.0×10^{15} p	275	Chromium concentration was reduced from CZ-41 and is reprcsented in lower ρ. As in GaAs grown out of Ga,[ ] THM-72 was p type with reasonable hole mobil-ity.

TABLE 13. (Continued)

Crystal	Resistivity Type	Resistivity ρ onm-cm	Carrier Concentration cm^{-3}	Electron or Hole Mobility, μ cm^2/volt-sec.	Discussion
GF-30 (undoped, vertical gradient freeze grown.)	N	10^7-10^8	very low	very low	Sample apparently highly compensated. Mass spectrometric data show high concentration of Cr, Fe, Cu and other impurities.
THM-76 (grown from three passes on GF-30.)	P	0.042	2.5 x 10^{16} p	60.4	Quality of crystal improved from GF-30. Resistivity is low and impurity concentration very low as indicated by mass spectrometric data. Low hole mobility unexplained.

TABLE 13. (Continued)

Crystal	Resistivity Type	Resistivity ρ ohm-cm	Carrier Concentration cm^{-3}	Electron or Hole Mobility, μ cm^2/volt-sec.	Discussion
THM-81 (Zn doping, ~0.5×10^{19} atoms per cc Ga.)	P	1.166	2.6×10^{16} p	180	No mass spectrometric results obtained. Mobility is fair.
THM-71 (Te doping ~1×10^{19} atoms per cc Ga.)	N	0.022	2.8×10^{17} n	1007	No mass spectrometric results obtained. Electron mobility is low probably because of compensating impurities.

measured. The low hole mobility is not readily explainable, however. It indeed appears that THM growth not only purified the feed material CZ-41 and GF-30, it also improved their electrical properties.

Mass spectrometric analyses were not obtained for THM-81 (Zn-doped) and THM-71 (Te-doped). It must be remembered that impurity concentrations as indicated in mass spectrometric results could only be used qualitatively in such a discussion as the actual electrical measurements are a result of the complex interactions between the different impurities and other defects. The possible presence of carbon was considered. The cause for the consistently lower-than-ideal mobilities of different crystals grown by different methods in our laboratory still remains a mystery. The primary objectives in this research were accomplished and further investigative effort would be necessary to improve the seeding, doping uniformity and electrical properties of the THM-grown crystals.

9. Temperature Profile Measurement During THM Growth

It was desired to obtain temperature measurements inside a growth ampoule during a THM growth run. Information such as the actual temperature in the Ga zone (which should be lower than the heater temperature), the temperature gradients at the top and bottom GaAs-Ga interfaces, etc., would be instrumental in improving our understanding of the crystal growth process in THM. There were a number of technical difficulties involved in situating a minute

thermocouple inside the bulk of the GaAs ingot in an evacuated ampoule and maintaining it at a high temperature. The dimensions and arrangements of all the components had to be chosen to ensure the best accuracy under the difficult conditions and everything had to perform correctly throughout the long growth period. These problems were eventually solved after careful planning and experimentation and the temperature profile inside a GaAs crystal was measured during a THM growth run over 13-1/2 days at a lowering rate of 1.5 mm/day and heater temperature of about 1000°C.

Insulation or coating was found that would prevent corrosive attack of a thermocouple by arsenic and molten gallium at the high operating temperature. Sauereisen (Sauereisen Cement Co., Pittsburgh, Pennsylvania) and other high temperature sealing compounds either could not form a uniform protective coating around the time thermocouple or were too porous to maintain a vacuum for that length of time. Finally, this temperature measurement was accomplished by using a 0.003 in Pt-Pt 10% Rh thermocouple, the leads to which were inserted in a two-holed 1/32-inch diameter alumina protection tube. This in turn was inserted into a long, thin-walled (0.012-inch thick) quartz well which was welded and sealed to the quartz ampoule. This fit into a 0.14 cm diameter 26-cm deep hole drilled in the center of a GaAs feed rod of diameter 1.02 cm. Details

of the experimental setup are shown in Figure 44.

During the actual THM run, the shielded thermocouple was initially at about 6.0 mm above the top GaAs-Ga interface, passed through the 7 mm Ga zone and was finally located at about 6.0 mm into the grown crystal at the end of the travel. During this entire time period, the thermocouple output was continuously recorded on a chart recorder using a second Pt-Pt 10% Rh thermocouple immersed in an ice-bath as a reference junction. The result was converted to temperature and is plotted in Figure 45, together with the heater temperature profile measured with a thermocouple placed outside an identically loaded ampoule.

The measured "crystal temperature" cannot be analyzed quantitatively because the measurement conditions were not ideal for obtaining results with great accuracy. The silica wall which protected the thermocouple from the corrosive environment in which it was located also introduced errors in the temperature thus measured. Initially, the silica wall and the thermocouple were situated in the 0.14 cm diameter hole drilled in the GaAs feed rod. Measured temperatures were lower than the true crystal temperature because of the temperature drop between the thermocouple and the GaAs. At point B, the hole touched the top interface of the Ga zone. The subsequent sudden increase in temperature B-C was due to hot liquid Ga coming in contact and surrounding the silica well and the thermocouple. In a

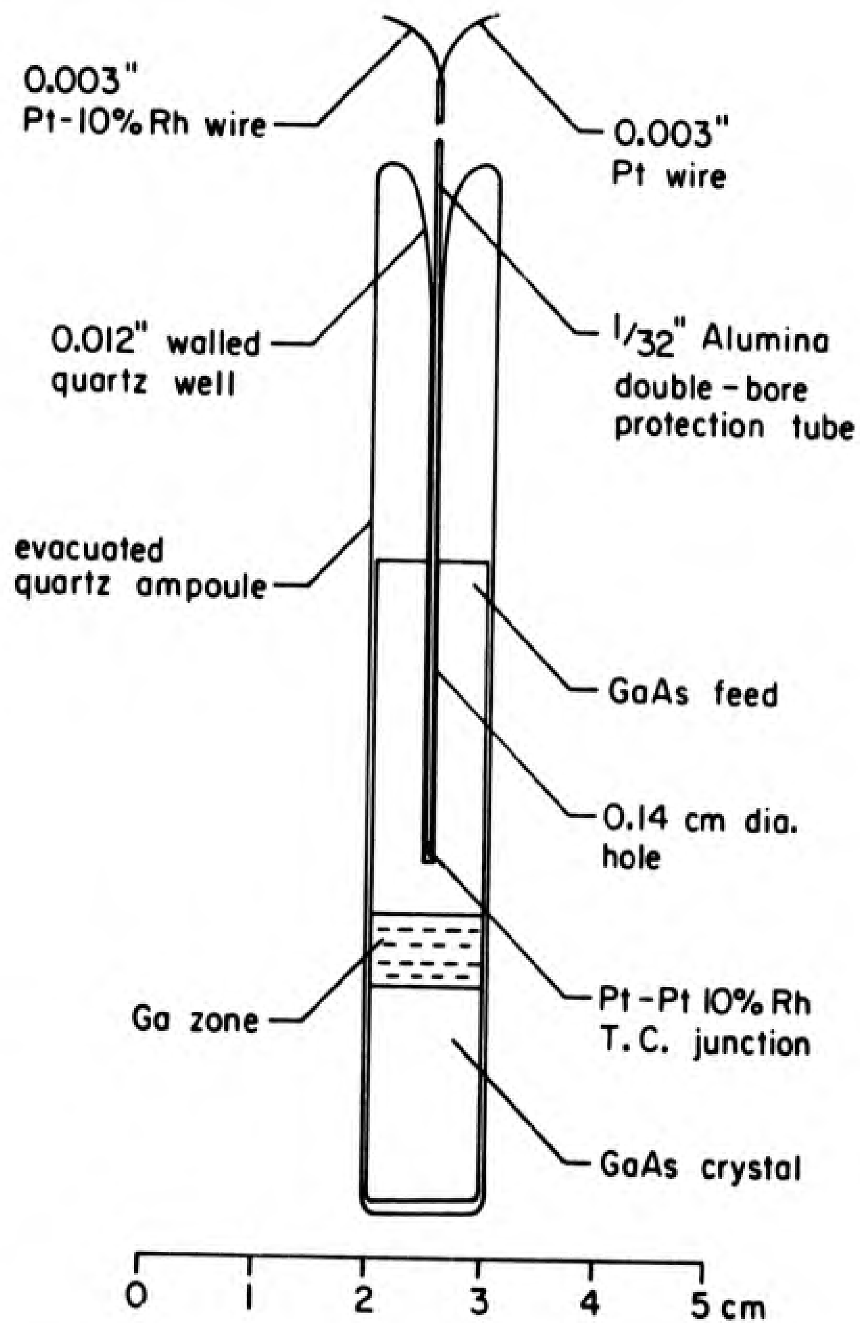

Figure 44: Assembled ampoule for measurement of temperature profile during THM growth.

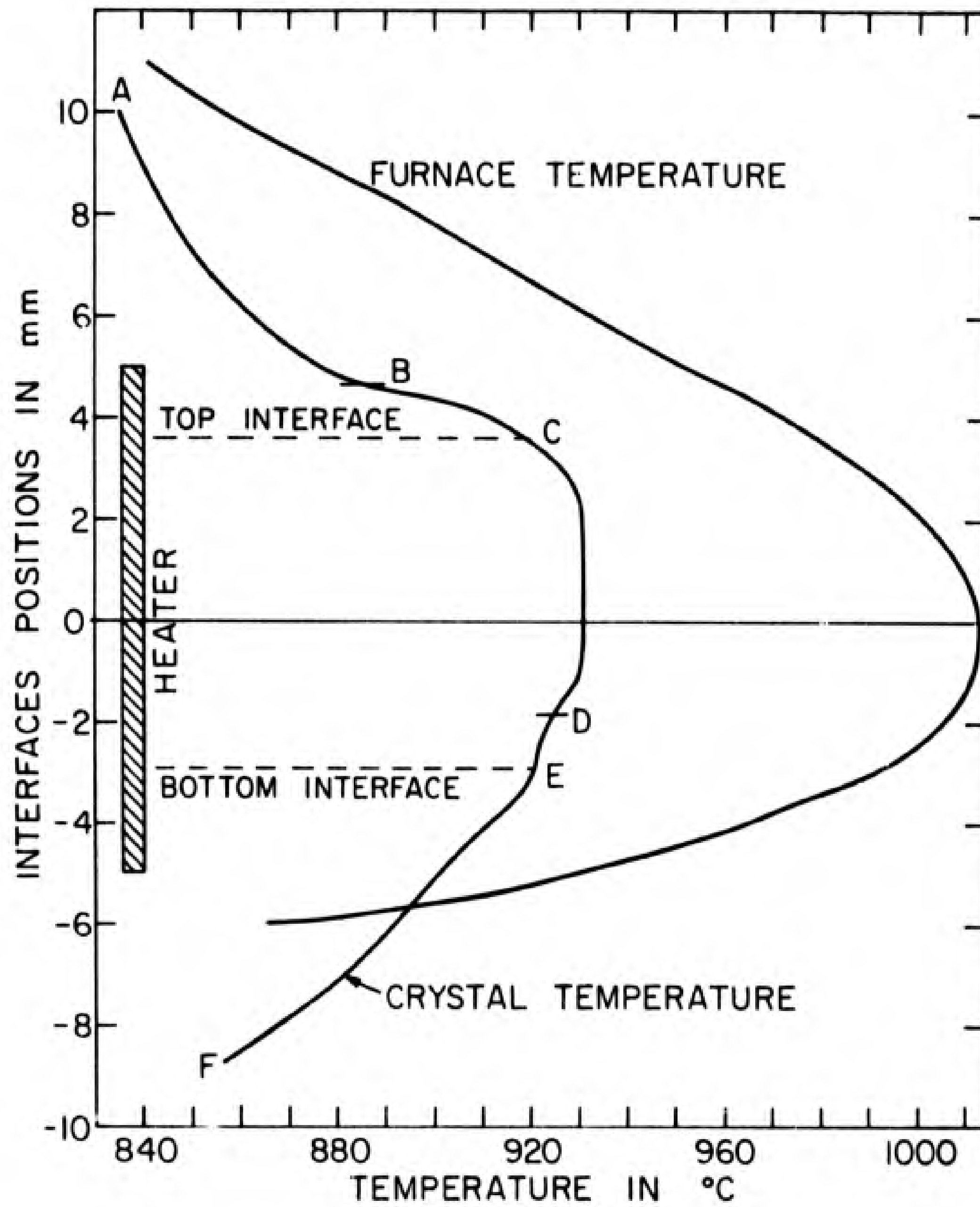

Figure 45: Measured temperature profiles inside and outside THM GaAs growth ampoule.

similar situation, the tip of the silica well (but not the thermocouple) first touched the bottom growth interface at point D and the temperature decreased until point E, where the thermocouple was surrounded by GaAs which had grown around it.

One important observation is that, except for some local fluctuations probably due to convection currents, the temperature within the Ga zone was uniform at 931°C. This gives a difference of 82°C from the measured maximum heater temperature of 1013°C outside the ampoule. This also points to the fact that it is important to consider and measure what the true growth temperature is in any crystal growth process, as it can be quite different from that measured outside the growth ampoule. It was also interesting to note from Figure 45, that, as expected, the temperature was about the same (~920°C) at the top (point C) and bottom (point E) interfaces, the top being a few degrees higher. Another important piece of information obtained was the temperature gradient at the bottom GaAs-Ga growth interface, about 40°C/cm.

The position of the thermocouple at different stages of the run was calculated using its initial and the final locations as reference points, the lowering rate was taken to be constant. The initial position was known from preparation of the ampoule, the exact final location of the thermocouple was determined by slicing the ingot

longitudinally after the run.

There are several limitations in the method of measurement employed here. The most important one being that the thermocouple was not in direct contact with the material whose temperature was to be measured. As mentioned previously, the silica well and other separations between the thermocouple and the surrounding introduced errors in the temperature readings. Conduction along the thermocouple leads is another source of error. As a whole, the measured readings would tend to be lower and any temperature gradients more "evened out" than the actual values. It is understood that the conditions of measurement were not ideal, the results obtained lack of accuracy and have only qualitative significance.

When the temperature measurement was terminated at point F, about 6 mm below the bottom interface, the heater power was abruptly turned off and the temperature was recorded with the ampoule stationary. In Figure 46 is plotted the difference between the thermocouple temperature and room temperature $(T-T_o)$ versus cooling time t in minutes. It was found that the temperature dropped rapidly from 798°C to 335°C in the first 30 minutes and afterwards followed an exponential decrease at a rate of approximately 1% per minute cooling time.

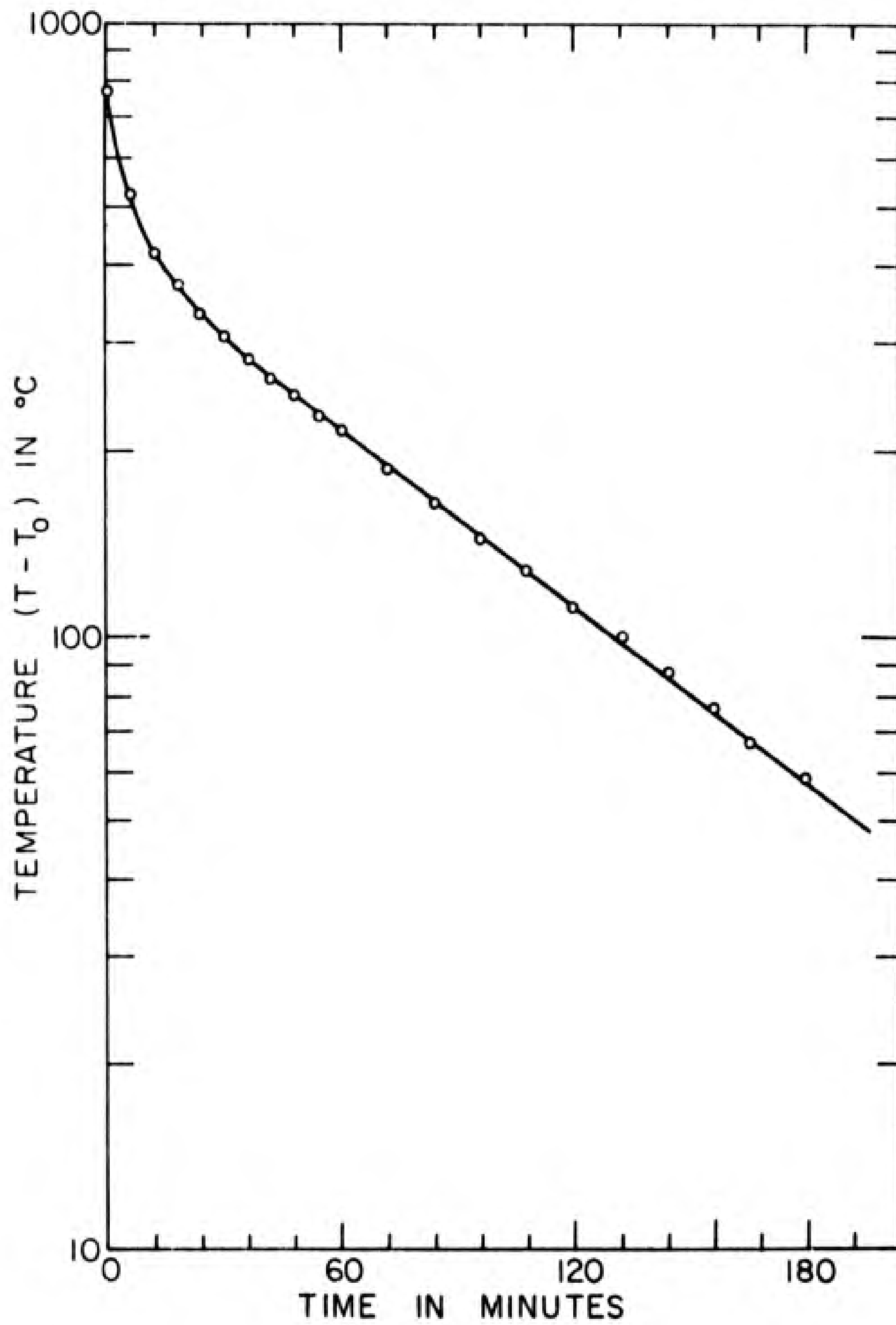

Figure 46: Excess crystal temperature versus cooling time at 6 mm below Ga zone at 931°C.

Chapter IV

TRAVELLING HEATER GROWTH OF MIXED III-V COMPOUNDS

Mixed III-V semiconductor compounds are used for acousto-electric, laser, optoelectronic, microwave and other electronic devices. The properties (such as the band gap and carrier mobility) of such material can be practically "tailor-made" by varying the composition. This makes crystal growth of mixed III-V compounds of great technological importance. This latter part of our research was devoted to a brief exploratory investigation of the THM growth of two such mixed compounds: $Ga_xIn_{1-x}Sb$ and $Ga_xAl_{1-x}As$. The former was chosen because of its low melting range and the availability of the material from another crystal growth project undertaken in our laboratory at that time. The $Ga_xAl_{1-x}As$ requires a higher growth temperature ($< 1000^oC$) but again the availability of the material was convenient for our investigation. The two systems chosen gave a good, representative experience in the investigation into THM growth of the mixed III-V's. The time and effort spent in this project was not intended to be exhaustive and the emphasis was on a qualitative, exploratory understanding which should lead to further extensive effort in this direction.

A. Travelling Heater Method Growth of $Ga_xIn_{1-x}Sb$

1. Sample preparation

As in THM growth of GaAs, cylindrical feed rods of $Ga_xIn_{1-x}Sb$ had to be prepared separately prior to assembly of the growth ampoule. Even though it is a ternary compound, the non-volatility of all three components and the low melting point (which should be between 525°C for InSb and 702°C for GaSb) makes the synthesis of the mixed compound into feed rods much simpler than for GaAs. Initially attempts were made to react quantities of the three elements in silica tubes with the head of an ordinary gas-oxygen torch. Passing a heater at a speed of several cm per minute over the tubes containing the material was also tried. The results in both cases were unsuccessful. The fused silica tubes cracked from solidification occurring at different parts simultaneously and the resultant ingots were inhomogeneous.

The appropriate amounts of six 9 parity elements corresponding to the desired $Ga_xIn_{1-x}Sb$ composition were placed in a carbonized fused silica tube. The carbon coating was necessary to prevent the cast ingots from sticking to the silica wall and cracking. The tubes were evacuated and sealed to yield ampoules for casting. Melting and mixing of the elements were done in the globar furnace used for vertical gradient freeze growth of GaAs (see Chapter III Section A2). The experimental requirements were not stringent here.

The elements were melted at a temperature of about 700°C. After the melt was mixed thoroughly by vigorously shaking the ampoule in the furnace, the ampoule was suddenly withdrawn and allowed to cool to room temperature. It was surprising that the ingots produced in this manner did not fracture and in most cases could be extracted by simply peeling away the cracked fused silica pieces surrounding them. Five ingots of the mixed compound prepared by casting are shown in Figure 47. The quenching and the vigorous mixing were necessary to avoid macro-inhomogeneities which would be undesirable for use in THM growth.

The preparation of the THM growth ampoule was similar to that for GaAs described in Chapter III. It was even simpler here since purity was not a concern and seeding was not used. The prepared ampoule consisted of a Ga-In melt zone (about 6 mm in length) of the desired composition and a $Ga_xIn_{1-x}Sb$ feed ingot contained in a sealed, evacuated fused silica tube.

2. Experimental Procedure

The same growth unit used for GaAs was employed here, although the technical requirements were less stringent because of the lower growth temperatures (below 600°C). The assembled ampoule was loaded with the Ga-In zone above the heater zone. After the steady state furnace temperature was reached, the ampoule was lowered at speeds in the range of 1 to 5 mm/day and self seeding

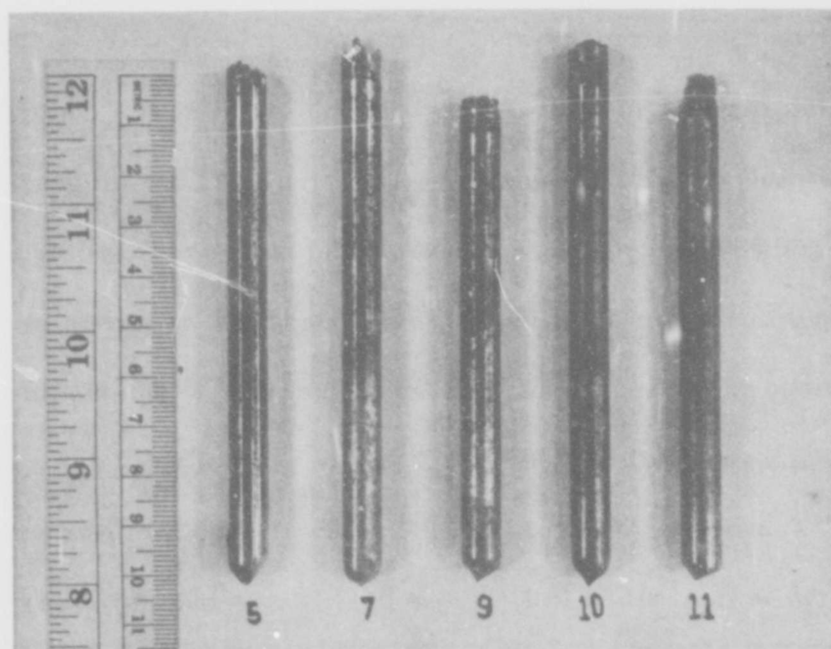

Figure 47: Five cast ingots of feed $Ga_xIn_{1-x}Sb$ material.

No. 5 and No. 7: $Ga_{0.9}In_{0.1}Sb$

No. 9 and No. 10: $Ga_{0.5}In_{0.5}Sb$

No. 11: $Ga_{0.7}In_{0.3}Sb$

growth began at the bottom of the ampoule. As a whole, the experimental procedure was similar to that adopted for THM growth of self-seeded GaAs without much modification.

3. Results and Discussions

The alloy system $Ga_xIn_{1-x}Sb$ has potential for use in Gunn oscillators and related devices. Bulk polycrystalline ingots have been grown by Plaskett and Wood[22] by the zone levelling technique with growth both from a stoichiometric melt and from a Sb-rich melt. They also grew epitaxial films of the compound from a Ga-In solution at 400°C. However, there are no reports on growth of the bulk material from a Ga, In or mixed Ga-In melts. In our investigation, two initial runs were made with a pure Ga melt and then a pure In melt, both at a heater temperature of 420°C. No material was found deposited at the bottom of the crucible after it travelled through the heater at 2 mm/day. A run (THM No. 74) was attempted, at a heater temperature 420°C, using a 1.4 Ga/In solvent zone and $Ga_{0.7}In_{0.3}Sb$ as feed and seed sections. Only about 2 mm of the material was deposited onto the polycrystalline seed section. Our experience from THM GaAs growth indicates that the solubility of the feed material in the solvent has to be greater than 5 to 6 at % for THM growth to be feasible. Thus the failures of THM growth attempts are not surprising. This is because the solubility of

GaSb in Ga is only 0.5 at % at 400°C.[41] The higher solubility of InSb in In (17 at % at 400°C) was insufficient to make growth possible since the feed material used was primarily GaSb. Therefore another attempt was made at a higher heater temperature of 600°C, which should correspond to a zone temperature of about 550°C (GaSb solubility in Ga is about 6 at % at this temperature). The run THM No. 75 proved successful and GaInSb grew by self-seeding on the bottom of the crucible. The details of this run and the unsuccessful runs mentioned earlier are listed in Table 14.

Subsequent to the initial attempts two successful growth runs were performed at a heater temperature of 600°C and a lowering rate of 2 mm/day. The feed composition was $Ga_{0.5}In_{0.5}Sb$ for THM No. 77 and $Ga_{0.9}In_{0.1}Sb$ for THM No. 87. The composition of the initial solvent zone was Ga/(Ga+In) = 0.58 (atom ratio) for the former and Ga/(Ga+In) = 0.8 for the latter. The details are summarized in Table 14. The longitudinal sections of the product ingots are shown in Figure 48 together with a section from an ingot which was grown by slow freezing from the melt. It appeared that the THM grown ingots contained large longitudinal grains a few mm in width as contrasted to the cellular grains in the melt-grown material. Under a low power optical microscope, no solvent inclusions were observed in the solution grown ingots, nor was there evidence of microsegregation of Ga Sb or InSb in the material. However, there

TABLE 14. SUMMARY OF TRAVELLING HEATER EXPERIMENTS ON $Ga_xIn_{1-x}Sb$.

Run THM	Heater Temp.	Seed	Original Zone Composition	Original Feed Length and Composition	Lowering Rate (mm/day)	Results
68	420°C	Self Seed	2.5 g Ga	3.0 cm $Ga_{0.7}In_{0.3}Sb$	2.0	No growth achieved.
69	420°C	Self Seed	5.5 g In	3.0 cm $Ga_{0.7}In_{0.3}Sb$	2.0	No growth achieved.
74	420°C	$Ga_{0.7}In_{0.3}Sb$	1.32 g Ga 1.57 g In	1.5 cm $Ga_{0.7}In_{0.3}Sb$	1.0	Only 2 mm deposited on seed. Temperature apparently too low for growth.
75	600°C	Self Seed	1.25 g Ga	2.0 cm $Ga_{0.7}In_{0.3}Sb$	1.0	Growth seemed successful.
77	600°C	Self Seed	1.33 Ga 1.57 g In Atom ratio Ga/In = 1.4	3.5 cm $Ga_{0.5}In_{0.5}Sb$	2.0	3.3 cm polycrystal successfully grown. Large grains were present with no solvent inclusion.
87	600°C	Self Seed	2.0 g Ga 0.82 g In Atom ratio Ga/In = 4.0	2.5 cm $Ga_{0.9}In_{0.1}Sb$	2.0	Large-grained polycrystal with no inclusions. There were cracks along the radial direction, as in THM-77

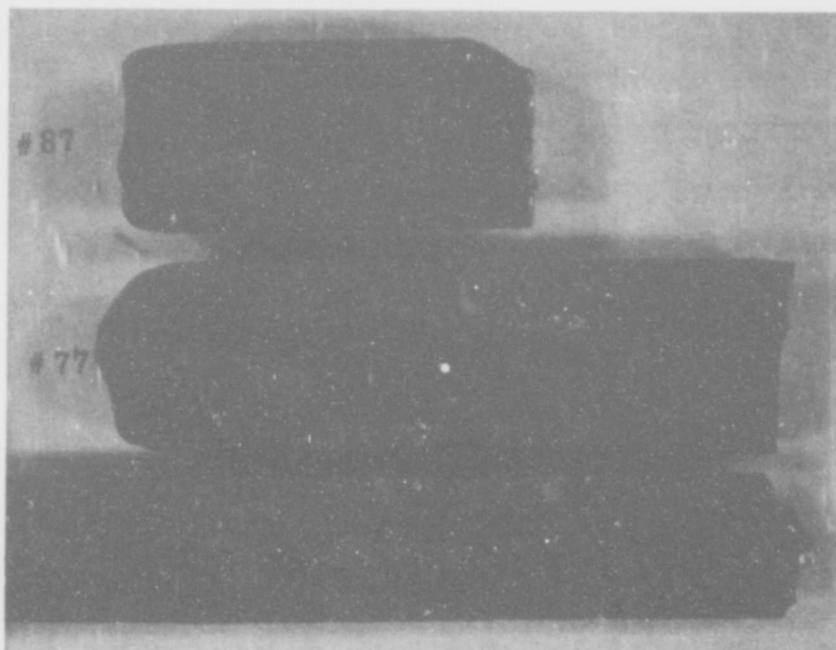

Figure 48: THM $Ga_xIn_{1-x}Sb$ ingots and slow-cooled casting grown from feed material $Ga_{0.5}In_{0.5}Sb$ (THM-77) and $Ga_{0.9}In_{0.1}Sb$ (THM-87 and casting).

appeared to be cracks along the radial direction throughout the length of the ingots. This could be due to stress from the compositional variations along the ingot.

Since this investigation was meant to be exploratory in nature, no extensive characterization of the properties of the grown material was performed. One of the most important and interesting properties of mixed compounds is the variation in composition of the grown material. Small cross-sectional pieces of material were sliced at intervals along ingots THM-77 and 87 and submitted for semi-quantitative analysis to Pacific Spectrochemical Laboratory (Los Angeles, California). The results were converted from weight % to atom % and summarized in Table 15 and Figure 49 for THM-77 and in Table 16 and Figure 50 for THM-87.

For THM-77, the concentration profile as shown in Figure 49 shows a downward dip towards the $Ga_{0.5}In_{0.5}Sb$ composition of the original feed material. Apparently steady state had not been reached after 33 mm of growth because the composition of the material was very different from that of the feed material. A more quantitative explanation can be found by referring to Ga-In-Sb solidus isotherm (Figure 51) presented in the work of Blom and Plaskett.[42] In our experiment, the initial solvent zone was of x = 0.58 in composition with a total weight of about 2.9 gm. The amount of feed

TABLE 15. ATOM RATIO x = Ga/(Ga+In) CALCULATED FROM Ga AND In WEIGHT % OBTAINED BY SPECTRO-CHEMICAL ANALYSIS OF SLICES TAKEN ALONG THE LENGTH OF INGOT THM-77 GROWN FROM A $Ga_{0.5}In_{0.5}Sb$ FEED AND A x = 0.58 ZONE.

Slice No.	Growth Distance	Ga wt. %	In wt. %	Calculated Atom Ratio x = Ga/(Ga+In)
77-1	2.0 mm	48.6	3.2	0.962
77-2	7.5 mm	46.3	3.6	0.955
77-3	14.0 mm	46.8	6.1	0.927
77-4	20.5 mm	41.4	6.5	0.913
77-5	26.5 mm	44.7	9.2	0.889
77-7	32.5 mm	32.9	16.0	0.772

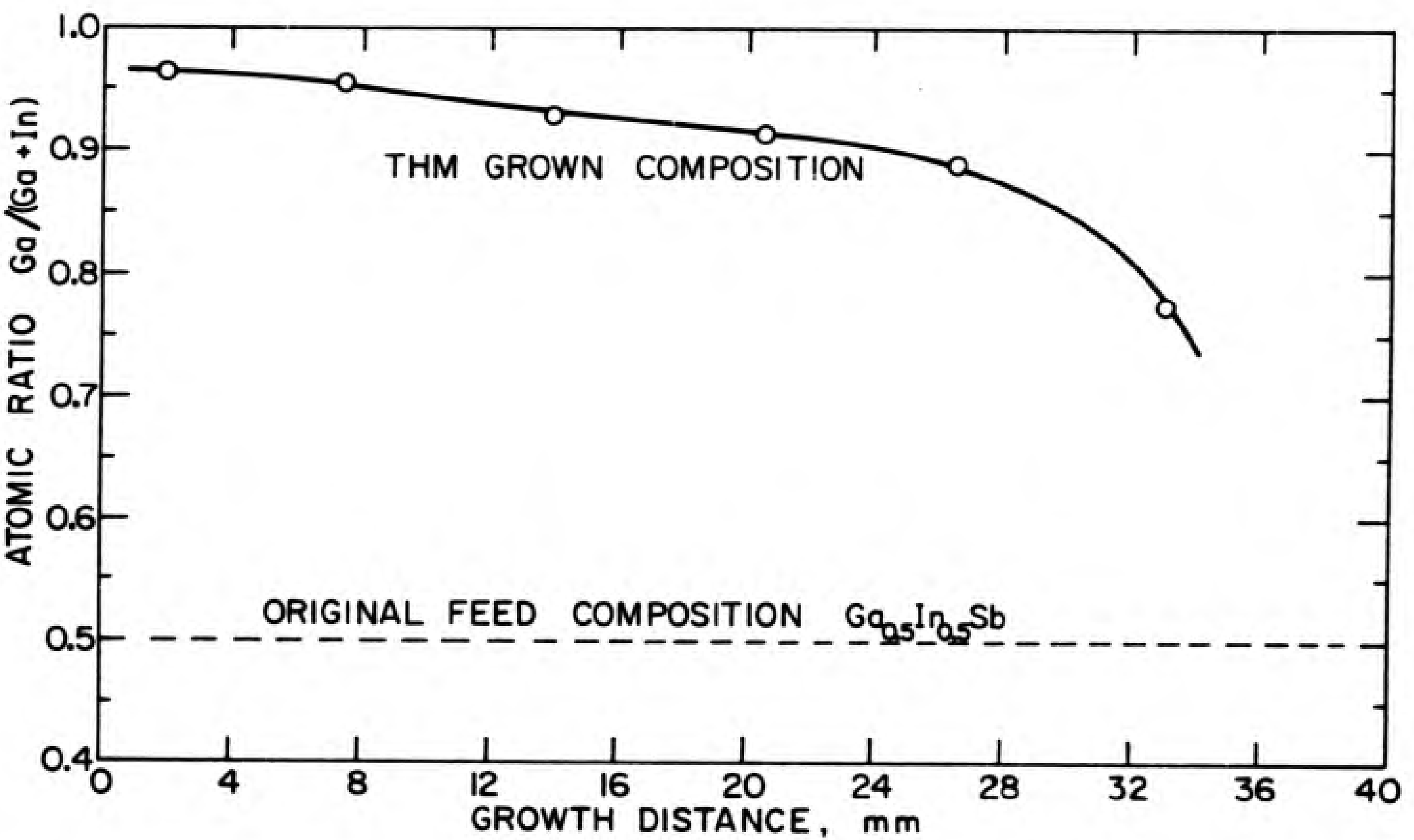

Figure 49: Atom fraction Ga/(Ga+In) versus distance along growth direction of ingot THM-77.

TABLE 16. ATOM RATIO x = Ga/(Ga+In) CALCULATED FROM Ga AND In WEIGHT % OBTAINED FROM SPECTRO-CHEMICAL ANALYSES OF SLICES TAKEN ALONG THE LENGTH OF INGOT THM-87 GROWN FROM A $Ga_{0.9}In_{0.1}Sb$ FEED AND A x = 0.8 ZONE.

Slice No.	Growth Distance	Ga wt. %	In wt. %	Calculated Atom Ratio x = Ga/(Ga+In)
87-1	2 mm	46.6	2.3	0.971
87-2	4 mm	51.7	2.2	0.975
87-3	10 mm	47.0	2.9	0.964
87-4	15 mm	47.4	4.6	0.945
87-5	17 mm	39.0	7.0	0.902
87-6	20 mm	49.2	3.8	0.964

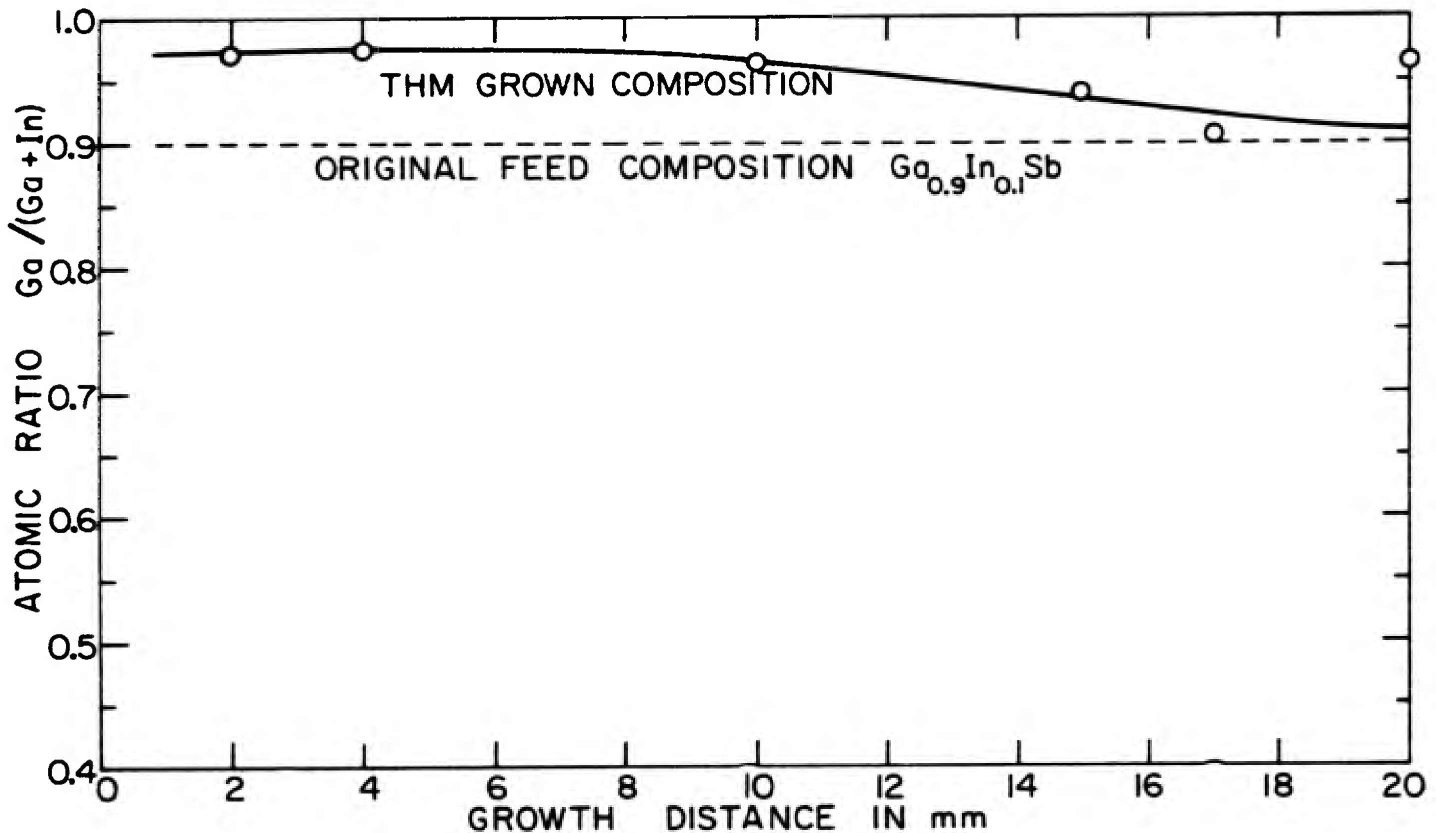

Figure 50: Atom ratio Ga/(Ga+In) versus distance along growth direction of ingot THM-87.

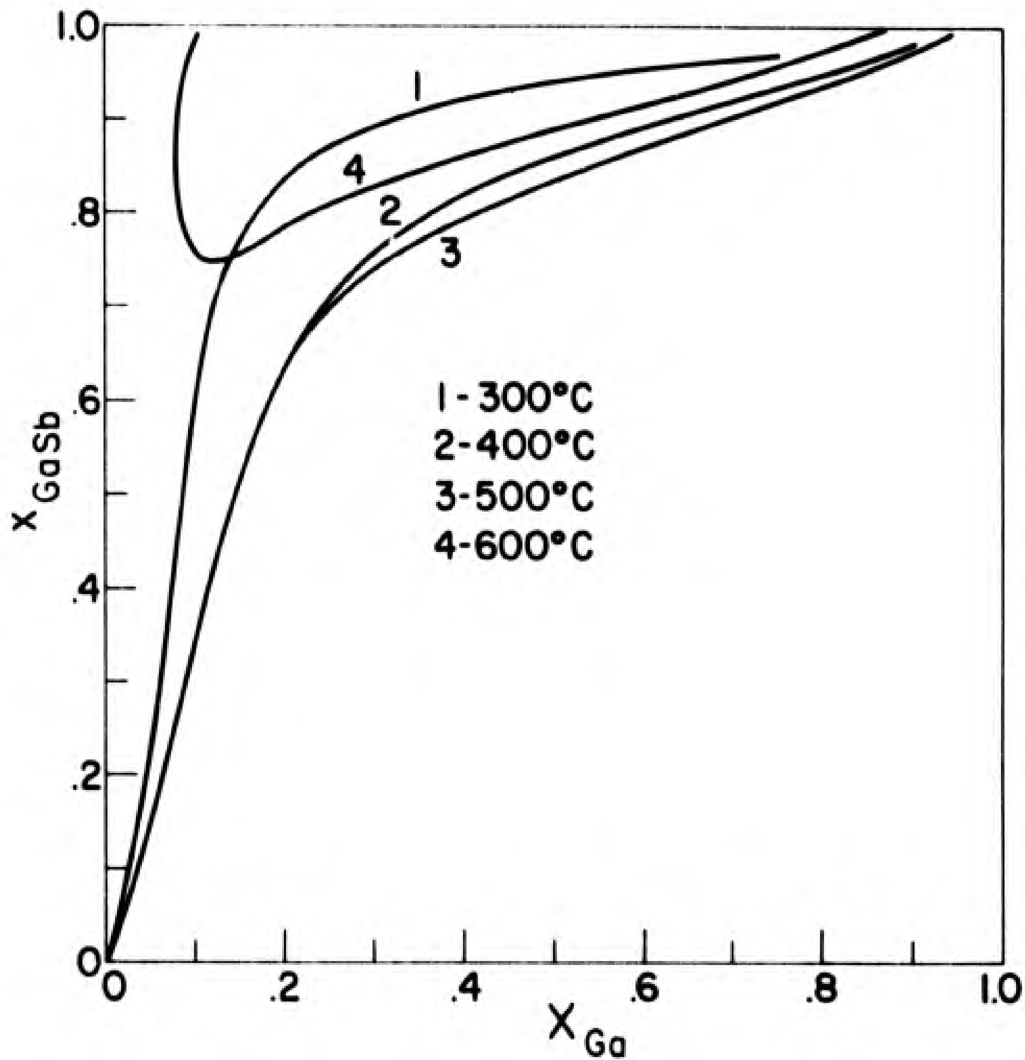

Figure 51: Calculated solidus isotherms for the Ga-In-Sb system. The GaSb fraction in the solid is plotted as a function of the Ga fraction in the liquid for four different temperatures. After Blom and Plaskett.[42]

$Ga_{0.5}In_{0.5}Sb$ dissolved when the zone was heated to ~550°C was probably small comparable to the original zone. The equilibrium zone should contain a Ga fraction of close to but slightly less than 0.58. Then, according to the theoretically calculated solidus curves of Fig. 51, the $Ga_xIn_{1-x}Sb$ crystallizing out of such a zone at ~550°C should have a Ga ratio $x \simeq 0.86$. The actual material first crystallized out was closer to $x \simeq 0.95$. This agrees with the work by Antypass[43] which showed experimentally that the x ratio in the crystallized solid is larger than that calculated by Blom and Plaskett.[42] Since x = 0.5 in the feed material, Ga was continuously being depleted from the zone during growth causing a gradual decrease in x of the solid crystalizing out. The composition of Ga in the final left-over zone was calculated from spectrochemical analysis as about 0.31. The solid crystallized out should be close to $Ga_{0.75}In_{0.25}Sb$ and this agrees well with the experimental data point at 33 mm in Figure 49. Apparently the composition of the solvent zone and the feed material was not chosen wisely in this case, which accounts for the undesirable non-uniform composition profile in the grown material. A solution zone with a Ga fraction of about 0.16 should be used for a feed of $Ga_{0.5}In_{0.5}Sb$, as could be deduced from Fig. 51.

On the other hand, the profile of THM-87 appears reasonably uniform with only 20 mm of growth. This can also be explained by

referring to the Ga-In-Sb solidus curves. The initial zone has a Ga ratio of about 0.8. The equilibrium solid composition should be approximately $Ga_{0.93}In_{0.07}Sb$, which was very close to the feed composition of $Ga_{0.9}In_{0.1}Sb$. The final zone contains Ga ratio of about 0.73 which should yield a solid composition $Ga_{0.9}In_{0.1}Sb$. This means that the steady state was reached and the material grown thereafter would have a uniform composition $Ga_{0.9}In_{0.1}Sb$.

In addition to the above qualitative discussion of the results of the two runs, a semi-quantitative material balance of the growth process could be applied here. Consider the THM configuration where the solution zone is of radius R and length ℓ. Let the composition of the component Ga be X_{fi} in the feed, X_{zi} in the zone and X_{ci} in the crystallized solid. If Y is the total number of moles crystallized at that stage and Z is the composition of the zone in g-atoms, then

$$Y = \frac{\pi R^2 y \rho_c}{M_c} \quad \text{and} \quad Z = \frac{\pi R^2 \ell \rho_z}{M_z} \qquad (1) \text{ and } (2)$$

Where y is the length of the crystallized solid, ρ_c and ρ_z are the densities of the crystal and zone respectively, M_c and M_z are the average atomic weight of the crystal and zone respectively.

Then from material balance consideration,

$$\begin{matrix}\text{gm at of component i} \\ \text{added to zone}\end{matrix} - \begin{matrix}\text{gm at of i} \\ \text{subtracted from zone}\end{matrix} = \begin{matrix}\text{change in gm at} \\ \text{in zone}\end{matrix}$$

That is,

$$X_{fi}dY - X_{ci}dY = ZdX_{zi} \qquad (3)$$

Since in the feed and crystal, half the atoms are antimony atoms, $X_{fi} = 2x_{fi}$ and $X_{ci} = 2x_{ci}$, where x_{ci} and x_{fi} are the ratio Ga/(Ga+In) in the crystal and feed respectively. So,

$$x_{fi}dY - x_{ci}dY = ZdX_{zi}$$

or

$$\frac{dY}{Z} = \frac{dX_{zi}}{(x_{fi} - x_{ci})} \qquad (4)$$

Figure 51 is in fact a plot of x_{ci} vs X_{zi} for Ga, it appears that for all the four temperatures (300, 400, 500, 600°C), the solidus isotherms for the range $X_{zi} = 0.3$ to 1.0 can be approximated by linear equations of the form

$$x_{ci} = a + kX_{zi} \qquad (5)$$

where a and k are constants.

Then equation (4) becomes

$$\left(\frac{\rho_c}{M_c}\right)\left(\frac{M_z}{\rho_z}\right)\frac{dy}{\ell} = \frac{dx_{ci}}{2k(x_{fi} - x_{ci})} \qquad (6)$$

The zone length ℓ is assumed constant. If the compositions of the zone and the crystallized solid do not change drastically during growth, the ratio $\left(\frac{\rho_c}{M_c}\right)\left(\frac{M_z}{\rho_z}\right)$ can be considered constant. The Eq. (6) is thereby integrated to yield,

$$y = \frac{\ell}{2k}\left(\frac{M_c}{\rho_c}\right)\left(\frac{\rho_z}{M_z}\right) \ln\left[\frac{(x_{fi}-x_{ci})}{(x_{fi}-x_{ci}^{o})}\right] \qquad (7)$$

where x_{ci}^{o} is the solid composition first crystallized out of the zone.

An exact quantitative reaction is known if the constant terms are known. In the present case there is some uncertainty regarding not only their values but the validity of the assumptions as well. However, it is instructive to replot the THM data in the form of Eq. (7) in order to compare with the theory developed above. Distance y versus $(x_{fi}-x_{ci})$ for THM-77 and 87 are summarized in Table 17 and plotted in Figure 52.

It appears that the plot for THM-77 is linear in excellent agreement with Eq. (66). The last data point at y = 32.5 mm deviated from the linear relationship because the sample had crystallized at the end of the run without contact with any feed material. There is a greater scatter in the data points of THM-87 from a linear relationship. This is expected as $x_{ci} - x_{fi} = 0.9$. The uncertainty in the crystal composition x_{ci} determined from spectrochemical analysis and the uncertainty in the feed composition x_{fi} are of the same order of magnitude as the difference term $(x_{fi}-x_{ci})$. Thus the error is the latter term is larger. The slopes of the two plots should be equal to $\frac{\ell}{k}\left(\frac{M_c}{\rho_c}\right)\left(\frac{\rho_z}{M_z}\right)$ and the intercepts should also be related to some constant related to that run. These were not evaluated here because several of the quantities needed were not known precisely. However, the general qualitative agreement with Eq. (66) has been demonstrated.

TABLE 17. GROWTH DISTANCE y(mm) VERSUS (x_{fi}-x_{ci}) FOR TWO $Ga_xIn_{1-x}Sb$ THM RUNS.

(A) THM-77 = x_{fi} = 0.5

distance y(mm)	x_{ci}	$x_{fi}-x_{ci}$
2.0	0.962	0.462
7.5	0.955	0.455
14.0	0.927	0.427
20.5	0.913	0.413
26.5	0.889	0.389
32.5	0.772	0.272

(B) THM-87: x_{fi} = 0.9

distance y(mm)	x_{ci}	$x_{fi}=x_{ci}$
2.0	0.971	0.071
4.0	0.975	0.075
10.0	0.964	0.064
15.0	0.945	0.045
17.0	0.902	0.002
20.0	0.964	0.064

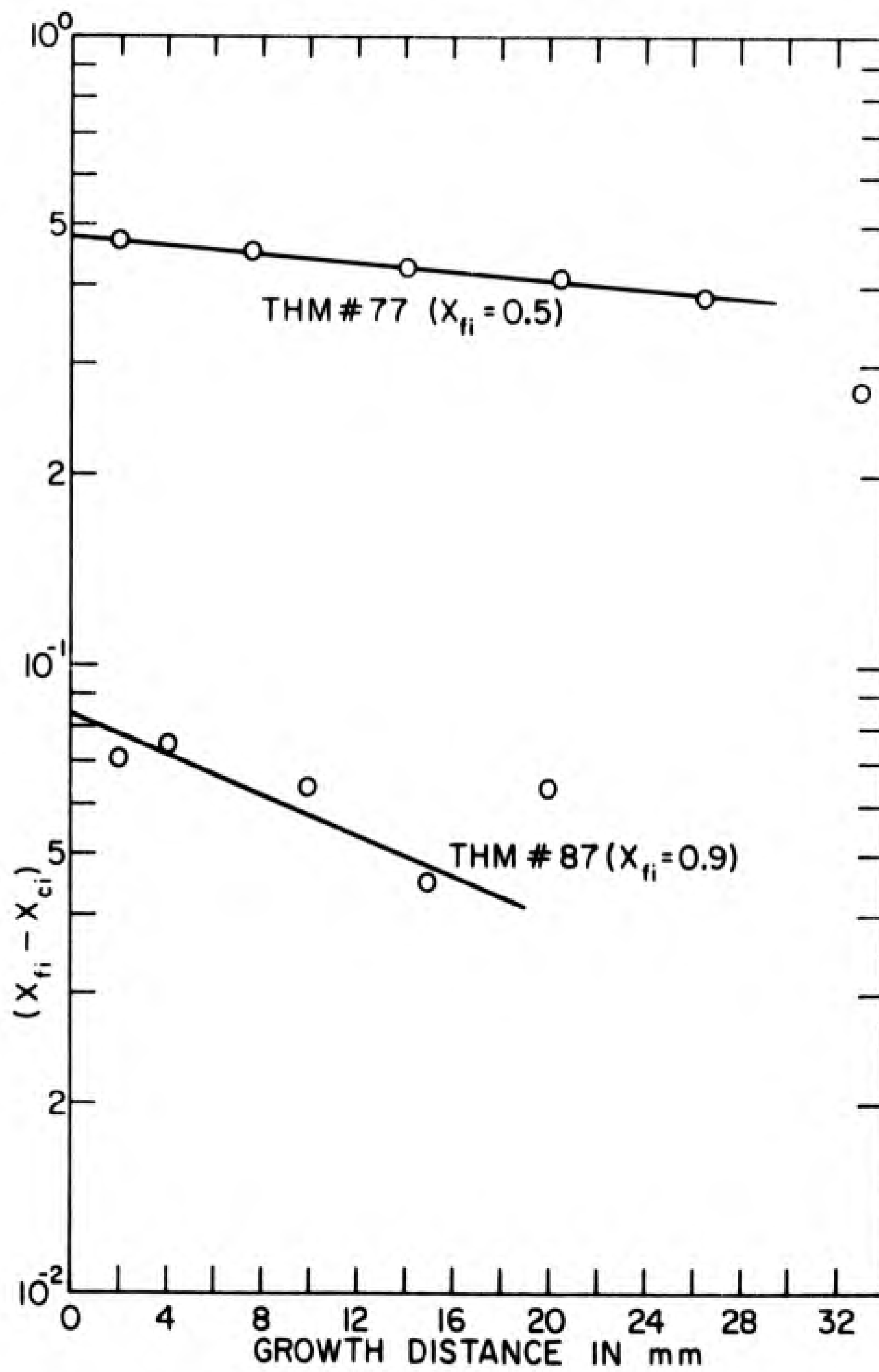

Figure 52: $(x_{fi}-x_{ci})$ versus growth distance in ingots THM-77 and THM-87.

B. Travelling Heater Method Growth of $Ga_xAl_{1-x}As$.

1. Sample preparation

The report by Bell et.al.[21] on THM growth of $Ga_xAl_{1-x}As$ was of great assistance in many aspects of the investigation carried out in our laboratory. For the growth of this particular mixed compound, the preparation of the feed material is a major problem. High purity AlAs is not available commercially, which makes the preparation of a sintered feed mixture of AlAs-GaAs impractical. It is not possible to use a Ga-Al-As elemental mixture as a feed charge because the Ga-Al alloy undergoes rapid oxidization and nitridization in air even at room temperature. A third alternative is to cast the feed ingot by slow cooling of solution. However, segregation of AlAs would make such material unattractive for THM use.

For the growth of a Ga-rich crystal of the mixed compound, it was found that an axially placed high purity Al wire(s), extending from the lower end of the Ga solvent zone to the top of a GaAs ingot, could be used satisfactory as feed material. The composition of the $Ga_xAl_{1-x}As$ feed material could be adjusted by using different relative amounts of Al and GaAs. This approach proved convenient and eliminated many of the problems previously mentioned. However, as will be discussed later in Section 3, the fused silica growth ampoules seriously reduced the concentration of Al in the solution

zone by chemical reaction at the high temperature used (> 1000°C). This difficulty was eliminated by performing the growth in a BN crucible, which was in turn enclosed in the usual evacuated fused silica ampoule. Single crystal GaAs was used as a seed in the growth of $Ga_xAl_{1-x}As$ because of availability and the small lattice mismatch between the two systems. A schematic of the assembled ampoule containing the BN crucible is shown in Fig. 53.

2. Experimental procedure

The procedure was similar to that employed in seeded growth of GaAs by THM. Unlike the growth of the low melting $Ga_xIn_{1-x}Sb$, a growth temperature in excess of 1000°C was necessary for $Ga_xAl_{1-x}As$ (see discussion in next section). This introduced several technical problems. To produce a growth temperature greater than 1000°C, the small diameter (gage 22) Pt-10% Rh heater temperature had to be raised to 1200-1300°C, which seriously shortened its life-time. Furthermore, the fused silica tube used as furnace core devitrified and fractured after several runs at that temperature. The opaque BN crucible made visual positioning of the Ga zone impossible. The introduction of BN, which has a thermal conductivity higher than that of quartz, also changed the thermal conditions of growth so that previous experience and knowledge on THM growth in fused silica ampoules could not be applied here directly. However,

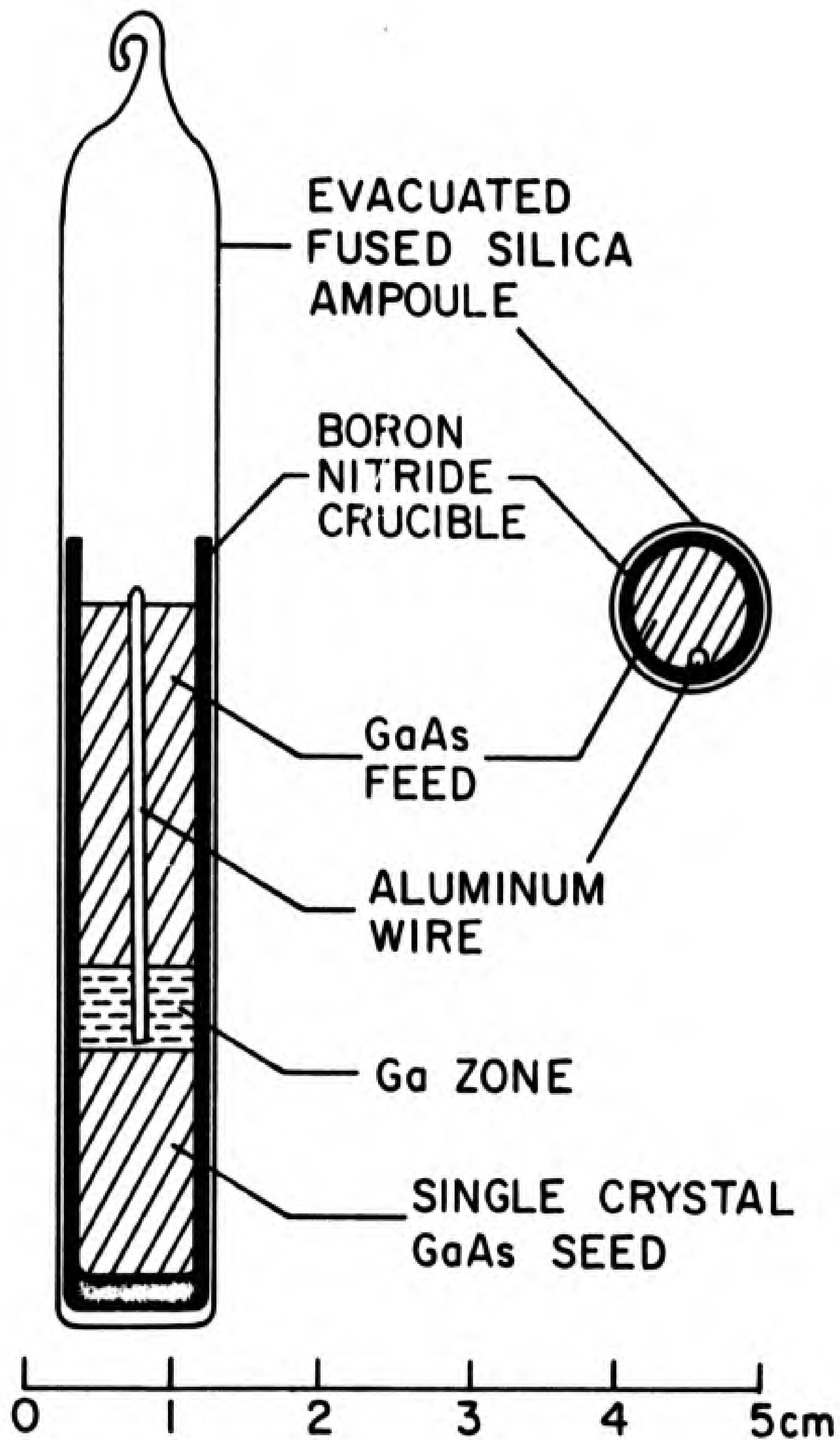

Figure 53: Ampoule showing axial Al wire together with GaAs feed, Ga zone and GaAs seed contained in a BN crucible assembled in the THM configuration.

an extensive research into THM growth of $Ga_xAl_{1-x}As$ was not the original intention, so that there was no effort at generating an ideal experimental procedure for its growth. One obvious immediate improvement which could be made is use of thicker gage heater wire wound on a larger diameter alumina (rather than fused silica) furnace core. The diameter of the ampoule could then be increased so that the mixed-alloy crystal grown in the BN crucible enclosed by the ampoule could be larger than the size (0.6 to 0.7 cm in dia.) possible with a 1 cm dia. ampoule.

3. Results and discussions

The results of three THM $Ga_xAl_{1-x}As$ runs are listed in Table 18. In the first two runs where the Ga-Al-As solution zone was in direct contact with the silica crucible wall, the growths were unsuccessful. The Al was depleted by the formation of white powder-like Al_2O_3 which ruined the seeding and disrupted the growths. This problem was eliminated by the use of a BN tube which was specially machined from a hot-pressed BN rod from the Carbon Products Division of Union Carbide Corporation (Chicago, Illinois). According to Bell et. al.[21], a pyrolytic BN tube would be better for the purpose because it will not tend to induce polycrystalline growth or introduce as much contamination, unlike the lower grade hot pressed material. However, the cost would be prohibitive.

TABLE 18. SUMMARY OF THM $Ga_xAl_{1-x}As$ GROWTH RUNS

Run THM	Heater Temp.	Seed	Original Zone Content	Original Feed Length and Composition	Lowering Rate (mm/day)	Results
80	1100°C	Self Seed	2.40 g Ga	13.12g GaAs + 0.07g Al $\approx Ga_{0.97}Al_{0.03}As$	4.0	White powder (Al_2O_3) on wall of quartz ampoule and on feed material. Unsuccessful.
82	1114°C	Self Seed	2.0 g Ga	$\sim Ga_{0.94}Al_{0.06}As$	2.0	Same as THM-80.
88	1110°C	GaAs seed 0.75 cm dia. 1.5 cm long ⟨111⟩As. direction	1.025 g Ga + 0.01 gAl	4.12 g GaAs + 0.024 g Al $\approx Ga_{0.97}Al_{0.03}As$	4.0	The growth took place inside a BN tube sealed inside the usual evacuated silica ampoule. No Al_2O_3 occurred and 1.5 cm of GaAlAs was seeded and successfully grown. New grains nucleated near the BN crucible wall and propagated into the bulk of the ingot.

One successful run (THM-88) was performed at 1110°C (which should correspond to about 1010°C zone temperature) and 4 mm/day lowering rate. Beginning at the (111) As seeding interface, new grains nucleated near the BN crucible wall (see Figure 53) and propagated into the bulk of the otherwise single crystal. This could possibly be due to a concave growth interface. There was no segregated Al_2O_3 or Ga solvent inclusions observed. The use of pyrolytic BN crucibles and better knowledge and control over the growth process should produce better results.

Slices were taken at different distances along the 1.5 cm grown material and submitted for spectrochemical analyses. The value of x in $Ga_xAl_{1-x}As$ was determined from the analytical results and presented in Table 19. Figure 55 shows a plot of atom ratio Ga/(Ga+Al) versus growth distance for the material. The lack of uniformity is probably due to the fact that the growth conditions had not reached steady state as the feed used and the grown length were small. The beginning end started from close to the GaAs seed composition and the final portion was also close to the pure GaAs composition. The apparent discrepancy of the low value of the point at 2.5 mm could be due to an error in the semi-quantitative analysis. More probably, it could be due to the analysis sample being taken from material which contained aluminum oxide. Apparently, more

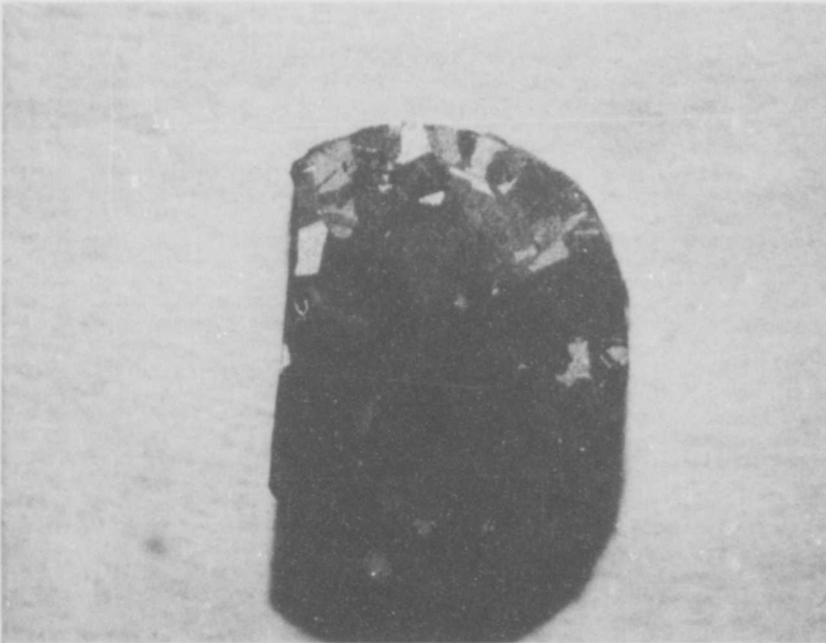

Figure 54: A slice from $Ga_xAl_{1-x}As$ THM-88 taken 2mm from the (111) As seed GaAs. The grains appeared to have nucleated at the BN crucible wall.

TABLE 19. ATOM RATIO Ga/(Ga+Al) CALCULATED FROM Ga AND Al WEIGHT % OBTAINED FROM SPECTROCHEMICAL ANALYSES OF SLICES TAKEN ALONG THE LENGTH OF CRYSTAL THM-88 WHICH WAS GROWN FROM A FEED OF $Ga_{0.97}Al_{0.03}As$.

Slice No.	Growth Distance	Ga wt. %	Al wt. %	Atom Ratio Ga/(Ga+Al)
88-1	Seed	56.0	0.005	0.999
88-2	0.5 mm	55.42	0.55	0.976
88-3	2.5 mm	52.39	1.6	0.927
88-4	5.0 mm	54.19	0.80	0.963
88-5	8.5 mm	54.21	0.39	0.982
88-6	11.5 mm	52.61	0.066	0.997

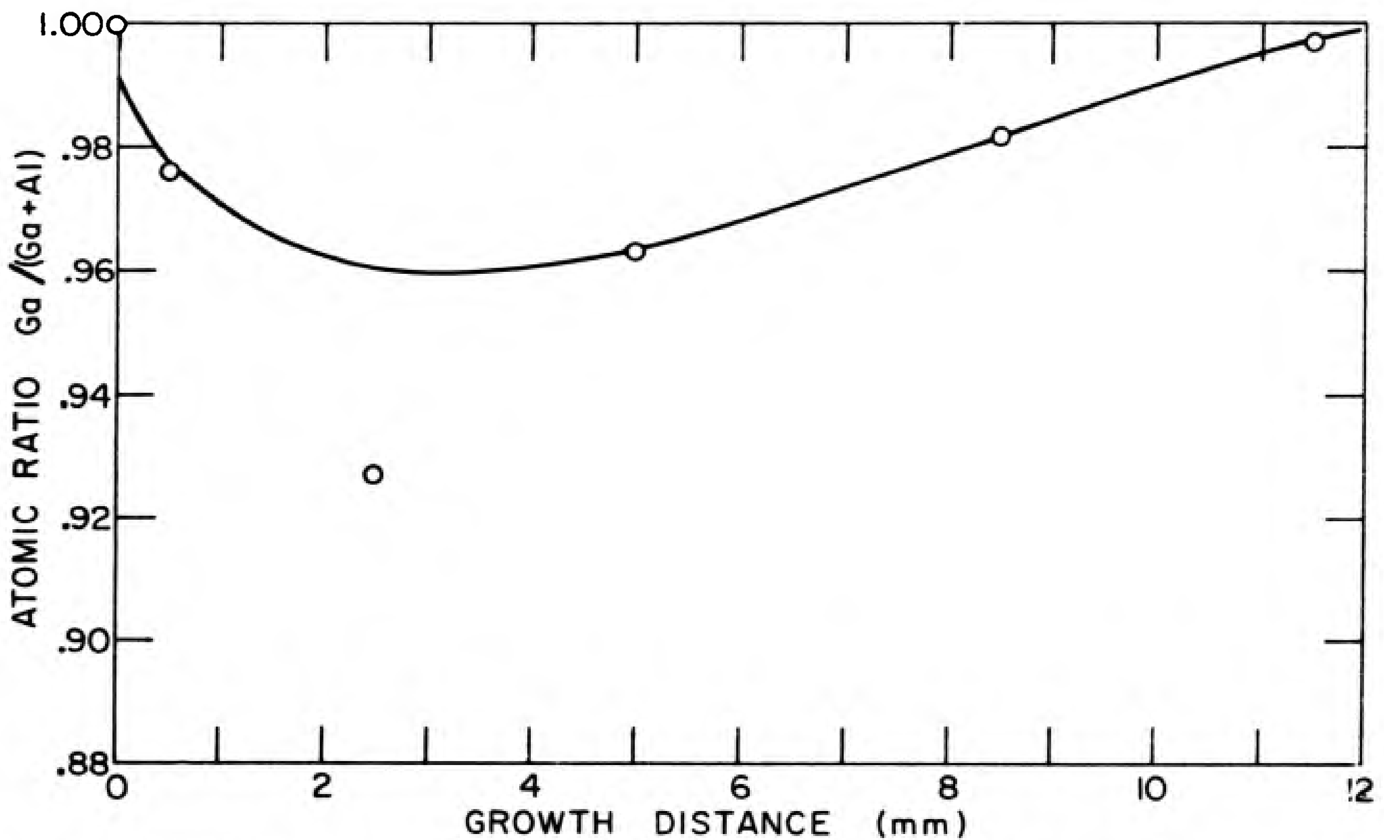

Figure 55: Atom ration Ga/(Ga+Al) versus growth distance in THM-88. Feed composition=$Ga_{0.97}Al_{0.03}As$, initial zone composition Ga/(Ga+Al)=0.975.

extensive theoretical and experimental work has to be done to achieve better understanding and control over the THM growth of $Ga_xAl_{1-x}As$. The sole successive growth run reported in this investigation only served as an exploratory attempt establishing the feasibility and some of the technical requirements of the experiment.

Chapter VI

CONSTITUTIONAL SUPERCOOLING IN TRAVELLING HEATER METHOD GROWTH

A. Expression for Constitutional Supercooling

Constitutional supercooling is a major problem in crystal growth because it causes breakdown of the growth interface resulting in formation of defects such as inclusions, and possibly new grains and twins . In crystallization of GaAs from a Ga solution onto a seed, the arsenic atom fraction X as a function of distance y from the crystal into the solution is shown in Figure 56(a). The corresponding equilibrium liquidus temperature distribution $T_L(y)$ determined from the Ga-As phase diagram is also shown in Figure 56(b) as a function of y.

At the solid-liquid interface, the gradient of the liquidus temperature can be expressed as:

$$\left.\frac{dT_L}{dy}\right)_{y=0} = \left.\frac{dT_L}{dX}\right)_{y=0} \left.\frac{dX}{dy}\right)_{y=0} = m \left.\frac{dX}{dy}\right)_{y=0} \qquad (8)$$

where m is the slope of the liquidus line at the interface temperature.

If the actual temperature gradient G in the liquid conformed to the dashed line A'B in Figure 56(b), the shaded region BB' would

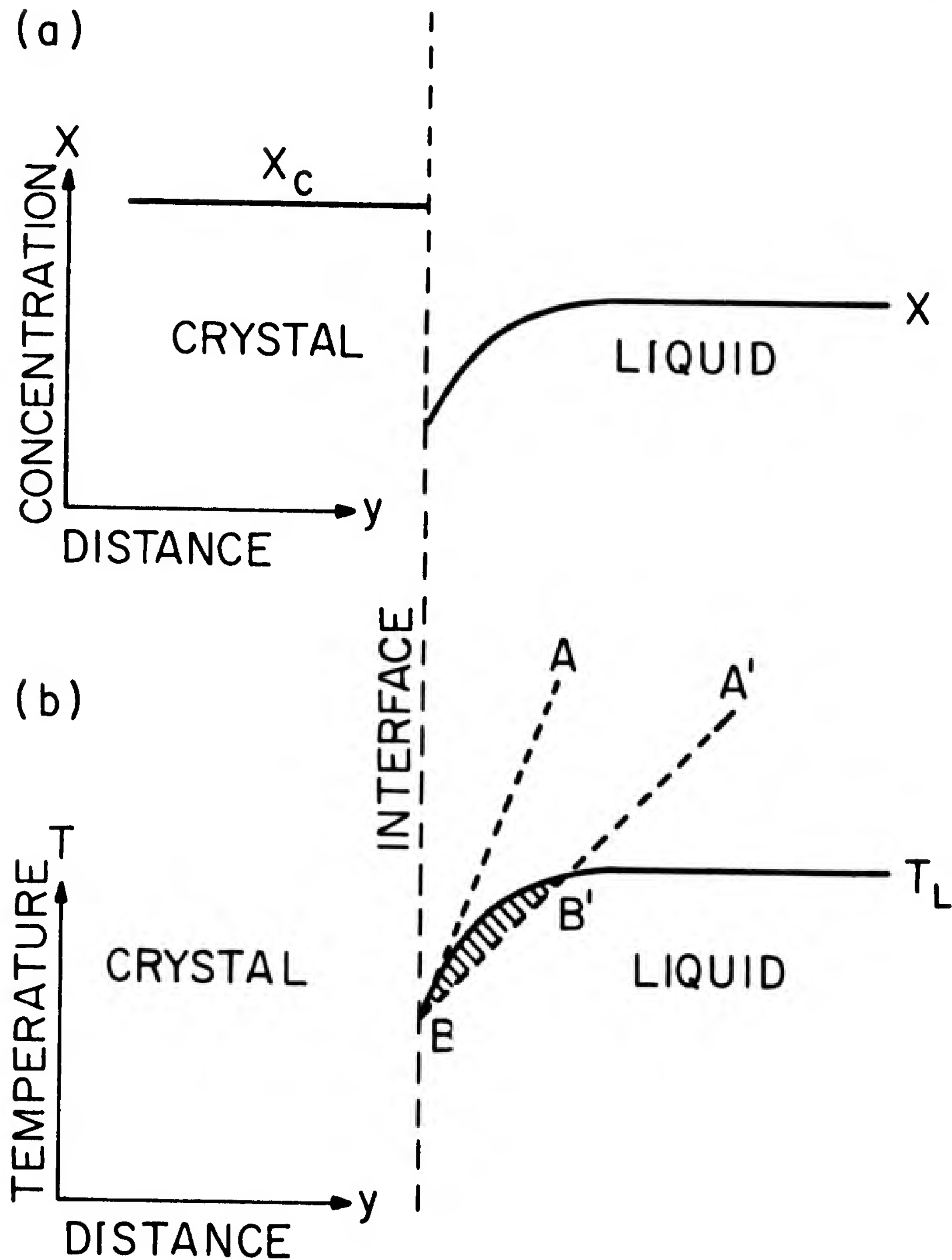

Figure 56(a): Atom fraction X of arsenic as a function of distance y into the Ga melt.

Figure 56(b): Equilibrium temperature distribution $T_L(y)$ determined from X(y) and the phase diagram.

be constitutionally supercooled, indicating that the interface morphology would be unstable with breakdown to cells, dendrites, etc. The criterion for no constitutional supercooling is thus given by:

$$\left.\frac{dT}{dy}\right)_{y=0} > \left.\frac{dT_L}{dy}\right)_{y=0}$$

or

$$G > m \left.\frac{dX}{dy}\right)_{y=0} \tag{9}$$

The dashed line AB indicates such a gradient which would prevent constitutional supercooling.

It is desired to derive an expression similar to Equation 9 in terms of specific parameters and quantities in THM growth. One returns to the basic concept of mass transfer at a crystallization interface where, for the component i,

total mass flux = diffusive flux + convective flux

In the crystallization flow formulation,[44] this can be expressed in the mole average velocity system as

$$VX_c C_c = J_i^* + V_{cf}^* C_\ell X \tag{10}$$

where V is the growth rate and V_{cf} is the crystallization flow X_c and X are the atom fraction of the solute in the crystal and in the liquid respectively, C_c and C_ℓ is the total atomic concentration in gm atom per volume in the crystal and in the liquid respectively.

Substituting the relations

$$V^*_{cf} C_\ell = V C_c \qquad (11)$$

and

$$J^* = -DC_\ell \frac{dX}{dy} \qquad (12)$$

for a binary, where D is the diffusion coefficient and $\frac{dX}{dy}$ is the concentration gradient of the solute, into Eqn. (9):

$$V X_c C_c = -DC_\ell \frac{dX}{dy} + V C_c X \qquad (13)$$

therefore

$$\frac{dX}{dy} = \frac{V C_c}{DC_\ell} (X_c - X) \qquad (14)$$

Substituting Eqn. (13) back into Eqn. (8), the criterion for no constitutional supercooling:

$$G > \frac{dT_L}{dy} = \frac{dT_L}{dX} \frac{dX}{dy} = m \frac{dX}{dy}$$

$$G > m \frac{V C_c}{DC_\ell} (X_c - X) \qquad (15)$$

We can thus define a "critical growth rate" V_c, below which constitutional supercooling can be prevented

$$V_c = \frac{GDC_\ell}{mC_c} \frac{1}{(X_c - X)} \qquad (16)$$

In THM growth, if the lowering speed is continuously increased beyond the value V_c, there will be a maximum value V_{max} above

which crystal growth fails, i.e. the growth rate is less than the lowering rate so that the zone moves out of the heater entirely. This phenomenon can be explained by considering the mass transfer equation,

$$V_c C_c X_c = K^* C_\ell \Delta X + V_c C_c X_\ell \tag{17}$$

where X_c and X_ℓ are the solute concentration in the crystal and the zone respectively, K^* is the overall mass transfer coefficient through the zone and ΔX is the concentration difference between the top and bottom interface. Consider a zone of approximately the same length as the heater being displaced downwards by a distance y (as shown in Figure 57(a)) which creates a concentration difference ΔX. We note that ΔX is proportional to ΔT, the temperature difference between the interfaces. Therefore the value ΔX should increase with increasing y and reach a maximum when the top interface is slightly below the center of the heater, as shown in Figure 57(b). However, the concentration X_ℓ in the zone decreases as y increases because the zone moves out of the heater and so the interface temperatures fall. Since from Eq. (17), the crystal growth rate V is proportional to both ΔX and X_ℓ, its value would also have a maximum value V_{max} with increased zone displacement y as shown in Fig. 57(d). Thus, if the lowering rate of the zone exceeds this value V_{max}, crystal growth will soon terminate. This phenomenon has been observed

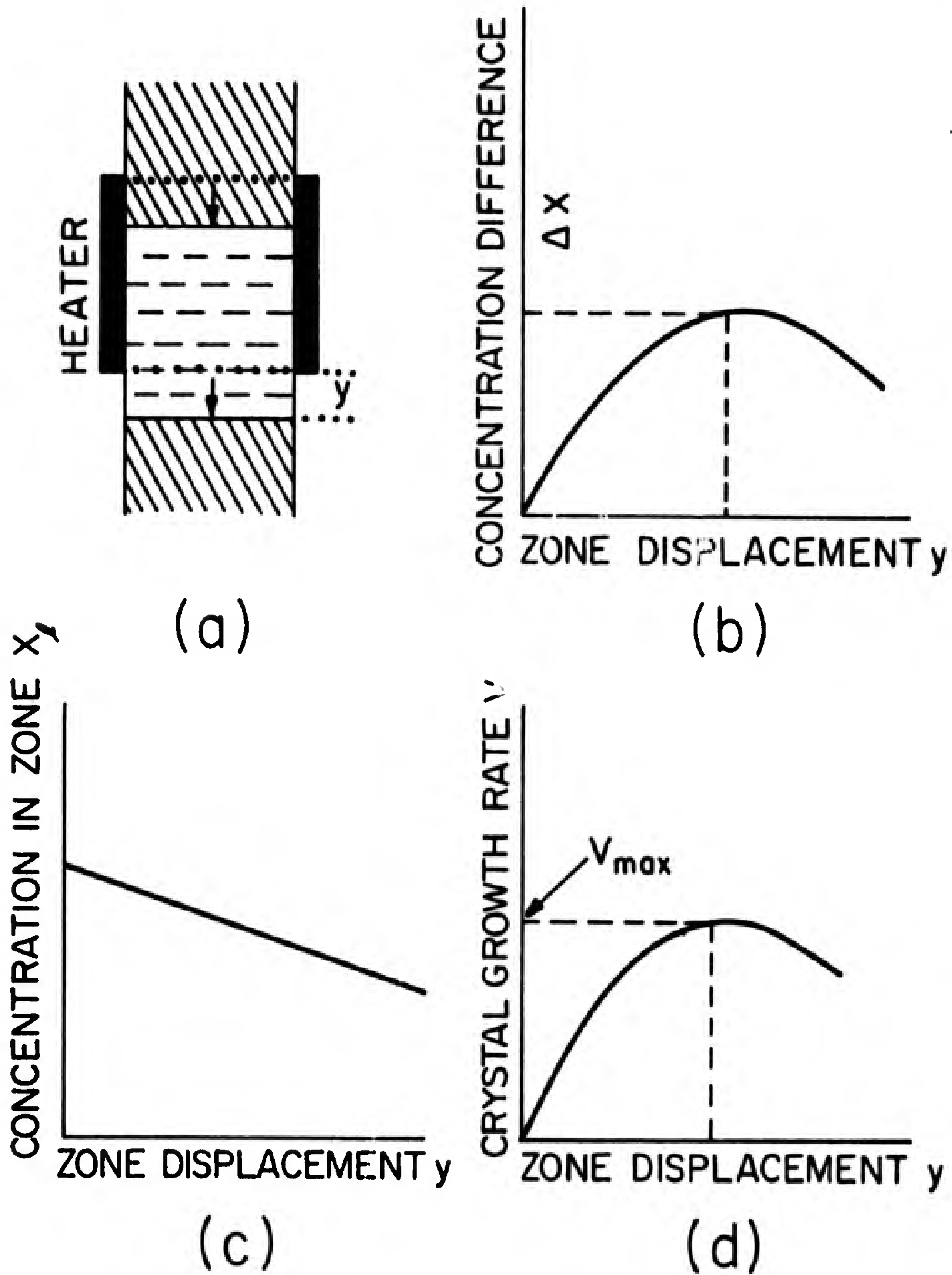

Figure 57: Illustration of the factors which determine the maximum lowering rate for THM growth.

in our THM growth of GaAs and $Ga_xIn_{1-x}Sb$ when the lowering speed is excessively high. Sometimes, at moderately high lowering rates, dissolution of the feed material would occur at the hotter periphery of the feed rod but not the center. In this case too, the crystal growth is essentially considered disrupted as there was no more travelling of a complete zone through the feed material. The end result is a feed rod with Ga smeared around the outside surface. The appearance resembled a corroded cylindrical rod of the material.

B. Constitutional Supercooling in THM Growth of GaAs.

In considering Eqn. (16) in relation to the GaAs system, X = 50 at. % for arsenic in the crystal. The ratio C_ℓ/C_c at growth temperature T can be approximated by:

$$\left(\frac{C_\ell}{C_c}\right)_T \simeq \frac{1}{2}\left(\frac{\rho_{Ga}}{\rho_{GaAs}}\right)_{T_0}\left(\frac{M_{GaAs}}{M_{Ga}}\right) \qquad (18)$$

where ρ_{Ga} and ρ_{GaAs} are the densities of Ga and GaAs respectively, M_{Ga} and M_{GaAs} are the atomic weight of Ga and molecular weight of GaAs respectively. At room temperature T_0 (27°C), ρ_{Ga} = 6.10 g/c.c. and ρ_{GaAs} = 5.32 g/c.c. and we have

$$\frac{C_\ell}{C_c} \simeq \frac{1}{2}\left(\frac{6.10}{5.32}\right)\left(\frac{144.64}{69.72}\right) \simeq 1.189 \qquad (19)$$

The liquidus slope m and solubility X can be read off the Ga-As

phase diagram in Hansen (See Appendix A). However, the solubility data for As in Ga in Hall's work [41] is provided in much greater detail in the temperature range of interest here (500-1000°C). This data as shown in Figure 58, is used for the determination of m in $^{\circ}$C/at.% and X at.%.

Unfortunately, measurements of the actual temperature gradient G at the GaAs-Ga growth interface during THM growth are difficutl to obtain. The only temperature measurement performed is described earlier in Chapter IV, Section C9. The value of G is found to be approximately 40°C/cm for an interface temperature of 920°C from Figure 45. The value $D = 1 \times 10^{-4}$ cm^2/sec from Mlavsky et.al[2] is used and m = 23°C/at.% and X = 7 at.% are taken from Figure 57 to calculate V_c at 920°C:

$$V_c = \frac{40 \times 2 \times 10^{-4}}{23(50-7)} \times 1.189 \frac{cm}{sec}$$

$$= 4.94 \frac{mm}{day} \qquad (20)$$

From the THM experimental evidence described in Chapter IV, Section C4, it was determined that at a interference temperature of 900°C, the ingot grown at 4.44 mm/day contained Ga inclusions. This value appears to correspond reasonably well to the V_c which was calculated above based on classical constitutional supercooling consideration.

As indicated earlier, the values of X and m are readily available

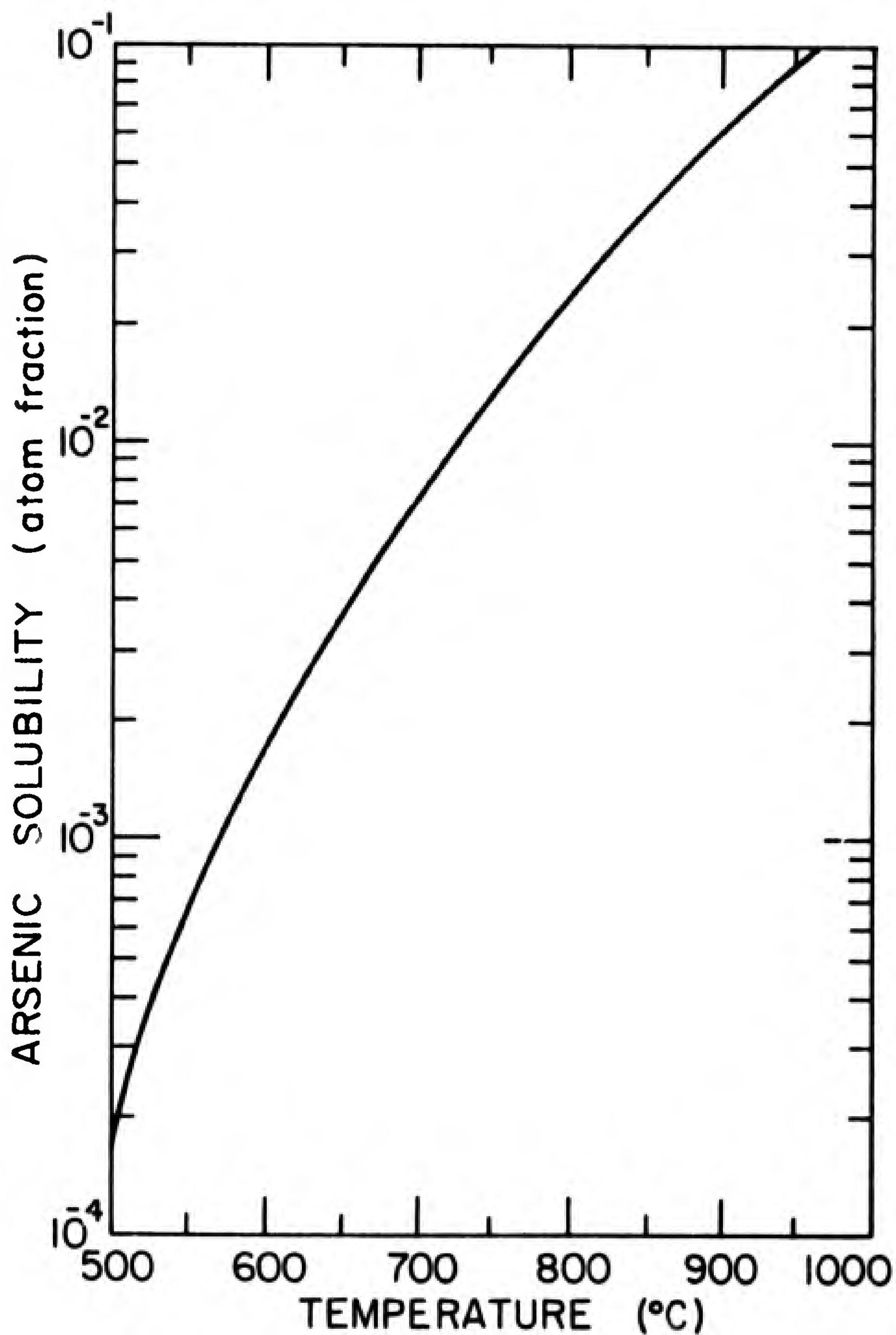

Figure 58: Arsenic solubility in Ga over the temperature range 500-1000°C. After R. N. Hall.[41]

from existing data in the literature. In order to calculate V_c at different temperatures the corresponding values of D and G must be known. There are only two known attempts at determining the diffusion coefficient D of As in a Ga melt. Mlvasky et. al.[2] obtained $D = 1 \times 10^{-4}\ cm^2 sec^{-1}$ from results on TSM growth of GaAs at 900°C. Lainer et. al.[45] determined the diffusion coefficient in a GaAs melt at 1255°C to be $1.5 \times 10^{-4}\ cm^2 sec^{-1}$. Since at the temperatures of interest for THM growth of GaAs, the concentration of As in Ga is not more than 10 at. %, the Nernst-Einstein relation $\frac{D\eta}{T}$ = constant was used to estimate values of D using values of the viscosity η of Ga at different temperatures taken from Reference 46 (plotted in Figure 59). The $D = 1 \times 10^{-4}\ cm^2 sec^{-1}$ at 900°C (1173°K) was taken as a reference value. The estimated values of D are tabulated in Table 20. It is interesting to note that the value for 1255°C is $1.516 \times 10^{-4}\ cm^2 sec^{-1}$, and it agrees with that determined by Lainer et. al.,[45] even though the former was calculated using the viscosity of a pure Ga melt rather than a GaAs melt.

Chang[33] used the system of naphthalene with benzoic acid as a solvent as the organic analog of THM growth of GaAs. The experimental conditions are similar to that in our investigation. The major difference was that the regions above and below the heater zone of temperature T_h were kept at a constant temperature T_c by cooler chambers with circulating fluid at that temperature. The temperature

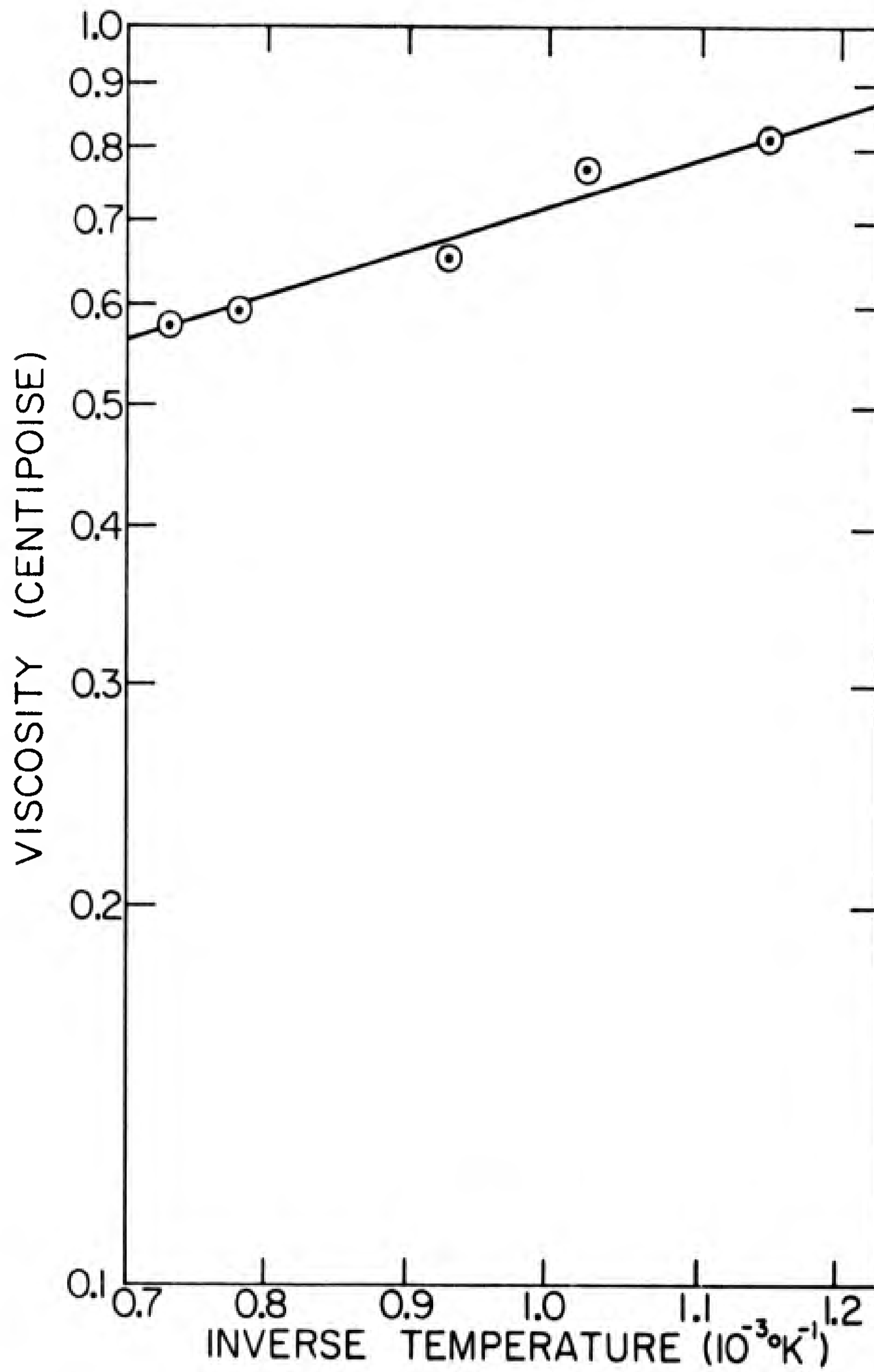

Figure 59: Plot of viscosity of pure Ga melt for the temperature range 500°C - 1000°C.

TABLE 20. CALCULATED VALUES OF DIFFUSION COEFFICIENT D USING VALUES OF Ga VISCOSITY η IN EQUATION $D\eta/T = 1.656 \times 10^{-7}$. THE * VALUES OF η ARE ESTIMATED FROM THE η vs 1/T PLOT IN FIGURE 59.

$T(^{o}C)$	$T(^{o}K)$	$\frac{1}{T}(10^{-3}\,{}^{o}K^{-1})$	η(cp)	D = $0.604(10^{-7})\frac{T}{\eta}\left(\frac{cm^2}{sec}\right)$
500	873	1.195	0.811	0.649×10^{-4}
600	973	1.028	0.770	0.758×10^{-4}
740	1013	0.990	0.711*	0.855×10^{-4}
775	1048	0.955	0.686*	0.918×10^{-4}
806	1079	0.925	0.652	0.993×10^{-4}
900	1173	0.857	0.648*	1.00×10^{-4}
920	1193	0.838	0.620*	1.155×10^{-4}
1010	1283	0.783	0.591	1.303×10^{-4}
1100	1373	0.730	0.578	1.425×10^{-4}
1255	1428	0.708	0.565*	1.516×10^{-4}

profile was thus close to a step-function type instead of the approximately Gaussian temperature profile in our system where solid insulation (bubbled alumina) surrounded the heater. For his system, an analytical expression for the temperature gradient G at the bottom interface which is inside the heater was derived by Chang as:

$$G = -\frac{V\rho\Delta H_f}{k} - a_1[(T_h - T_c)\exp(-a_2\delta_b) - (T_h - T_i)] \quad (21)$$

where V is the growth rate, ρ is the density of the crystal, ΔH_f is the latent heat of fusion, k is the thermal conductivity of the crystal,

$$a_1 = \frac{1}{2}\left[\frac{V_\rho C_\rho}{k} - \sqrt{\left(\frac{V_\rho C_\rho}{k}\right)^2 + \frac{8h}{Rk}}\right] \quad (22)$$

$$a_2 = \frac{1}{2}\left[\frac{V_\rho C_\rho}{k} + \sqrt{\left(\frac{V_\rho C_\rho}{k}\right)^2 + \frac{8h}{Rk}}\right] \quad (23)$$

T_h is the heater temperature, T_c is the cold bath temperature, T_i is the interface temperature, C_p is the heat capacity of the solid, δ_b is the height of the bottom interface above the bottom of the heater, h is the heat transfer coefficient at the crystal surface and R is the radius of the crystal.

The following properties of GaAs at 23°C are taken from Reference 47: ρ = 5.3 gm/cc , C_p = 0.084 cal/gm$^\circ$C, k = 0.193 cal/gm$^\circ$C sec, and ΔH_f = 73 cal/gm. The typical value of growth rate V, which is taken to be equal to the lowering rate of the ampoule, was of the order of mm/day or about 10^{-6} cm/sec. This value is

several orders of magnitude smaller than all the other parameters quoted above and so the terms $\frac{V\rho\Delta H_f}{k}$ and $\frac{V_\rho C_p}{k}$ are negligible. Thus Eq. (21) reduces to

$$G = -a_1[(T_h - T_c)\exp(a_2\delta_b) - (T_h - T_i)] \quad (24)$$

where

$$a_2 = -a_1 = \sqrt{\frac{8h}{Rk}} \quad (25)$$

Equations (24) and (25) can be used to estimate the temperature gradient G for THM growth of GaAs if δ_b is known. The temperatures T_h and T_c have to be interpreted according to the particular experimental conditions because the original expression (Eq. 21) was derived for a step-function temperature profile for the heater-cooler system.

It appears that unless the thermal conditions of growth are clearly defined and known, it is not possible to calculate the value of G from Eq. (24) and (25) since the values of T_i, T_c, δ_b, h and k are either not known or cannot be estimated accurately. Instead, the $G = 40^\circ C/cm$ measured for $T_h = 1010^\circ C$ was used as a reference and values of G at other temperatures could be estimated by assuming G proportional to the difference between the heater temperature and room temperature,

$$G = a(T_h - T_0)\frac{^\circ C}{cm} \quad (26)$$

However, at high temperatures where radiative heat loss is predominant, the heat transfer varies as the fourth power of absolute temperature. Thus it was assumed that,

$$G = b[(T_h+273)^4 - (T_0+273)^4] \simeq b(T_h+273)^4 \ \frac{^\circ C}{cm} \qquad (27)$$

In Eqs. 26 and 27, T_0 is the room temperature in $^\circ$C, a and b are constants. By equating to G = 40°C/cm at T_h = 1010°C, the constants are determined as $a \simeq 4 \times 10^{-2}$ cm^{-1} and $b \simeq 4.9 \times 10^{-12}$ c^{-3} cm^{-1}.

All the values necessary for the calculation of the critical growth rate V_c are now known or estimated. Estimated critical growth rates, $V_c = \frac{GD}{m} \frac{C_\ell}{C_c} \frac{1}{(X_c - X)}$, for the five heater temperatures (800, 850, 980, 1010, 1100°C) at which actual THM runs were performed are presented in Table 21. The eleven THM runs in Table 9 of Chapter III are plotted (with indication whether or not the resultant crystal contained Ga inclusions) in Figure 60 together with the critical growth rates V_c calculated with the two different estimated values of G. It appears that the classical constitutional supercooling criterion predicts fairly accurately the occurrence of Ga inclusions in THM. The discrepancy at higher zone temperatures such as at 1010°C, where inclusion free GaAs was grown at lowering rates as high as 20 mm/day, can be accounted for qualitatively by referring

TABLE 21. CALCULATIONS OF CRITICAL GROWTH RATE V_c BASED ON CONSTITUTIONAL SUPERCOOLING CRITERION IN THM GROWTH OF GaAs. THE * VALUES ASSUMED $G\alpha(T_h-T_0)$ AND THE ** VALUES ASSUMED $G\alpha(Th+273)^4$.

Heater Temp. Th(°C)	Zone Temp. T_i (°C)	Arsenic Solubility X(at. %)	Liquidus Slope $m\left(\frac{°C}{at.\ \%}\right)$	Diffusion Coefficient $D(cm^2 sec^{-1})$	Temperature Gradient $G\left(\frac{°C}{cm}\right)$	Critical Growth Rate $V_c\left(\frac{mm}{day}\right)$
800	740	1.2	60	$0.855(10^{-4})$	30.8* 19.6**	0.92* 0.59**
850	775	2.0	44	$0.918(10^{-4})$	32.8* 23.5**	1.47* 1.05**
980	900	6.0	25	$1.0(10^{-4})$	38.0* 23.5**	3.55* 3.40**
1010	920	7.0	23	$1.155(10^{-4})$	40* 40**	4.32* 4.32**
1100	1000	12.0	18	$1.300(10^{-4})$	46.8* 52.5**	7.25* 8.13**

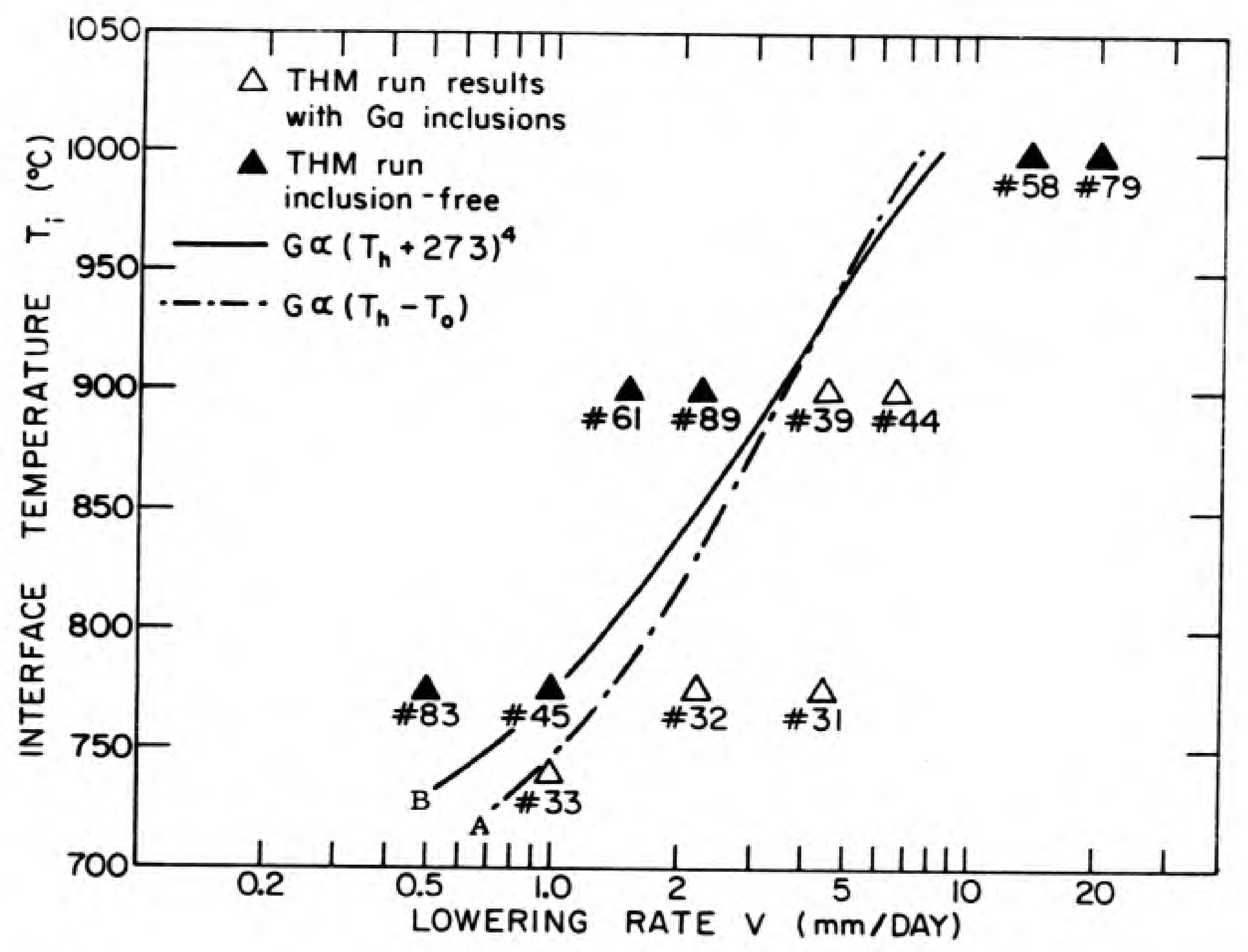

Figure 60: THM GaAs experimental results shown with curves calculated from criterion for constitutional supercooling. Curve A assumes $G\alpha(T_h - T_o)$. Curve B assumes $G\alpha(T_h + 273)^4$.

back to Eq. (21). The arsenic solubility in Ga is about 1 to 6 at. % for the 700 to 900°C range and increases markedly to 12 at. % at 1010°C. The larger As solubility increases the size of the zone relative to the heater for a fixed mass of Ga initially in the zone, thus decreasing the parameter δ_b for temperatures above about 900°C. Referring back to Eq. (21), this will increase the temperature gradient G. The corresponding values of V_c would be larger than that calculated in Table 21 and plotted in Figure 60.

In summary, the onset of constitutional supercooling estimated for THM growth of GaAs agrees fairly well with experimental evidence of interface breakdown and Ga inclusion trapping. It seems that interface temperatures of about 900°C which correspond to a V_c of about 3 to 4 mm/day in the present apparatus, are most convenient for THM GaAs growth. Lower temperatures necessitate inconveniently small lowering rates (below 1 mm/day) which may be hard to achieve because of small fluctuations in ampoule movement and temperatures. Temperatures higher than 1000°C introduce technical problems and increase contamination from the silica crucible.

C. Constitutional Supercooling in Multicomponent Systems

The growth of mixed alloy systems (such as mixed III-V compounds) in the gas and solution phase is of great technological

interest and importance. Unfortunately, the diffusion and mass transfer phenomena in such complex situations are not well understood, especially for multi-component growth from solution. Consequently, important theoretical information such as the criterion for constitutional supercooling is not available for use as a guideline for use in liquid-phase epitaxy or THM. There was an attempt by Tiller[48] to elucidate the constitutional supercooling criterion (c.s.c.) for a poly-component liquid system. The variation of the liquidus surface, $T_L(y)$, of the alloy ahead of the growing crystal face is a function of the solute contents $C_i(y)$ of its i constituents. The constitutional supercooling criterion was derived as,

$$\frac{G}{V} < \frac{1}{D_0} \sum_{i=1}^{n} \frac{[(\partial \overline{T}_L/\partial C_i)(k_0^i - 1)C_i(0)]}{D_i/D_0} \tag{28}$$

where D_0 is the diffusion coefficient of the solvent, $(\partial \overline{T}_L/\partial C_i)$ is the average value for the liquidus slope in the liquid, D_i is the diffusion coefficient of the i component, and $k_0^i = C_{ci}/C_i$ (where C_{ci} and C_i are the atom concentration of the ith component in the crystal and in the liquid respectively).

Equation (28) is not strictly correct as it was derived from the constitutional supercooling criterion for a binary system assuming that at the crystallization surface the concentration gradient dC_i/dy is given by,

$$D_i\left(\frac{dC_i}{dy}\right)_{y=0} = V(C_{ci}-C_i) \tag{29}$$

Actually, diffusion and mass transfer in a multi-component system are complex phenomena and a simple relationship such as Eq. (28) is not applicable. To derive a correct relationship, it is necessary to start with the fundamental mass transfer concept:

$$\begin{matrix}\text{total mass transfer flux} \\ \text{of component i}\end{matrix} = \begin{matrix}\text{diffusion flux} \\ \text{of i}\end{matrix} + \begin{matrix}\text{convective flux} \\ \text{of i}\end{matrix}$$

Expressed in a form similar to Eq. (10) given earlier in section A, it becomes,

$$VX_{ci}C_c = J_i^* + V_{cf}^*C_\ell X_i \tag{30}$$

where the following conditions are true:

$$\sum_i^n J_i^* = 0 \tag{30a}$$

$$\sum_i^n X_i = 1 \tag{30b}$$

Eq. (30) is rewritten as

$$VX_{ci}C_c = J_i^* + VC_cX_i \tag{31}$$

Now, the constitutional supercooling criterion for an n-component system is expressable as,

$$G < \nabla T_L = \sum_{i=1}^{n-1} \left(\frac{\partial T_L}{\partial X_i}\right)_0 \nabla X_i \qquad (32)$$

because the liquidus temperature T_L can be expressed in terms of the concentration of the components:

$$T_L = T_L(X_1, \ldots X_i, \ldots X_{n-1}) \qquad (33)$$

To obtain the terms ∇X_i it is necessary to refer to the formula[49] for the mass flux J_i^*,

$$J_i^* = \frac{c^2}{\rho RT} \sum_{\substack{j=1 \\ i \neq j}} M_i M_j D_{ij} \left[X_j \sum_{k=1}^{n} \left(\frac{\partial \mu_i}{\partial X_i}\right)_{\substack{T, p, X_s \\ s \neq j, k}} \nabla X_k \right] \qquad (34)$$

where C is the total molar concentration of the fluid, ρ is the fluid density, R is the gas constant, T is the temperature, M_i and M_j are the molecular weights of the i and j components, D_{ij} are the multi-component diffusion coefficients, μ_j are the chemical potentials.

If all the parameters in Eqn. (34) are known except ∇X_k, there are n equations with n unknowns so that the latter could be determined, at least in principle.

For the simple case of an ideal solution (activity coefficient $\gamma = 1$) where $\mu_j = \mu_j^o + RT \ln X_j$, and therefore Eq. (34) reduces to

$$J_i^* = \frac{c^2}{\rho} \sum_{\substack{j=1 \\ i \neq j}}^{n} M_j D_{ij} \nabla X_j \qquad (34a)$$

For a binary system A-B,

$$J_A^* = \frac{c^2}{\rho} M_B D_{AB} \nabla X_B \tag{34b}$$

Since, $X_A + X_B = 1$ and $\nabla X_A + \nabla X_B = 0$, Eq. (34b) becomes $J_A = -\frac{c^2}{\rho} M_B D_{AB} \nabla X_A$, which is the ordinary diffusion flux equation for component A in a solution of A-B. This confirms the validity of Eq. (34).

Since mixed III-V and other three component systems are of the greatest importance, we will examine in detail the present case where n = 3 for Eq. (34). Thus we have,

$$
\begin{aligned}
J_1^* &= \frac{c^2}{\rho RT} \sum_{\substack{j=1 \\ j \neq i}}^{3} M_1 M_j D_{ij} X_j \left[\frac{\partial \mu_j}{\partial X_1} \nabla X_1 + \frac{\partial \mu_j}{\partial X_2} \nabla X_2 + \frac{\partial \mu_j}{\partial X_3} \nabla X_3 \right] \\
&= \frac{c^2}{\rho RT} \left\{ M_1 M_2 D_{12} X_2 \left[\frac{\partial \mu_2}{\partial X_1} \nabla X_1 + \frac{\partial \mu_2}{\partial X_2} \nabla X_2 + \frac{\partial \mu_2}{\partial X_3} \nabla X_3 \right] \right. \\
&\qquad \left. + M_1 M_3 D_{13} X_3 \left[\frac{\partial \mu_3}{\partial X_1} \nabla X_1 + \frac{\partial \mu_3}{\partial X_2} \nabla X_2 + \frac{\partial \mu_3}{\partial X_3} \nabla X_3 \right] \right\} \\
&= \frac{c^3}{\rho RT} M_1 \left[M_2 D_{12} X_2 \frac{\partial \mu_2}{\partial X_1} + M_3 D_{13} X_3 \frac{\partial \mu_3}{\partial X_1} \right] \nabla X_1 \\
&\quad + \frac{c^2}{\rho RT} M_1 \left[M_2 D_{12} X_2 \frac{\partial \mu_2}{\partial X_2} + M_3 D_{13} X_3 \frac{\partial \mu_3}{\partial X_2} \right] \nabla X_2 \\
&\quad + \frac{c^2}{\rho RT} M_1 \left[M_2 D_{12} X_2 \frac{\partial \mu_2}{\partial X_3} + M_3 D_{13} X_2 \frac{\partial \mu_3}{\partial X_3} \right] \nabla X_3
\end{aligned}
$$

We let,

$$J_1^* = (\alpha_{11} + \beta_{11}) \nabla X_1 + (\alpha_{12} + \beta_{12}) \nabla X_2 + (\alpha_{13} + \beta_{13}) \nabla X_3 \tag{35}$$

where,

$$\alpha_{11} = \frac{c^2}{\rho RT} M_1 M_2 D_{12} X_2 \frac{\partial \mu_2}{\partial X_1} \tag{35a}$$

$$\alpha_{12} = \frac{c^2}{\rho RT} M_1 M_2 D_{12} X_2 \frac{\partial \mu_2}{\partial X_2} \tag{35b}$$

$$\alpha_{13} = \frac{c^2}{\rho RT} M_1 M_2 D_{12} X_2 \frac{\partial \mu_2}{\partial X_3} \tag{35c}$$

$$\beta_{11} = \frac{c^2}{\rho RT} M_1 M_3 D_{13} X_3 \frac{\partial \mu_3}{\partial X_1} \tag{35d}$$

$$\beta_{12} = \frac{c^2}{\rho RT} M_1 M_3 D_{13} X_3 \frac{\partial \mu_3}{\partial X_2} \tag{35e}$$

$$\beta_{13} = \frac{c^2}{\rho RT} M_1 M_3 D_{13} X_3 \frac{\partial \mu_3}{\partial X_3} \tag{35f}$$

Similarly, we can expand Eq. (34) for i = 2 and obtain,

$$\begin{aligned} J_2^* &= \frac{c^2}{\rho RT} M_2 \left[M_1 D_{21} X_1 \frac{\partial \mu_1}{\partial X_1} + M_3 D_{23} X_3 \frac{\partial \mu_3}{\partial X_1} \right] \nabla X_1 \\ &+ \frac{c^2}{\rho RT} M_2 \left[M_1 D_{21} X_1 \frac{\partial \mu_1}{\partial X_2} + M_3 D_{23} X_3 \frac{\partial \mu_3}{\partial X_2} \right] \nabla X_2 \\ &+ \frac{c^2}{\rho RT} M_2 \left[M_1 D_{21} X_1 \frac{\partial \mu_1}{\partial X_3} + M_3 D_{23} X_3 \frac{\partial \mu_3}{\partial X_3} \right] \nabla X_3 \\ &= (\alpha_{21} + \beta_{21}) \nabla X_1 + (\alpha_{22} + \beta_{22}) \nabla X_2 + (\alpha_{23} + \beta_{23}) \nabla X_3 \end{aligned} \tag{36}$$

where

$$\alpha_{21} = \frac{c^2}{\rho RT} M_2 M_1 D_{21} X_1 \frac{\partial \mu_1}{\partial X_1} \qquad (36a)$$

$$\alpha_{22} = \frac{c^2}{\rho RT} M_2 M_1 D_{21} X_1 \frac{\partial \mu_1}{\partial X_2} \qquad (36b)$$

$$\alpha_{23} = \frac{c^2}{\rho RT} M_2 M_1 D_{21} X_2 \frac{\partial \mu_1}{\partial X_3} \qquad (36c)$$

$$\beta_{21} = \frac{c^2}{\rho RT} M_2 M_3 D_{23} X_3 \frac{\partial \mu_3}{\partial X_1} \qquad (36d)$$

$$\beta_{22} = \frac{c^2}{\rho RT} M_2 M_3 D_{23} X_3 \frac{\partial \mu_3}{\partial X_2} \qquad (36e)$$

$$\beta_{23} = \frac{c^2}{\rho RT} M_2 M_3 D_{23} X_3 \frac{\partial \mu_3}{\partial X_3} \qquad (36f)$$

For $i = 3$,

$$J_3^* = \frac{c^2}{\rho RT} M_3 \left[M_1 D_{31} X_1 \frac{\partial \mu_1}{\partial X_1} + M_2 D_{32} X_2 \frac{\partial \mu_2}{\partial X_1} \right] \nabla X_1$$

$$+ \frac{c^2}{\rho RT} M_3 \left[M_1 D_{31} X_1 \frac{\partial \mu_1}{\partial X_2} + M_2 D_{32} X_2 \frac{\partial \mu_2}{\partial X_2} \right] \nabla X_2$$

$$+ \frac{c^2}{\rho RT} M_3 \left[M_1 D_{31} X_1 \frac{\partial \mu_1}{\partial X_3} + M_2 D_{32} X_2 \frac{\partial \mu_2}{\partial X_3} \right] \nabla X_3$$

$$= (\alpha_{31} + \beta_{31}) \nabla X_1 + (\alpha_{32} + \beta_{32}) \nabla X_2 + (\alpha_{33} + \beta_{33}) \nabla X_3 \qquad (37)$$

where,

$$\alpha_{31} = \frac{c^2}{\rho RT} M_3 M_1 D_{31} X_1 \frac{\partial \mu_1}{\partial X_1} \quad (37a)$$

$$\alpha_{32} = \frac{c^2}{\rho RT} M_3 M_1 D_{31} X_1 \frac{\partial \mu_1}{\partial X_2} \quad (37b)$$

$$\alpha_{33} = \frac{c^2}{\rho RT} M_3 M_1 D_{31} X_1 \frac{\partial \mu_1}{\partial X_3} \quad (37c)$$

$$\beta_{31} = \frac{c^2}{\rho RT} M_3 M_2 D_{32} X_2 \frac{\partial \mu_2}{\partial X_1} \quad (37d)$$

$$\beta_{32} = \frac{c^2}{\rho RT} M_3 M_2 D_{32} X_2 \frac{\partial \mu_2}{\partial X_2} \quad (37e)$$

$$\beta_{33} = \frac{c^2}{\rho RT} M_3 M_2 D_{32} X_2 \frac{\partial \mu_2}{\partial X_3} \quad (37f)$$

If we return to Eq. (32) and write it for i = 1, 2, 3, we obtain:

$$VX_{c1}C_c = J_1^* + VC_cX_1 \quad (38)$$

$$VX_{c2}C_c = J_2^* + VC_cX_2 \quad (39)$$

$$VX_{c3}C_c = J_3^* + VC_cX_3 \quad (40)$$

Rearranging them gives,

$$J_1^* = VC_c(X_{c1} - X_1) \quad (41)$$

$$J_2^* = VC_c(X_{c2} - X_2) \quad (42)$$

$$J_3^* = VC_c(X_{c3} - X_3) \quad (43)$$

We now equate Eqs. (35), (36), (37) with Eq. (41), (42) and (43) respectively:

$$C_1 = (\alpha_{11}+\beta_{11})\nabla X_1 + (\alpha_{12}+\beta_{12})\nabla X_2 + (\alpha_{13}+\beta_{13})\nabla X_3 \tag{44}$$

$$C_2 = (\alpha_{21}+\beta_{21})\nabla X_1 + (\alpha_{22}+\beta_{22})\nabla X_2 + (\alpha_{23}+\beta_{23})\nabla X_3 \tag{45}$$

$$C_3 = (\alpha_{31}+\beta_{31})\nabla X_1 + (\alpha_{32}+\beta_{32})\nabla X_3 + (\alpha_{33}+\beta_{33})\nabla X_3 \tag{46}$$

which can be written in the matrix form as,

$$\begin{bmatrix} C_1 \\ C_2 \\ C_3 \end{bmatrix} = \begin{bmatrix} (\alpha_{11}+\beta_{11})\nabla X_1 & (\alpha_{12}+\beta_{12})\nabla X_2 & (\alpha_{13}+\beta_{13})\nabla X_3 \\ (\alpha_{21}+\beta_{21})\nabla X_1 & (\alpha_{22}+\beta_{22})\nabla X_2 & (\alpha_{23}+\beta_{23})\nabla X_3 \\ (\alpha_{31}+\beta_{31})\nabla X_1 & (\alpha_{32}+\beta_{32})\nabla X_3 & (\alpha_{33}+\beta_{33})\nabla X_3 \end{bmatrix} \tag{47}$$

which can be written as,

$$\begin{bmatrix} C_1 \\ C_2 \\ C_3 \end{bmatrix} = \begin{bmatrix} a_{11}\nabla X_1 & a_{12}\nabla X_2 & a_{13}\nabla X_3 \\ a_{21}\nabla X_1 & a_{22}\nabla X_2 & a_{23}\nabla X_3 \\ a_{31}\nabla X_1 & a_{32}\nabla X_2 & a_{33}\nabla X_3 \end{bmatrix} \tag{48}$$

where

$$a_{11} = (\alpha_{11}+\beta_{11}) \tag{48a}$$

$$a_{21} = (\alpha_{21}+\beta_{21}) \tag{48b}$$

$$a_{31} = (\alpha_{31}+\beta_{31}) \tag{48c}$$

$$a_{12} = (\alpha_{12}+\beta_{12}) \tag{48d}$$

$$a_{22} = (\alpha_{22}+\beta_{22}) \tag{48e}$$

$$a_{32} = (\alpha_{32}+\beta_{32}) \quad (48f)$$

$$a_{13} = (\alpha_{13}+\beta_{13}) \quad (48g)$$

$$a_{23} = (\alpha_{23}+\beta_{23}) \quad (48h)$$

$$a_{33} = (\alpha_{33}+\beta_{33}) \quad (48i)$$

With the aid of Cramer's rule, the matrix equation (48) is solved to yield:

$$\nabla X_1 = \frac{|A_1|}{|A|} \quad (49)$$

$$\nabla X_2 = \frac{|A_2|}{|A|} \quad (50)$$

and

$$\nabla X_3 = \frac{|A_3|}{|A|} \quad (51)$$

where $|A|$ is the determinant:

$$|A| = \begin{vmatrix} a_{11} & a_{12} & a_{13} \\ a_{21} & a_{22} & a_{23} \\ a_{31} & a_{32} & a_{33} \end{vmatrix}$$

$$= a_{11}(a_{22}a_{33}-a_{23}a_{32}) - a_{12}(a_{21}a_{33}-a_{23}a_{31}) + a_{13}(a_{21}a_{32}-a_{22}a_{31}) \quad (52)$$

and

$$|A_1| = \begin{vmatrix} C_1 & a_{12} & a_{13} \\ C_2 & a_{22} & a_{23} \\ C_3 & a_{32} & a_{33} \end{vmatrix}$$

$$= C_1(a_{22}a_{33}-a_{23}a_{32}) - a_{12}(C_2a_{33}-C_3a_{23}) + a_{13}(C_2a_{32}-C_3a_{22}) \quad (53)$$

and

$$|A_2| = \begin{vmatrix} a_{11} & C_1 & a_{13} \\ a_{21} & C_2 & a_{23} \\ a_{31} & C_3 & a_{33} \end{vmatrix}$$

$$= a_{11}(C_2a_{33}-C_3a_{23}) - C_1(a_{21}a_{33}-a_{23}a_{31}) + a_{13}(a_{21}C_3-a_{31}C_2) \quad (54)$$

and

$$|A_3| = \begin{vmatrix} a_{11} & a_{12} & C_1 \\ a_{21} & a_{22} & C_2 \\ a_{31} & a_{32} & C_3 \end{vmatrix}$$

$$= a_{11}(C_3a_{22}-C_2a_{32}) - a_{12}(C_3a_{21}-C_2a_{31}) + C_1(a_{21}a_{32}-a_{22}a_{31}) \quad (55)$$

There is actually a relation which connects Eqs. (49), (50) and (51). Since from Eq. (30b):

$$\sum_{i=1}^{3} X_i = X_1 + X_2 + X_3 = 1$$

therefore

$$\nabla X_1 + \nabla X_2 + \nabla X_3 = 0 \quad (56)$$

and from Eq. (30a):

$$\sum_{i=1}^{3} J_i^* = J_1^* + J_2^* + J_3^* = C_1 + C_2 + C_3 = 0 \quad (57)$$

Returning to Eq. (32) for the constitutional supercooling criterion for three component system:

$$G < \nabla T_L = \sum_{i=1}^{2} \left.\frac{\partial T_L}{\partial X_i}\right)_0 \nabla X_i$$

$$= \left.\frac{\partial T_L}{\partial X_1}\right)_0 \nabla X_1 + \left.\frac{\partial T_L}{\partial X_2}\right)_0 X_2 \qquad (58)$$

As was discussed earlier, if $T_L = T_L(X_1, X_2)$ is known, then the terms $\left.\frac{\partial T_L}{\partial X_1}\right)_0$ and $\left.\frac{\partial T_L}{\partial X_2}\right)_0$ can be calculated. The terms ∇X_1 and ∇X_2 were derived and expressed in equations (49) and (50). So the constitutional supercooling criterion for the three component system, as expressed in equation (58) is determined. The expression should reduce to that for a simple binary system for n = 2.

Chapter VII

CONCLUSIONS

The research described in this dissertation was primarily concerned with three experimental projects: the vertical gradient freeze growth of GaAs, the THM growth of GaAs, and the THM growth of $Ga_xIn_{1-x}Sb$ and $Ga_xAl_{1-x}As$. The objectives accomplished are discussed here under three individual investigations.

In the vertical gradient freeze growth investigation, we have demonstrated the feasibility of routinely preparing reasonably large (1 cm dia., 10 cm long), fracture-free cylindrical ingots of GaAs from pre-reacted polycrystalline material. Growth from elemental Ga and As was also been successfully accomplished. There was definite evidence of grain selection towards single crystallinity in all the ingots grown. The product material was comparable in purity to GaAs produced by conventional methods such as horizontal Bridgman and Czochralski techniques. Macroscopic defects such as peripheral voids and central cracks frequently occurred in the grown material. In addition, compositional inhomogeneities, a high dislocation content and relatively poor electrical properties rendered the GaAs grown undesirable for direct device application. It is suspected that some, if not all, of the above problems are due to the

rapid (0.05 to 0.5 cm/min) solidification rates and relatively poor control of the growth conditions. However, the vertical gradient freeze method has been proven to be a fast and convenient technique for producing cylindrical ingots of GaAs for use as feed material in THM and floating zone melting growths of GaAs.

The major portion of our research effort was centered on the travelling heater method growth of GaAs. The accomplishments are summarized below:

1. A relatively simple, low cost but reliable apparatus for THM growth of crystals was constructed. A procedure for preparing the THM GaAs growth ampoule was developed and perfected so that samples could be produced routinely and with ease. The apparatus also allowed convenient loading and positioning of the growth ampoule. The position of the GaAs-Ga interfaces relative to the heater could be visually monitored and measured by a stereomicroscope-camera setup positioned outside the apparatus.
2. A systematic investigation was performed on the influence of the various parameters such as temperature and lowering rate, feed and crystal lengths, zone length and growth interface shape on THM growth and the quality of GaAs crystals grown. It was found that at the beginning of a THM growth in which the crystal length is much smaller than its diameter, and at the end of a

run when the remaining feed length becomes small, the actual growth rate exceeds the lowering rate, resulting in accelerated growths. In other words, the zone does not remain stationary relative to the heater throughout the run.

Because of this end effect, it is preferable to use a feed length at least twice the diameter. The size of the Ga zone was found to determine the GaAs-Ga growth interface shape, which in turn strongly influenced the crystallinity of the grown crystal. A zone-to-heater ratio of 0.6 to 1.0 was found to yield a convex growth interface which was conducive to single crystal growth. Twinning sometimes occurred when the interface was too convex. On the other hand, the concave interface of a large zone tended to produce polycrystalline growth and trap Ga inclusions in the center. The temperature and lowering rate are two closely related parameters. Higher temperatures generally increase the lowering rate feasible for THM growth but are expected to increase impurity contamination and introduce other problems, whereas lower temperatures necessitate inconveniently low growth rates and also increase the possibility of constitutional supercooling. It was found that a zone temperature about 900°C and lowering rate of about 1.5 to 2 mm/day were optimal for THM GaAs growth in the present apparatus.

3. Several inclusion-free, good quality single crystals of GaAs were grown with seeding in the ⟨111⟩ Ga, ⟨111⟩ As and ⟨110⟩ directions. The preferential seeding direction could not be determined conclusively. The crystals were either not intentionally doped or were doped with Te, Zn or Cr. Hall measurements showed that the electrical properties of the material were only fair. There was a sudden increase in density of dislocations parallel to the growth direction at the seeding interface. It decreased abruptly for the first one to two mm and followed an exponential decrease thereafter at a rate of about 17 to 27% per mm of growth. The etch pit density of dislocations normal to the growth direction was found to remain at the same level as that of the seed material. The dislocation elimination phenomenon is thought to involve the "loop formation" effect of dislocation annilation observed in TSM grown GaAs and the dislocation "growing out" effect of a convex GaAs-Ga growth interface. Impurity concentrations of THM grown GaAs showed a decrease from that of the Czochralski and gradient freeze grown feed material. This effect was especially marked for a crystal subjected to three Ga zone passes. Most of the impurities were reduced by a factor of from 1 to 30, down to a level of 10^{14} to 10^{15} atoms/cm^3.

4. The temperature profile inside a GaAs crystal was measured for a THM growth run over 13.5 days at a lowering rate of 1.5 mm/day. The maximum heater temperature outside the ampoule was 1013°C and the Ga zone temperature was measured as 931°C. The temperature gradient G in the liquid at the GaAs-Ga growth interface was ~40°c/cm.

5. An expression for the critical growth rate V_c for the onset of constitutional supercooling in THM growth of GaAs was derived. The value of V_c depends not only on the diffusion coefficient D but also the temperature gradient G, the arsenic solubility X and the liquidus slope m. Higher values of V_c are strongly favored by higher temperatures. The predicted values of V_c agree reasonably well with THM experimental runs. A general expression for V_c for a multicomponent system was also successfully derived.

Two systems were chosen for exploratory research into THM growth of mixed III-V compounds. $Ga_xIn_{1-x}Sb$ was grown from a mixed Ga-In zone by THM. The variation of the composition ratio X was determined for two different ingots grown at heater temperature ~600°C from a feed of $Ga_{0.5}In_{0.5}Sb$ (with an initial zone of $X \simeq 0.58$) and $Ga_{0.9}In_{0.1}Sb$ (with an initial zone of $X \simeq 0.8$). A similar compositional profile was determined for a crystal grown

with a GaAs seed and a $Ga_{0.97}Al_{0.03}As$ feed at heater temperature ~1100°C. The results were satisfactorily explained by material balance-phase diagram considerations.

Chapter VIII

RECOMMENDATIONS

The results of our research discussed in this dissertation were satisfactory and the main objectives accomplished. However, the planning, execution and characterization of the results were by no means perfect or ideal. Based on the knowledge and experience gained thus far, the following recommendations are made for future work:

A. Vertical gradient freeze growth of GaAs.

1. A resistance furnace with perhaps three separate temperature zones would be better than the globar furnace setup used. The furnace bore should be a closer fit to the growth ampoule and baffles could be used to reduce the convection currents in the furnace chamber in such vertical growth units. Better temperature control is definitely needed and lower cooling rates should be made possible.
2. Investigate the cause of the peripheral voids and the central cracks in the GaAs material produced and adopt improvements to eliminate these defects. Attempt seeding the growth and adding impurity dopants to the material. The eventual aim would be to grow larger diameter single crystals of

higher perfection and better electrical properties which could be used in fabrication of devices.

3. Obtain better theoretical understanding of the heat and mass transfer and other aspects of the crystal growth process and compare it with experiments.

B. Travelling heater method growth of GaAs.

1. Further improvements on the present THM growth apparatus could be made. A motor with variable speed would make speed changes between different runs convenient and allow speed changes (if wanted) during a run without disturbing the growth. An alundum furnace core would be more durable than the quartz furnace tube. The lack of visibility in loading could be overcome by standardizing the ampoule length and the seed-zone-feed configuration.

2. Investigate further the seeding and impurity doping of THM growth of GaAs and possible growth at higher lowering rates. This could be done by making the heater zone profile sharper, thus increasing the temperature gradient G at the growth interface and the critical growth rate V_c. If larger crystals of perhaps lower dislocation content and better electrical properties could be grown at a production level, the THM could conceivably be developed into a competitive

method of growing GaAs crystals. This is an even more plausible proposition for growth of GaP and other crystals which are difficult and thus expensive to grow by other methods.

3. Perform more extensive characterization of the GaAs crystals and investigate possible application in device fabrication.

C. Travelling heater method growth of mixed III-V compounds.

1. Pursue further the investigation of growth of $Ga_xIn_{1-x}Sb$ and $Ga_xAl_{1-x}As$ along similar lines as that adopted for the growth of GaAs. The solvent zone and feed compositions which could produce uniform grown material should be deduced from known phase diagrams and investigated experimentally. The emphasis should be on sound coupling between theoretical understanding and experimental work.

2. Investigate the growth of other mixed III-V compounds, such as $GaAs_xP_{1-x}$, $Ga_xIn_{1-x}As$, etc. If high quality crystals of these mixed III-V compounds are successfully grown, extensive characterization and device work could be performed.

A final note on the THM growth of III-V compounds is appropriate here. That is, we have barely scratched the surface of a crystal growth method with great potential and technological importance.

The topic could well be developed into a whole new important field of crystal growth of mixed III-V compounds. It is thus strongly recommended that future effort concentrate in this direction.

NOMENCLATURE

a	Constant
a_{ij}	Matrix element, i, j = 2, 3, 3 (see Chapter VI)
A	Solvent
b	Constant
B	Solute
c	Total molar concentration of the fluid, g-atom/cm^3
C	Solute concentration, g atom/cm^3
C_{1-3}	Matrix element (see Chapter VI)
C_i	Atom concentration of i component in liquid, g-atom/cc
C_{ci}	Atom concentration of i component in crystal, g-atom/cc
C_c	Total atomic concentration in crystal, g-atom/cc
C_ℓ	Total atomic concentration in liquid, g-atom/cc
C_p	Specific heat at constant pressure, cal/g^{o}C
D	Diffusion coefficient, cm^2/sec
D_i	Diffusion coefficient of i component, cm^2/sec
D_{ij}	Multicomponent diffusion coefficient, cm^2/sec
D_0	Diffusion coefficient of solvent, cm^2/sec
G	Temperature gradient in liquid at crystallizing interface, ^{o}C/cm
h	Heat transfer coefficient from the surface of crystal, cal/cm^2 sec^{o}C
ΔH_f	Latent heat of fusion, cal/b

J	Diffusion flux of solute in the zone, g-atom/cm^{2}sec
k	Thermal conductivity, cal/cm sec$^\circ$C
k	segregation coefficient = $\frac{\text{concentration of component in solid}}{\text{concentration of component in liquid}}$
K^*	Overall mass transfer coefficient in the zone between interfaces, cm/sec
ℓ	Length of zone in Travelling Heater Method
m	Slope of liquidus on phase diagram, dT_L/dX, $^\circ$C/atom %
M	Molecular weight
M_c	Average molecular weight of crystal
M_z	Average molecular weight of zone
R	Radius, cm
R	Gas constant, cal/g-atom $^\circ$K
t	Time, sec
T	Temperature, $^\circ$C
T_c	Cooler temperature, $^\circ$C
T_h	Heater temperature, $^\circ$C
T_i	Interface temperature, $^\circ$C
T_L	Liquidus temperature, $^\circ$C
T_0	Room temperature, $^\circ$C
ΔT	Actual temperature difference between top and bottom interfaces, $^\circ$C
V	Lowering rate (steady state growth rate), cm/sec or mm/day

V_c	Critical Growth rate above which constitutional supercooling occurs, cm/sec
V_{cf}	Crystallization flow, cm/sec
x	Atom fraction of group III element in a mixed III-V compound
x_{ci}	Atom fraction x for element i in crystal
x_{fi}	Atom fraction x for element i in feed
X_{ci}	Atom fraction of i component in crystal
X_{fi}	Atom fraction of i component in feed
X_{zi}	Atom fraction of i component in zone
X	Atom fraction solubility
∇X	Gradient of atom fraction of solute, cm^{-1}
∇X_i	Gradient of atom fraction of i component, $i = 1, 2, 3$, cm^{-1} (see Chapter VI)
ΔX	Concentration difference between top and bottom interfaces, g-atom/cc
X_c	Atom fraction of solute in crystal
X_{ci}	Atom fraction of i component in crystal
X_i	Atom fraction of i component in liquid
y	Distance, cm or mm
Y	Total number of g-atoms crystallized in travelling heater method growth of mixed compound
Z	Total g-atoms in zone

Greek Symbols

α_{ij} Matrix elements, i, j = 1, 2, 3 (see Chapter VI)

δ_b Distance between the bottom interface of zone and the lower heater boundary, cm

γ Activity coefficient

η Viscosity, g/sec cm

μ Chemical potential, cal/mole

μ Mobility of electrons or holes, cm^2/v-sec

ρ Density, g/cc

ρ Resistivity, ohm-cm

REFERENCES

1. W. G. Pfann, Trans. AIME 203, 961 (1955).

2. A. I. Mlavsky, and M. Weinstein, J. Applied Physics 34 2885 (1963).

3. N. Hemmat, and F. Wald, "Gallium Arsenide," Final Technical Report, NR 017-730/1-23-70, Tyco Labs., Waltham, Mass. (June 1970).

4. W. G. Pfann, "Zone Melting," John Wiley & Sons, Inc., New York (1958), p. 201.

5. F. A. Trumbore, E. M. Porbansky, and A. A. Tartaglia, J. Phys. Chem. Solids 11, 239 (1959).

6. G. A. Wolff, A. I. Mlavsky, Proc. Intern. Conf. on Adsorption and Crystal Growth, Nancy, France, No. 152, p. 711 (1965).

7. J. J. Brissot, and C. Belin, J. Crystal Growth 8, 213 (1971).

8. C. Berlin, J. J. Brissot, and R. E. Jesse, J. Crystal Growth 13/14, 597 (1972).

9. D. R. Mason, and J. S. Cook, J. Applied Physics 32, 475 (1961).

10. N. Hemmat, C. B. Lamport, A. A. Mena, and G. A. Wolff, Proc. ACCG Conf. on Crystal Growth, p. 79 (1969).

11. N. Hemmat, and M. Weinstein, J. Electrochem. Soc. 114, 403 (1967).

12. R. O. Bell, N. Hemmat, and F. Wald, Phys. Stat. Sol. 1, 375 (1970).

13. B. J. Perner, J. Crystal Growth 6, 86 (1969).

14. J. J. Brissot, and A. Lemogne, Phillips Technical Review No. 8/9/10, 261 (1969).

15. "New Methods for Growth and Characterization of GaAs and Mixed III-V Semiconductor Crystals," USCEE Report 437, ARPA, Grant No. DAHC 15-72-G7 (1 July 1972 - 31 December 1972), pp. 16-17.

16. T. S. Plaskett, S. E. Blum, and L. M. Foster, J. Electrochem. Soc. 114, 1304 (1967).

17. F. J. Reid, R. D. Baxter, and S. E. Miller, J. Electrochem. Soc. 113, 713 (1966).

18. G. A. Wolff, H. E. LaBelle, Jr., and B. N. Das, Trans. AIME 242, 436 (1968).

19. J. D. Broder, and G. A. Wolff, J. Electrochem. Soc. 110, 1150 (1963).

20. R. O. Bell, S. C. Foote, C. B. Lamport, and G. A. Wolff, "Electroluminescent Light Sources," Third Quarterly Report Contract No. NAS 12-2044, Tyco Labs., Waltham, Mass., (August 1969).

21. R. O. Bell, S. C. Foote, C. B. Lamport, A. H. Menna, and G. A. Wolff, "$Ga_xAl_{1-x}As$ Laser Diodes," Final Technical Report, Contract No. DAAK02-69-C-0071, Tyco Labs., Waltham, Mass. (December 1969).

22. T. S. Plaskett, and J. F. Woods, J. Crystal Growth 11, 341 (1971).

23. R. Ueda, O. Ohtsuki, K. Shinohara, and Y. Ueda, J. Crystal Growth 13/14, 668 (1972).

24. "New Methods for Growth and Characterization of GaAs and Mixed III-V Semiconductor Crystals," USCEE Report to ARPA for Grant No. DAHC15-71-G6 (1 July 1971 - 30 June 1972), Semi-Annual Report (January 1972), pp. 8-16.

25. B. DiBenedetto, C. J. Cronan, J. Am. Ceram. Soc. 51, 364 (1968).

26. C. C. Hein, U. S. Patent 2,747,196 to Westinghouse Electric Corp. (May 29, 1956).

27. G. A. Wolff, B. N. Das, C. B. Lamport, A. I. Mlavsky, and E. A. Trickett, Mat. Res. Bull. 4, S67 (1969).

28. L. L. Abernethy, T. H. Ramsey, and J. W. Ross, J. Applied Phys. 32, 376S (1961).

30. V. Yip and W. R. Wilcox, Bull. Am. Phys. Soc. 15, 1624 (1970).

31. V. F. Yip and W.R. Wilcox, Bull. Am. Phys. Soc. 17, 1185 (1972).

32. N. Hemmat, C. B. Lamport, A. A. Menna, and G. A. Wolff, Proc. of 67th National Meeting of the American Institute of Chemical Engineers in Atlanta, Georgia (August 1970), pp. 112-121.

33. "New Methods for Growth and Characterization of GaAs and Mixed III-V Semiconductor Crystals," USCEE Report 423, ARPA, Grant No. DAHC 15-71-G6 (1 July 1971 - 30 June 1972), pp. 34-50 .

34. "New Methods for Growth and Characterization of GaAs and Mixed III-V Semiconductor Crystals," USCEE Report, ARPA, Grant No. DAHC 15-70-G-14 (1 July 1970 - 30 June 1971), pp. 1-4.

35. W. A. Tiller, p. 277 in "The Art and Science of Growing Crystals," J. J. Gilman, ed., John Wiley & Sons, New York (1963).

36. John H. Perry, "Perry's Chemical Engineering Handbook," 4th edition, McGraw Hill, New York (1963), pp. 3-96.

37. M. Weinstein, H. E. LaBelle, Jr., and A. I. Mlavsky, J. Applied Physics 37, 2913 (1966).

38. F. Nicolau, J. Mat. Sci. 5 623 (1970).

39. "New Methods for Growth and Characterization of GaAs and Mixed III-V Semiconductor Crystals," USCEE Report 437, ARPA, Grant No. DAHC 15-72-G7 (1 July 1972 - 31 December 1972), pp. 35-41.

40. V. J. Vieland, and S. Skalski, pp. 303-315 in Metallurgy of Elemental and Compound Semiconductors, R. O. Grubble, ed., Interscience, New York (1960).

41. R. N. Hall, J. Electrochem. Soc. 110, 385 (1963).

42. G. M. Blom, and J. S. Plaskett, J. Electrochem. Soc. 118, 1831 (1971).

43. G. A. Antypas, J. Crystal Growth 16, 181 (1972).

44. W. R. Wilcox, J. Crystal Growth 12, 93 (1972).

45. B. D. Lainer, V. V. Rakov, M. G. Mil'vidiskii, and I. A. Magidson, Dokl. Akad. Nank SSSR, 185(1), 142-144 (1969) (Russ.).

46. Colin J. Smithells, "Metals Reference Book," Interscience, New York (1949), p. 415.

47. A. S. Grove, "Physics and Technology of Semiconductor Devices," John Wiley & Sons, Inc., New York (1967), pp. 102-103.

48. W. A. Tiller, J. Crystal Growth 2, 69 (1968).

49. R. B. Bird, W. E. Stewart, and E. N. Lightfoot, "Transport Phenomena," John Wiley & Sons, Inc., New York (1966), pp. 563-572.

APPENDIX A

GALLIUM - ARSENIC PHASE DIAGRAM FROM HANSEN*

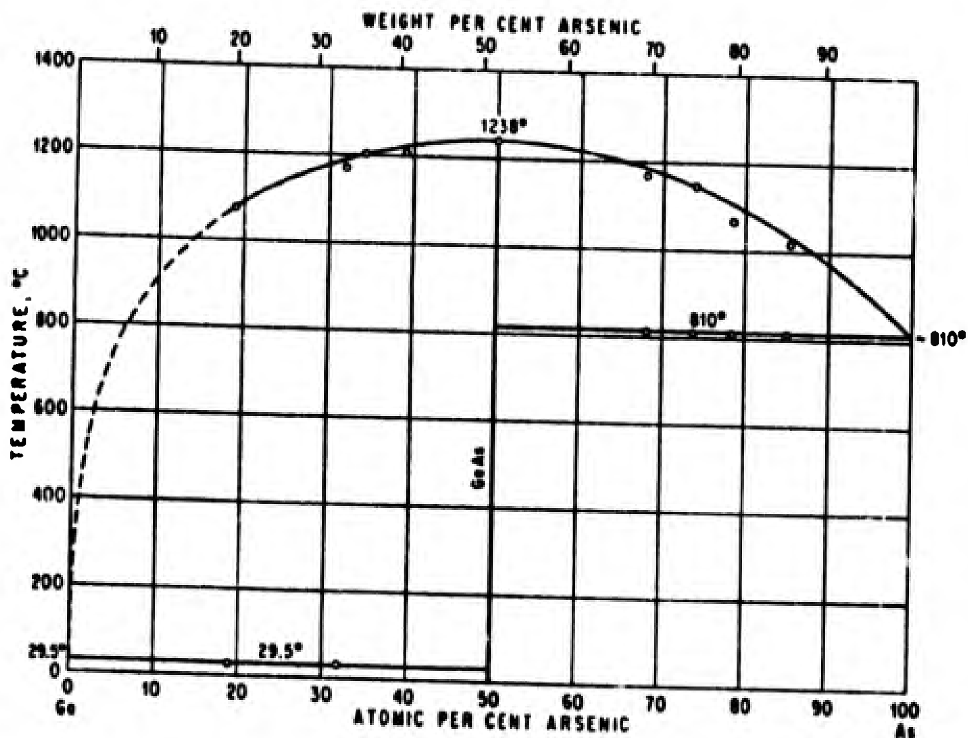

* Max Hansen, "Consitution of Binary Alloys," McGraw-Hill, Inc., New York(1958), p. 165.

APPENDIX B

CATHODOLUMINESCENCE INTENSITY DATA FOR FIGURE 12.

Horizontal Distance (mm)	Total Cathodoluminescence Intensity (microamp.)
-4.0 (point C)	0.92
-2.0	0.68
0.0 (point B)	1.04
+2.0	0.94
+4.0 (point A)	0.86

Vertical Distance (mm)	Total Cathodoluminescence Intensity (microamp.)
-8.0 (point E)	0.98
-6.0	0.74
-4.0	0.71
-2.0	0.65
0.0 (point B)	1.04
+2.0	1.34
+4.0	1.04
+6.0	1.25
+8.0 (point D)	1.15

APPENDIX C

ETCH PIT DENSITY DATA FOR FIGURE 41.

Slice No.	Growth Distance (mm)	Etch Pits per cm^2
72-1	-1.0 (seed)	$(2.65 \pm 0.5) \times 10^4$
72-2	0.0	$(2.50 \pm 1.0) \times 10^5$
72-3	1.0	$(1.40 \pm 0.7) \times 10^5$
72-4	2.0	$(1.25 \pm 0.5) \times 10^5$
72-5	4.0	$(7.00 \pm 2.0) \times 10^4$
72-6	6.0	$(3.20 \pm 0.5) \times 10^4$
72-7	8.0	$(2.95 \pm 0.5) \times 10^4$
72-8	10.0	$(2.25 \pm 0.3) \times 10^4$
72-9	12.0	$(1.55 \pm 0.2) \times 10^4$
72-10	15.0	$(1.00 \pm 0.1) \times 10^4$
72-11	19.0	$(4.00 \pm 0.3) \times 10^3$

APPENDIX D

ETCH PIT DENSITY FOR FIGURE 42.

Slice No.	Growth Distance (mm)	Etch Pits per cm^2
71-1	-1.0 (seed)	$(3.5 \pm 0.5) \times 10^4$
71-2	0.0	$(1.75 \pm 0.7) \times 10^5$
71-3	1.0	$(1.70 \pm 0.7) \times 10^5$
71-4	2.0	$(1.00 \pm 0.3) \times 10^5$
71-5	3.0	$(8.00 \pm 1.0) \times 10^4$
71-6	4.0	$(6.00 \pm 0.6) \times 10^4$
71-7	6.0	$(3.25 \pm 0.3) \times 10^4$
71-8	7.5	$(2.00 \pm 0.2) \times 10^4$
71-9	9.0	$(4.00 \pm 0.5) \times 10^4$
71-10	10.5	$(7.00 \pm 1.0) \times 10^4$
71-11	12.5	$(7.00 \pm 1.0) \times 10^4$
71-12	14.5	$(8.00 \pm 1.0) \times 10^4$
71-13	16.5	$(2.00 \pm 0.7) \times 10^5$

APPENDIX E

ETCH PIT DENSITY DATA FOR CURVE THM-84 IN FIGURE 43.

Slice No.	Growth Distance (mm)	Etch Pits per cm^2
84-1	-1.0 (seed)	$(2.10 \pm 0.2) \times 10^4$
84-2	0.0	$(2.60 \pm 0.3) \times 10^4$
84-3	0.5	$(2.60 \pm 0.3) \times 10^4$
84-4	1.0	$(2.60 \pm 0.3) \times 10^4$
84-5	2.0	$(2.75 \pm 0.3) \times 10^4$
84-6	3.0	$(2.90 \pm 0.4) \times 10^4$
84-7	4.0	$(2.90 \pm 0.4) \times 10^4$
84-8	5.0	$(2.55 \pm 0.3) \times 10^4$

APPENDIX F

ETCH PIT DENSITY DATA FOR CURVE THM-86 IN FIGURE 43

Slice No.	Growth Distance (mm)	Etch Pits per cm^2
86-1	-1.0 (seed)	$(3.50 \pm 0.5) \times 10^4$
86-2	0.0	$(3.90 \pm 0.5) \times 10^4$
86-3	1.0	$(3.70 \pm 0.5) \times 10^4$
86-4	2.0	$(3.45 \pm 0.3) \times 10^4$
86-5	3.0	$(3.30 \pm 0.4) \times 10^4$
86-6	4.0	$(3.20 \pm 0.3) \times 10^4$
86-7	5.0	$(3.20 \pm 0.3) \times 10^4$
86-8	6.0	$(3.40 \pm 0.4) \times 10^4$
86-9	7.0	$(3.50 \pm 0.4) \times 10^4$
86-10	8.0	$(3.30 \pm 0.4) \times 10^4$
86-11	9.0	$(3.30 \pm 0.4) \times 10^4$

APPENDIX G

MASS SPECTROMETRIC RESULTS FOR CALCULATION OF TABLE 12. (Concentrations in parts per million weight)

Element	C2-41	THM-72	GF-30	THM-76
Li	< 0.003	< 0.003	< 0.003	< 0.002
Be	≤ 0.004	≤ 0.004	0.04	< 0.002
B	0.005	< 0.003	0.05	< 0.003
F	< 0.1	< 0.1	< 0.3	< 0.1
Mg	0.03	0.03	< 0.1	≤ 0.03
Si	< 1	< 1	0.7	0.6
Cl	0.1	0.1	0.02	0.05
K	< 0.2	0.1	0.06	0.03
Ca	< 0.3	< 0.3	0.03	< 0.06
Cr	0.1	< 0.02	< 0.03	< 0.01
Mn	< 0.02	< 0.02	< 0.02	< 0.01
Fe	0.4	0.07	0.2	1
Co	< 0.01	< 0.01	0.03	< 0.01
Ni	< 0.04	< 0.04	0.1	< 0.02
Cu	< 0.03	< 0.03	0.6	< 0.02
Zn	0.1	0.1	0.2	< 0.02
Sn	< 0.1	< 0.1	0.1	< 0.05

Element	C2-41	THM-72	GF-30	THM-76
Te	< 0.05	< 0.05	< 0.06	< 0.06
Pb	< 0.06	< 0.06	0.6	< 0.06

APPENDIX H

TEMPERATURE PROFILE DATA FOR FIGURE 45

Interfaces Positions (mm)	Crystal Temperature (^{o}C)	Furnace Temperature (^{o}C)
10.0	834	856
9.5	839	866
9.0	840	876
8.5	850	886
8.0	842	896
7.5	844	906
7.0	853	915
6.5	861	923
6.0	866	932
5.5	868	942
5.0	870	952
4.5	897	963
4.0	912	972
3.5	922	981
3.0	926	989
2.5	929	996
2.0	931	1001
1.5	931	1006

Interfaces Positions (mm)	Crystal Temperature (°C)	Furnace Temperature (°C)
1.0	931	1009
0.5	931	1012
0.0	931	1013
-0.5	931	1012
-1.0	930	1011
-1.5	927	1010
-2.0	923	1007
-2.5	922	999
-3.0	920	990
-3.5	918	977
-4.0	906	965
-4.5	904	949
-5.0	904	930
-5.5	897	908
-6.0	892	860
-6.5	887	-
-7.0	882	-
-7.5	874	-
-8.0	867	-

APPENDIX I

TEMPERATURE DATA FOR FIGURE 46.

Cooling Time (min.)	Temperature $(T-T_0)^oC$
0	770
6	520
12	419
18	371
24	332
30	307
36	282
42	262
48	246
54	228
60	214
72	186
84	163
96	143
108	128
120	111
132	100

Cooling Time (min)	Temperature $(T-T_0)^oC$
144	88
156	76
168	67
180	59